



Calhoun: The NPS Institutional Archive
DSpace Repository

Theses and Dissertations

Thesis and Dissertation Collection

1976-06

Computer prediction of tropospheric radio
transmission loss for selected paths in the
Pacific northwest

Cassidy, Richard Michael

<http://hdl.handle.net/10945/17704>

Downloaded from NPS Archive: Calhoun



Calhoun is a project of the Dudley Knox Library at NPS, furthering the precepts and goals of open government and government transparency. All information contained herein has been approved for release by the NPS Public Affairs Officer.

Dudley Knox Library / Naval Postgraduate School
411 Dyer Road / 1 University Circle
Monterey, California USA 93943

<http://www.nps.edu/library>

COMPUTER PREDICTION OF TROPOSPHERIC
RADIO TRANSMISSION LOSS FOR SELECTED
PATHS IN THE PACIFIC NORTHWEST

Richard Michael Cassidy

JUDLEY KNOX LIBRARY
NAVAL POSTGRADUATE SCHOOL
MONTEREY, CALIFORNIA 93940

NAVAL POSTGRADUATE SCHOOL

Monterey, California



THESIS

Computer Prediction of Tropospheric
Radio Transmission Loss for Selected
Paths in the Pacific Northwest

by

Richard Michael Cassidy, Jr.

June 1976

Thesis Advisor:

J. B. Knorr

Approved for public release; distribution unlimited.

Prepared for:
Naval Torpedo Station
Keyport, Washington 98345

T174974

UNCLASSIFIED

SECURITY CLASSIFICATION OF THIS PAGE (When Data Entered)

REPORT DOCUMENTATION PAGE

**READ INSTRUCTIONS
BEFORE COMPLETING FORM**

1. REPORT NUMBER		2. GOVT ACCESSION NO.	3. RECIPIENT'S CATALOG NUMBER
4. TITLE (and Subtitle) Computer Prediction of Tropospheric Radio Transmission Loss for Selected Paths in the Pacific Northwest		5. TYPE OF REPORT & PERIOD COVERED Master's Thesis June 1976	
7. AUTHOR(s) Richard Michael Cassidy, Jr.		8. CONTRACT OR GRANT NUMBER(s)	
9. PERFORMING ORGANIZATION NAME AND ADDRESS Naval Postgraduate School Monterey, CA 93940		10. PROGRAM ELEMENT, PROJECT, TASK AREA & WORK UNIT NUMBERS	
11. CONTROLLING OFFICE NAME AND ADDRESS Naval Postgraduate School Monterey, CA 93940		12. REPORT DATE June 1976	13. NUMBER OF PAGES
14. MONITORING AGENCY NAME & ADDRESS (if different from Controlling Office) Naval Postgraduate School Monterey, CA 93940		15. SECURITY CLASS. (of this report) UNCLASSIFIED	15a. DECLASSIFICATION/DOWNGRADING SCHEDULE
16. DISTRIBUTION STATEMENT (of this Report) Approved for public release; distribution unlimited.			
17. DISTRIBUTION STATEMENT (of the abstract entered in Block 20, if different from Report)			
18. SUPPLEMENTARY NOTES			
19. KEY WORDS (Continue on reverse side if necessary and identify by block number)			
20. ABSTRACT (Continue on reverse side if necessary and identify by block number) In order to characterize the propagation conditions along known paths at VHF and S Band frequencies, transmission loss predictions are produced by computer methods. An attempt is made to define the standard atmospheric conditions along these paths through the presentation of the statistics for normal and super-refractive propagation conditions.			

NAVAL POSTGRADUATE SCHOOL
Monterey, California

Rear Admiral Ishan Linder
Superintendent

Jack Borsting
Provost

This thesis prepared in conjunction with research supported in part by Naval Torpedo Station, Keyport, Washington under work order N00253-76-WR-00025.

Reproduction of all or part of this report is authorized.

Released as a
Technical Report by:

I. Linder

Computer Prediction of Tropospheric Radio Transmission
Loss for Selected Paths in the Pacific Northwest

by

Richard Michael Cassidy, Jr.
Lieutenant, United States Navy
A.B., University of North Carolina, 1970

Submitted in partial fulfillment of the
requirements for the degree of

MASTER OF SCIENCE IN ELECTRICAL ENGINEERING

from the

NAVAL POSTGRADUATE SCHOOL
June 1976

ABSTRACT

In order to characterize the propagation conditions along known paths at VHF and S Band frequencies, transmission loss predictions are produced by computer methods. An attempt is made to define the standard atmospheric conditions along these paths through the presentation of the statistics for normal and super-refractive propagation conditions.

TABLE OF CONTENTS

I. INTRODUCTION -----	12
II. COMPUTER-AIDED PATH LOSS PREDICTION -----	16
A. PROGRAM DESCRIPTION -----	16
B. ACTUAL PATH LOSS MEASUREMENTS -----	30
1. Procedure -----	30
2. Results -----	31
III. PROPAGATION IN A NON-STANDARD ATMOSPHERE -----	63
A. THEORY -----	64
B. IREPS -----	79
APPENDIX A - PATH PLOTTING PROGRAM -----	104
APPENDIX B - INPUT PARAMETER COMPUTATION -----	107
COMPUTER PROGRAM -----	113
LIST OF REFERENCES -----	116
INITIAL DISTRIBUTION LIST -----	118

LIST OF TABLES

I.	Input Values for Various TROPOPLOT Runs -----	20
II.	Range of Refractive Index Gradient for Various Propagation Conditions -----	67
III.	Relationship of Refractivity Gradient to Various Propagation Variables -----	69
IV.	K Factor Guide -----	70
V.	Variability of M Curves with Type of Transmission Conditions -----	78

LIST OF FIGURES

1.	NAVTORPSTA Keyport Ranges and Vicinity -----	14
2.	Path Geometry -----	18
3.	Example of Least Square Line Fit to Terrain -----	21
4.	Sample TROPOPLOT Output -----	23
5.	Sample TROPOPLOT Output -----	24
6.	Sample TROPOPLOT Output -----	25
7.	Sample TROPOPLOT Output -----	26
8.	Terrain Profile for the Zelatched Point to Keyport Path -----	32
9.	Terrain Profile for the Makah to Striped Peak Path -----	33
10.	Terrain Profile for the Lookout Mt. to Keyport Path -----	34
11.	Terrain Profile for the Zelatched Point to Bangor Path -----	35
12.	Terrain Profile for the Mt. Constitution to Gold Mt. Path -----	36
13.	Terrain Profile for the Striped Peak to Mt. Constitution Path -----	37
14.	Terrain Profile for the Bangor to Gold Mt. Path ---	38
15.	Terrain Profile for the Keyport to Gold Mt. Path --	39
16.	Terrain Profile for the Lookout Mt. to NOEF, Bangor Path -----	40
17.	Terrain Profile for the NOEF, Bangor to Gold Mt. Path -----	41
18.	Terrain Profile for the Zelatched Point to NOEF, Bangor Path -----	42
19.	Terrain Profile for the Lookout Mt. to Bangor Path -----	43
20.	Transmission Loss vs. Distance for the Zelatched Pt. to Keyport Path -----	45

21. Transmission Loss vs. Distance for the Makah to Striped Peak Path -----	46
22. Transmission Loss vs. Distance for the Lookout Mt. to Keyport Path -----	47
23. Transmission Loss vs. Distance for the Zelatched Point to Bangor Path -----	48
24. Transmission Loss vs. Distance for the Mt. Constitution to Gold Mt. Path -----	49
25. Transmission Loss vs. Distance for the Striped Peak to Mt. Constitution Path -----	50
26. Transmission Loss vs. Distance for the Bangor to Gold Mt. Path -----	51
27. Transmission Loss vs. Distance for the Keyport to Gold Mt. Path -----	52
28. Transmission Loss vs. Distance for the Lookout Mt. to NOEF, Bangor Path -----	53
29. Transmission Loss vs. Distance for the NOEF, Bangor to Gold Mt. Path -----	54
30. Transmission Loss vs. Distance for the Zelatched Point to NOEF, Bangor Path -----	55
31. Transmission Loss vs. Distance the Lookout Mt. to Bangor Path -----	56
32. Antenna Height Variation for an Unmodified Version of TROPOPLOT Transmission.Loss vs. Distance -----	57
33. Antenna Height Variations for the Modified Version of TROPOPLOT Transmission.Loss vs. Distance -----	58
34. Variation in ϵ and σ for the Lookout to Keyport Path Transmission.Loss vs. Distance -----	59
35. Variation in Δh for the Lookout Mt. to Keyport Path Transmission.Loss vs. Distance -----	60
36. Path Profile for Lookout Mt. to Keyport ($K=\frac{1}{2}$) -----	71
37. Path Profile for Lookout Mt. to Keyport ($K=1$) -----	72
38. Path Profile for Keyport to Gold Mt. ($K=\frac{1}{2}$) -----	73

39.	Path Profile for Keyport to Gold Mt. (K=1) -----	74
40.	Path Profile for Lookout Mt. to Bangor (K=½) -----	75
41.	Path Profile Lookout Mt. to Bangor (K=1) -----	76
42.	Historical Propagation Conditions for Tatoosh Island, Wash. -----	81
43.	Historical Propagation Conditions for Quillayute, Wash. -----	82
44.	Historical Meteorological Data for Tatoosh Island, Wash. -----	83
45.	Historical Meteorological Data for Quillayute, Wash. -----	84
46.	Median Profiles for Quillayute, Wash. -----	85
47.	Median Profiles for Tatoosh Island -----	86
48.	Winchelsea Island Ray Trace for Median Conditions -----	87
49.	Lookout Mt. Ray Trace for Median Conditions -----	88
50.	Makah Ray Trace for Median Conditions -----	89
51.	Striped Peak Ray Trace for Median Conditions -----	90
52.	Mt. Constitution Ray Trace for Median Conditions -----	91
53.	Profiles Required to Produce an Elevated Duct Between 1100-1400 Feet -----	92
54.	Ray Trace from Mt. Constitution for an Elevated Duct -----	93
55.	Ray Trace from Striped Peak for an Elevated Duct -----	94
56.	Ray Trace from Makah for an Elevated Duct -----	95
57.	Ray Trace from Lookout Mt. for an Elevated Duct --	96
58.	Profiles Required to Produce an Elevated Duct Between 2300-2900 Feet -----	97
59.	Ray Trace from Lookout Mt. for an Elevated Duct --	98

60.	Ray Trace from Mt. Constitution for an Elevated Duct -----	99
61.	Coverage Diagram (IREPS) -----	100
62.	Path Loss Display (IREPS) -----	101

ACKNOWLEDGMENT

I wish to express my appreciation to Mr. Herb Hitney of NELC for his kind assistance in providing the IREPS output used in this report.

I. INTRODUCTION

Numerous methods of estimating tropospheric propagation path loss are currently found in the literature. These include both graphical and computer techniques, of which the graphical methods are most widely presented. In conducting this particular study a program dealing with tropospheric path loss prediction (TROPOPLOT) was chosen as a computer method of analysis. This program was originally published by ESSA in a technical report [Ref. 6] and was subsequently modified for use at the Naval Postgraduate School [Ref. 7]. Tests were conducted by Longley and Reasoner [Ref. 8], in which the computer-predicted results of the program were compared with empirical data taken over a number of different paths. The results showed that TROPOPLOT can provide reasonably accurate predictions of path loss within certain constraints.

The paths selected for analysis in this study are located in the Puget Sound, Washington area. They comprise both existing and proposed communications links connecting the underwater range facilities operated by the Naval Torpedo Station at Keyport, Washington. The range operation centers are currently located at Winchelsea Island, British Columbia and on Zelatched Point near Dabob Bay. The present communications requirements include on-range communications with both range control vessels and the submarines and aircraft conducting tests, the capability to monitor telemetry information,

and the maintenance of telephone links with other sites. Proposals for expansion of the range facilities as the TRIDENT program progresses include possible at-sea range facilities and digital data transmission to a central computer processing center located at Bangor or Keyport. These proposals would increase the bandwidth requirements of the links and thus necessitate a change from the present VHF frequency range to an S-band (2 GHz) line of sight link.

The terminal and repeater sites are shown in Figure 1. The existing VHF link consists of paths from Winchelsea to Lookout Mt. (repeater) to Bangor and from Zelatched Point to Bangor. The proposed link at 2 GHz runs from Makah to Striped Peak (repeater) to Mt. Constitution (repeater) to Gold Mt. (repeater) to Bangor or Keyport, as well as from Zelatched Point to Bangor or Keyport. Each of these paths is computer-analyzed in Section II.

In addition to computing path loss, the historical meteorological data for this area was examined in an attempt to characterize the "typical" propagation conditions found in this vicinity. This was accomplished by means of the Integrated Refractive Effects Prediction System (IREPS) which provided output based on data taken from upper air sounding stations in the Puget Sound area. This information could also be useful in the determination of link service probability.

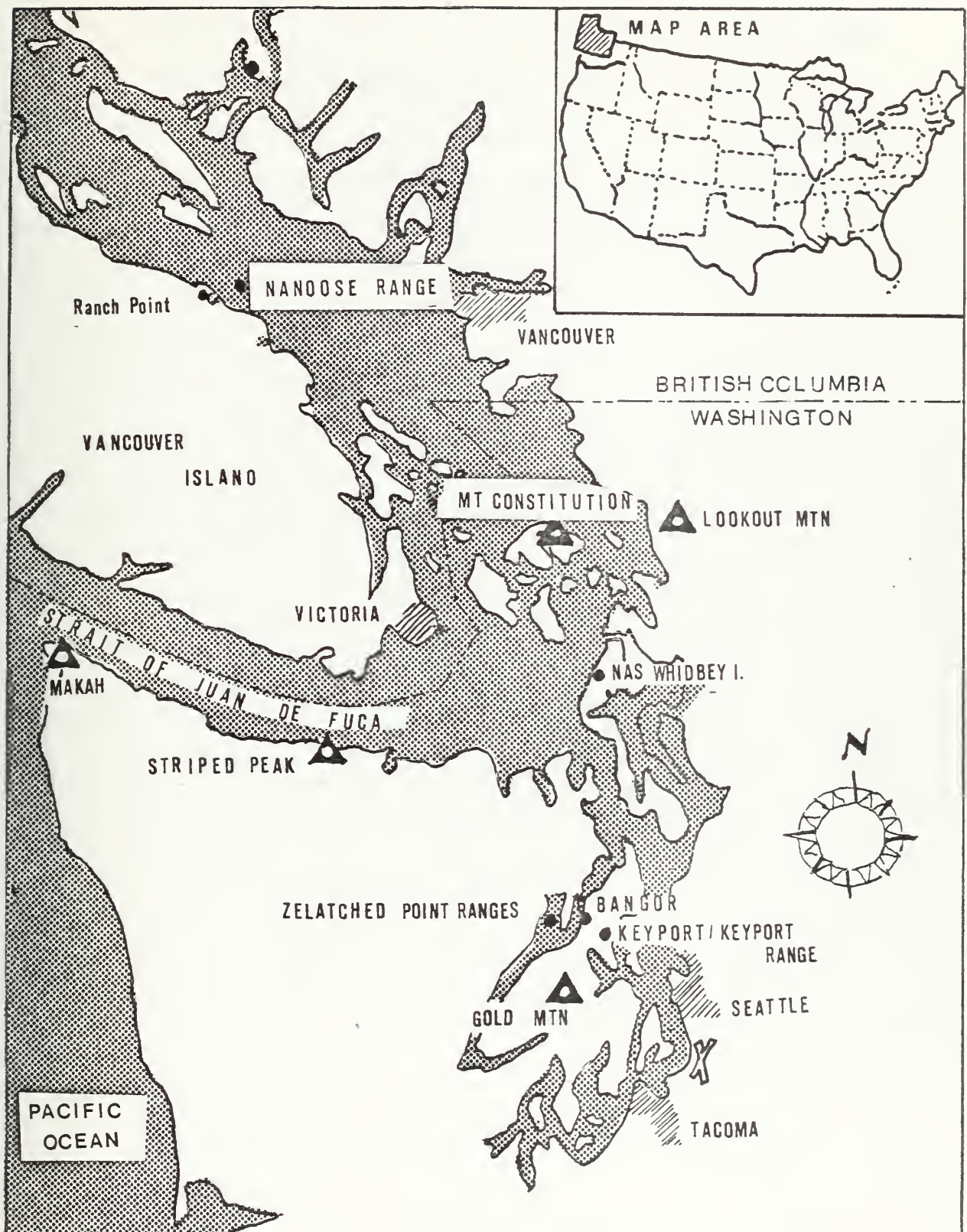


Figure 1
NAVTORPSTA Keyport Ranges and Vicinity

A listing of a computer program designed to plot path profiles and to aid in the determination of several input variables is included in the appendices, as is an explanation of the modifications required in order to use detailed terrain profile information in the TROPOPLOT program.

II. COMPUTER-AIDED PATH LOSS PREDICTION

A. PROGRAM DESCRIPTION

TROPOPOPLOT provides as an output a measure of the long-term attenuation over a given path. The program was primarily designed for use in cases where detailed terrain information was not available but can be used accurately with user-supplied data after a slight modification. The required input parameters include frequency, antenna heights, antenna gains, line losses, receiver sensitivity, path length, polarization, transmitter power out, surface refractivity, conductivity, permittivity, and a measure of the terrain roughness Δh . These parameters are for the most part well defined in Refs. 6 and 7 and are easily determined except in the case of user-supplied terrain profile information. For this sort of input there is some ambiguity concerning the selection of values for σ , ϵ , Δh , and the effective antenna heights.

In considering a path which includes both poor ground surfaces ($\epsilon=4$, $\sigma=.001$) and sea water surface ($\epsilon=81$, $\sigma=5$) the particular value to use as input is not specified, although a completely oversea path requires an adjustment to the program not available in the version used for this study. Thus the values of ϵ and σ chosen were based on the corresponding value for that portion of the terrain that constituted the largest portion of the dominant reflecting plane between the transmitter and receiver.

The path geometry considered is shown in Figure 2 and indicates $h_{g1,2}$ as the structural transmitter (receiver) height above ground. This input parameter is converted into an effective height, $h_{e1,2}$ by the program. It should be noted that Longley and Rice consider two cases: one for random antenna siting in which structural heights, $h_{g1,2}$ are considered equal to the effective heights, $h_{e1,2}$; and another in which the sites are carefully selected, as in the case of radio relay links, and the effective heights are larger than the structural heights as shown below:

$$h_{e1,2} = h_{g1,2} + k \exp(-2h_{g1,2}/\Delta h) \text{ meters}$$

The variable k is considered to have a maximum value of 50 as determined by the author's study of varied terrain conditions. The method presented below for the computation of k is valid only for antenna heights less than or equal to 10 meters. In Callaghan's version [Ref. 7] this determination was:

$$\begin{aligned} k &= 1 + 4 \sin(\pi h_{g1,2}/10) \text{ for } 0 \leq h_{g1,2} \leq 5 \\ &= 5 \quad \text{otherwise} \end{aligned}$$

Since most of the antennas in the links under study had structural heights in the neighborhood of 50 meters, it is obvious that predictions based on strictly $h_{g1,2}$ would in this case, produce an erroneous (higher than normal) prediction of path loss. This factor is recognized by the authors as an area requiring better definition and as a primary source of

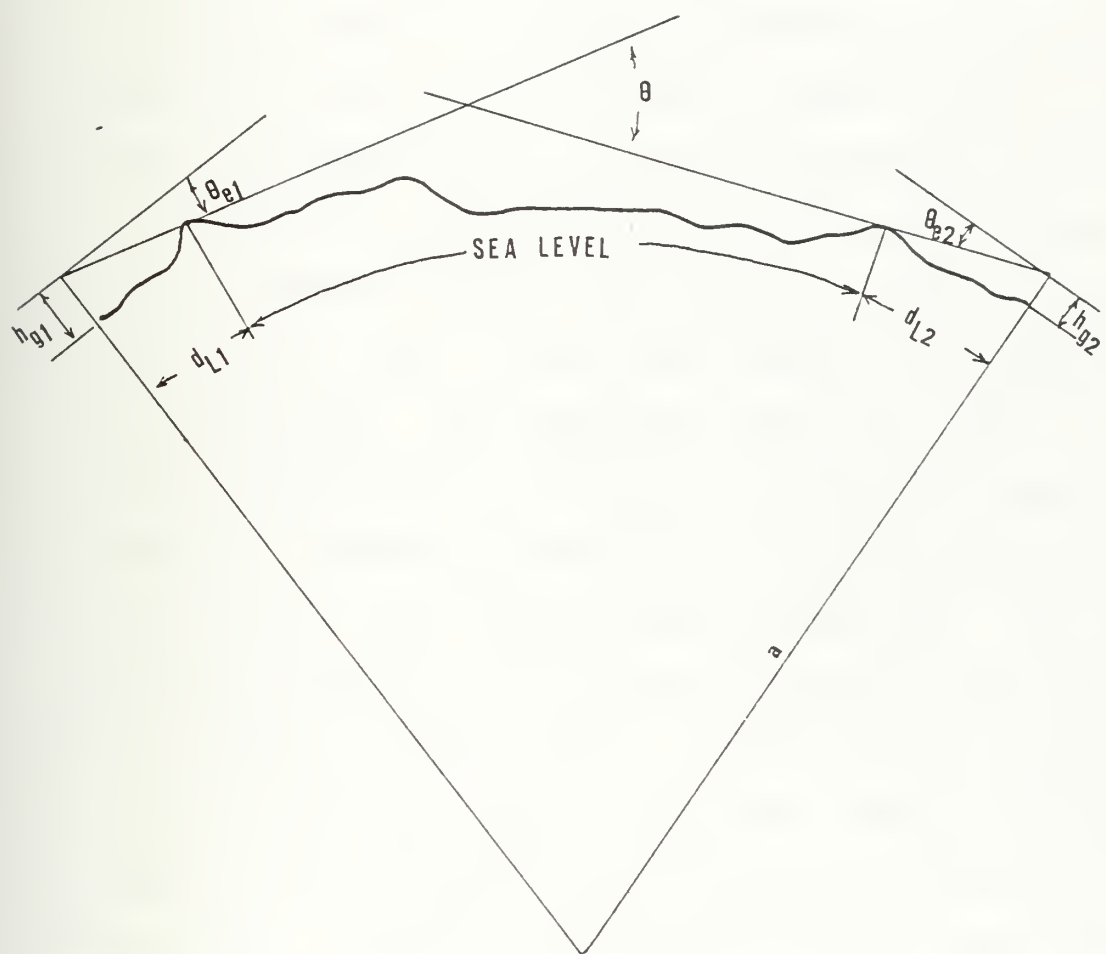


Figure 2
Path Geometry

prediction error. For this reason the modifications to TROPOPLOT which are detailed in Appendix B were necessary. The effect of varied antenna heights in the input of the unmodified program is shown in the output data presented later in this section.

The description of the terrain is accomplished by a statistical quantity, Δh , which is defined in Ref. 6 as "the asymptotic value of the interdecile range, $\Delta h(d)$, of terrain heights above and below a straight line fitted to elevations above sea level. The parameter $\Delta h(d)$ is calculated at fixed distances and its median value usually increases with path length to Δh ." For a single path profile these definitions are not adequate. The asymptotic value, Δh , used in this study as determined by taking the interdecile range of the difference between a straight line fitted to the path profile points and the path profile points themselves. The results of this estimation of Δh correlate favorably with those values listed in Table 1 [Ref. 7] which shows estimated values of Δh for particular types of terrain. Figure 3 shows an example of the straight line fit to the terrain profile between Lookout Mt. and Bangor. The details of the computation are found in Appendix B.

Having thus considered the variations in the input parameters the program constraints should be noted. TROPOPLOT is designed for use within the following constraints:

	Lookout Mt. to Bangor	Lookout Mt. to Gold Mt.	Lookout Mt. to Mt. Constituteion	Lookout Mt. to Stripped Peak	Lookout Mt. to Mt. Constituteion	Lookout Mt. to Gold Mt.	Lookout Mt. to Mt. Constituteion	Lookout Mt. to Stripped Peak	Lookout Mt. to Gold Mt.	Lookout Mt. to Mt. Constituteion	Lookout Mt. to Stripped Peak	Lookout Mt. to Gold Mt.	Lookout Mt. to Mt. Constituteion	Lookout Mt. to Stripped Peak	Lookout Mt. to Gold Mt.	Lookout Mt. to Mt. Constituteion	Lookout Mt. to Stripped Peak	Lookout Mt. to Gold Mt.	Lookout Mt. to Mt. Constituteion	Lookout Mt. to Stripped Peak	Lookout Mt. to Gold Mt.	Lookout Mt. to Mt. Constituteion	
TXPO watts	10 100	2 100	10 100	10 100	10 100	10 100	10 100	10 100	10 100	10 100	10 100	10 100	10 100	10 100	10 100	10 100	10 100	10 100	10 100	10 100	10 100	10 100	10 100
TAG=RAG db	31 12	31 12	31 12	31 12	31 12	31 12	31 12	31 12	31 12	31 12	31 12	31 12	31 12	31 12	31 12	31 12	31 12	31 12	31 12	31 12	31 12	31 12	31 12
FREQ MHz	2000 250	2000 250	2000 250	2000 250	2000 250	2000 250	2000 250	2000 250	2000 250	2000 250	2000 250	2000 250	2000 250	2000 250	2000 250	2000 250	2000 250	2000 250	2000 250	2000 250	2000 250	2000 250	2000 250
DIST(km)	15	81.9	109.5	8.1	124.3	85.35	16.5	20.5	110.3	17.8	6.2	111.9											
Δh (m)	57.43	171.72	87.86	59.96	140.68	208.99	80.25	96.52	120.6	67.67	40.87	103.61											
TE1(rad)	1.466	-0.7505	-0.9075	1.3089	-1.1345	-.06981	.8552	1.256	-.90757	+.89012	1.3177	-.82030											
TE2(rad)	1.3963	0.7505	1.2217	.244346	+1.1345	+.06981	-8552	-.7505	.94248	-.89012	1.0646	.82030											
HIG(m)	50	168.75	701.4	97.8	698.58	330	50	50	330	50	78	510.7											
H2G(m)	50	200	50	50	250	700	286.75	362.5	50	200	120	50											
DL1(km)	2.5	81.9	129	2	250	128.75	16.7	1.5	107.5	18	2.0	137.5											
DL2(km)	2.5	81.9	7.5	6.25	250	128.75	16.7	20	31.25	18	4.3	137.5											
ϵ	25.0	25	25	25	25	25	25	25	25	25	25	25											
N_s	N-units	308	298	297	307	292	299	306	301	297	308	306											

Table I

Input Values for Various TROPOPLOT Runs

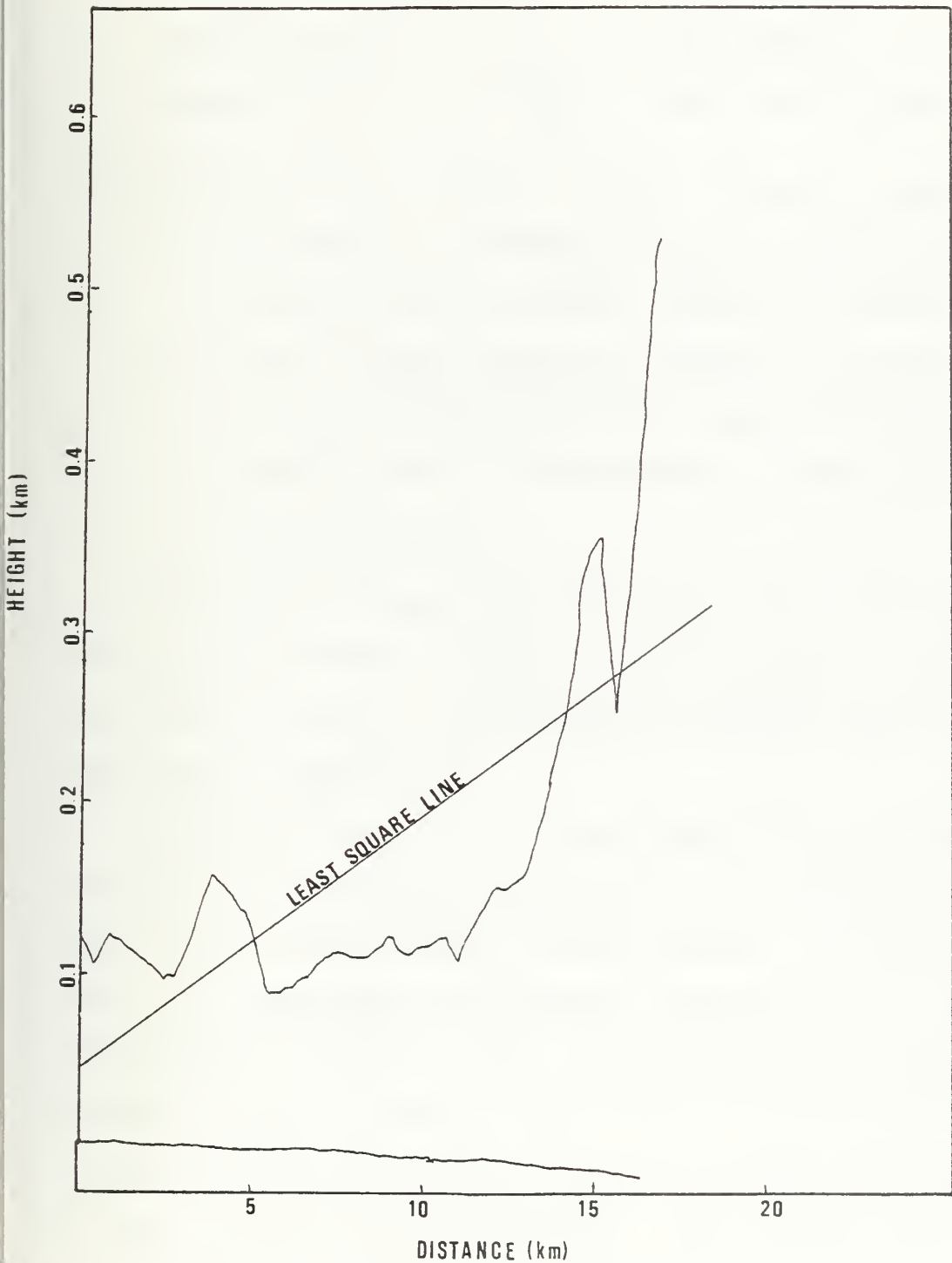


Figure 3
Examples of Least Square Line Fit to Terrain

<u>Parameter</u>	<u>Range</u>
frequency (f)	20 to 40,000 MHz
antenna height ($h_{g1,2}$)	0.5 to 3000 m
distance (dist)	1 to 2000 km
surface refractivity (N_s)	250 to 400 N-units

The antenna siting is subject to the following conditions:

1. The angle of elevation, $\theta_{e1,2}$, of each horizon ray from the horizontal should not exceed 12° .
2. The distance from each antenna to its horizon ($d_{L1,2}$) should not be less than 1/10 or more than 3 times the corresponding smooth earth distance (d_{LS}).

These limitations can be ignored if the values of $d_{L1,2}$, and $\theta_{e1,2}$ are entered directly into the program. As is the case with Δh and $h_{g1,2}$ the method of accomplishing this is contained in Appendix B.

Having resolved, or at least identified, the potential ambiguities in the input parameters, it is useful to briefly describe the output format of the program. As shown in Figs. 4-7, the output of TROPOPLOT consists of two tables containing transmission loss versus distance and signal strength versus distance, a plot of the transmission loss information and a printout of the calculated and input values of many of the program parameters. Some of the quantities in this figure may require some explanation as to their meaning or derivation. These include the variables AE, AES, AED, MS, → MD, ADX, DX, K1, K2, and ALS.

--- USER TERRAIN DATA ---

FREQUENCY OF SIGNAL - F- (MEG-HERTZ) 100.00000

	DISTANCE (KM)	TRANS LOSS (dB)	DISTANCE (KM)	TRANS-LCSS (dB)	DISTANCE (KM)	TRANS-LOSS (dB)	DISTANCE (KM)	TRANS-LOSS (dB)	DISTANCE (KM)	TRANS-LOSS (dB)
0.8000	-----114.41	16.8000-----150.25	32.8000-----160.75	48.8000-----168.12	64.8000-----174.50					
1.6000	-----121.11	17.6000-----151.09	33.6000-----161.16	49.6000-----168.46	65.6000-----174.80					
2.4000	-----125.19	18.4000-----151.90	34.4000-----161.56	50.4000-----168.79	66.4000-----175.10					
3.2000	-----128.21	19.2000-----152.70	35.2000-----161.95	51.2000-----169.13	67.2000-----175.40					
4.0000	-----133.65	20.0000-----153.32	36.0000-----162.34	52.0000-----169.46	68.0000-----175.70					
4.8000	-----132.71	20.8000-----153.86	36.8000-----162.73	52.8000-----169.78	68.8000-----176.00					
5.6000	-----134.52	21.6000-----154.38	37.6000-----163.11	53.6000-----170.11	69.6000-----176.30					
6.4000	-----136.15	22.4000-----154.89	38.4000-----163.49	54.4000-----170.44	70.4000-----176.59					
7.2000	-----137.63	23.2000-----155.39	39.2000-----163.87	55.2000-----170.76	71.2000-----176.89					
8.0000	-----138.99	24.0000-----155.88	40.0000-----164.24	56.0000-----171.08	72.0000-----177.18					
8.8000	-----140.27	24.8000-----156.36	40.8000-----164.61	56.8000-----171.40	72.8000-----177.47					
9.6000	-----141.47	25.6000-----156.84	41.6000-----164.97	57.6000-----171.72	73.6000-----177.76					
10.4000	-----142.61	26.4000-----157.30	42.4000-----165.33	58.4000-----172.03	74.4000-----178.05					
11.2000	-----143.65	27.2000-----157.75	43.2000-----165.69	59.2000-----172.34	75.2000-----178.24					
12.0000	-----144.73	28.0000-----158.20	44.0000-----166.05	60.0000-----172.66	76.0000-----178.63					
12.8000	-----145.75	28.8000-----158.64	44.8000-----166.40	60.8000-----172.97	76.8000-----178.91					
13.6000	-----146.65	29.6000-----159.08	45.6000-----166.75	61.6000-----173.28	77.6000-----179.20					
14.4000	-----147.62	30.4000-----159.50	46.4000-----167.09	62.4000-----173.59	78.4000-----179.49					
15.2000	-----148.52	31.2000-----159.53	47.2000-----167.44	63.2000-----173.89	79.2000-----179.77					
16.0000	-----149.40	32.0000-----160.34	48.0000-----167.78	64.0000-----174.20	80.0000-----180.05					

Figure 4

Sample TROPOPLOT Output

--- SIGNAL STRENGTH VERSUS DISTANCE FOR GIVEN SYSTEM PARAMETERS ---

DISTANCE (KM)	SIG-STRENGTH (dBm)	DISTANCE (KM)	SIG-STRENGTH (dBm)	DISTANCE (KM)	SIG-STRENGTH (dBm)	DISTANCE (KM)	SIG-STRENGTH (dBm)
0.8000----	-48.41	16.8600----	-84.25	32.8090----	-94.75	48.8000----	-102.12
1.6000----	-55.11	17.6500----	-85.99	33.6000----	-95.16	49.6000----	-102.46
2.4000----	-59.19	18.4000----	-85.50	34.4000----	-95.56	50.4000----	-102.79
3.2000----	-62.21	19.2000----	-86.70	35.2000----	-95.95	51.2000----	-103.13
4.0000----	-64.65	20.0000----	-87.32	36.0000----	-96.34	52.0000----	-103.46
4.8000----	-66.71	20.8000----	-87.86	36.8000----	-96.73	52.8000----	-103.78
5.6000----	-68.52	21.6000----	-88.38	37.6000----	-97.11	53.6000----	-104.11
6.4000----	-70.15	22.4000----	-88.89	38.4000----	-97.49	54.4000----	-104.44
7.2000----	-71.63	23.2000----	-89.39	39.2000----	-97.87	55.2000----	-104.76
8.0000----	-72.95	24.0000----	-89.88	40.0000----	-98.24	56.0000----	-105.08
8.8000----	-74.27	24.8000----	-90.36	40.8000----	-98.61	56.8000----	-105.43
9.6000----	-75.47	25.6000----	-90.84	41.6000----	-98.97	57.6000----	-105.72
10.4000----	-76.61	26.4000----	-91.30	42.4000----	-99.33	58.4000----	-106.03
11.2000----	-77.65	27.2000----	-91.75	43.2000----	-99.69	59.2000----	-106.34
12.0000----	-78.73	28.0000----	-92.20	44.0000----	-100.05	60.0000----	-106.66
12.8000----	-79.73	28.8000----	-92.64	44.8000----	-101.40	61.8000----	-106.97
13.6000----	-80.65	29.6000----	-93.08	45.6000----	-101.75	61.6000----	-107.28
14.4000----	-81.62	30.4000----	-93.53	46.4000----	-101.99	62.4000----	-107.59
15.2000----	-82.52	31.2000----	-93.93	47.2000----	-101.44	63.2000----	-107.89
16.0000----	-83.40	32.0000----	-94.34	48.0000----	-101.78	64.0000----	-108.20
						80.0000----	-114.05

* * * * * FOR A RECEIVER INPUT LEVEL OF -90.50 dBm. DISTANCE BETWEEN ANTENNAS CAN BE AT LEAST 24.00 KM

10

Figure 5

Sample TROPOPLOT Output

PLOT OF TRANS.-LCSS VERSUS DISTANCE

** NOTE ** TO FIND SIGNAL STRENGTH FROM GRAPH. SUBTRACT TRANS.-LCSS FROM 66.00

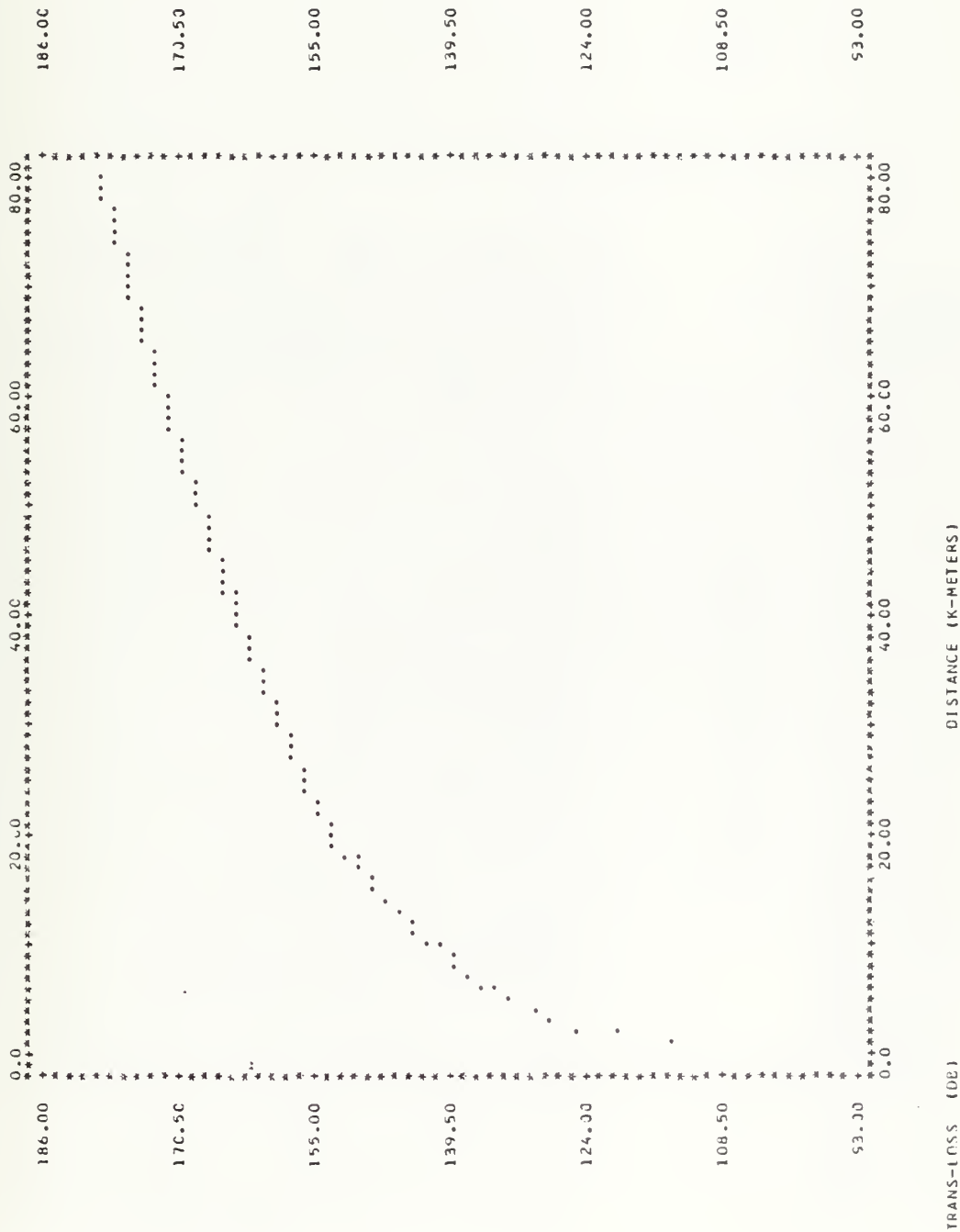


Figure 6

Sample TROPOPLOT Output

--- PROGRAM PARAMETERS ---

POLARIZATION (PCL)	-----	VERTICAL
FREQUENCY OF SIGNAL (F)	-----	100.00 MEG-HERTZ
SURFACE CONDUCTIVITY (S)	-----	0.01500 MH/OMETER
SURFACE REFRACTIVITY (NS)	-----	321.00 N-UNITS
SUM OF ELEVATION ANGLES (TE)	-----	3.1885 RADIAN
DISTANCE BETWEEN ANTENNAS (DIST)	-----	80.00 K-METERS
ATTENUATION BELOW FREE SPACE (A _B)	-----	43.57 DB
INTERDECILE RANGE OF TERRAIN HEIGHT (OH)	-----	580.00 METERS
SUM OF SMOOTH-EARTH HORIZON DISTANCES (CLS)	-----	19.44 K-METERS
DIFFRACTION ATTENUATION AT DISTANCE OLS (ALS)	-----	54.71 DB
PERMITTIVITY OR RELATIVE DIELECTRIC CONSTANT (E)	-----	2.00
ESTIMATED SCATTER ATTENUATION BELOW FREE SPACE (AES)	-----	95.45 DB
STRUCTURAL RECEIVER ANTENNA HEIGHT ABOVE GROUND (H2G)	-----	3.00 METERS
STRUCTURAL TRANSMITTER ANTENNA HEIGHT ABOVE GROUND (H1G)	-----	4.00 METERS
ESTIMATED DIFFRACTION ATTENUATION BELOW FREE SPACE (AEC)	-----	45.55 DB
COEFFICIENT THAT DEFINES SLOPE OF A SMOOTH CURVE OF ACR (K1)	-----	-0.51568 EB/KM
COEFFICIENT THAT DEFINES SLOPE OF A SMOOTH CURVE OF ACR (K2)	-----	-0.86222 DB/KM
SLOPE OF THE CURVE OF SCATTER ATTENUATION AS VERSUS DISTANCE (MS)	-----	-0.34735 DB/KM
DISTANCE WHERE DIFFRACTION AND SCATTER ATTENUATIONS ARE EQUAL (DX)	-----	230.35 K-METERS
ATTENUATION WHERE DIFFRACTION AND SCATTER ATTENUATION ARE EQUAL (ACX)	-----	-106.35 DB
SLOPE OF THE CURVE OF DIFFRACTION ATTENUATION AS VERSUS DISTANCE (MO)	-----	-0.24684 DB/KM
--- SIGNAL STRENGTH DATA INPUT ---		
TRANSMITTER POWER OUT	-----	100.00 WATTS
TRANSMITTER TRANSMISSION LINE LOSS	-----	2.00 DB
TRANSMITTER ANTENNA GAIN	-----	10.00 CB
RECEIVER SENSITIVITY	-----	-90.33 DBM
RECEIVER TRANSMISSION LINE LOSS	-----	2.00 CB
RECEIVER ANTENNA GAIN	-----	10.00 DB

Figure 7
Sample TROPOPLOT Output

In the process of describing these parameters a brief outline of how TROPOPLOT determines path loss is presented. A more detailed exposition can be found in Ref. 6. The median reference value of attenuation below free space, A_{cr} , is computed first. The reference value of transmission loss, L_{cr} , then becomes the sum of the free space attenuation, L_{bf} , and the reference attenuation, A_{cr} ,

$$L_{cr} = L_{bf} + A_{cr} \text{ dB.}$$

where the free space loss is defined as,

$$L_{bf} = 32.45 + 20 \log_{10} (f \text{ in MHz}) + 20 \log_{10} (d \text{ in km}).$$

The reference attenuation, A_{cr} , is determined using one of three subroutines depending on the particular mechanism of propagation; LOS for line of sight modes, DIFF for diffraction, and SCATT for tropo-scatter. Two ray optics is used to compute line of sight paths while diffraction paths are assumed to be over a double knife edge and a value of diffraction attenuation below free space, A_d , is computed. In the case of scattering the attenuation variable is designated as A_s . The reference attenuation A_{cr} is determined by the smaller value of A_d and A_s . In the line of sight case the attenuation is calculated for 2 values of distance (d_0, d_1) for which line of sight propagation is valid to produce corresponding values of attenuation A_0 and A_1 . The diffraction attenuation, A_{LS} , is computed at the distance

d_{LS} and together with A_0 and A_1 is used to determine the slopes, k_1 and k_2 , of a smooth curve of the reference attenuation versus distance over the range $1 \leq d \leq d_{LS}$

$$A_{cr} = A_0 + k_1(d-d_0) + k_2 \log_{10}(d/d_0) \text{ dB.}$$

The output parameter A_e is defined as

$$A_e = A_0 - k_1 d_0 - k_2 \log_{10} d_0 \text{ (i.e., } d=1)$$

so for $1 \leq d \leq d_{LS}$

$$A_{cr} = A_e + k_1 d + k_2 \log_{10} d$$

When the diffraction attenuation is computed the output variables A_{ed} and m_d come into consideration. The diffraction attenuation is computed as the weighted average of the diffraction attenuation over smooth earth, A_r , and the attenuation over a double knife edge surface, A_k , where

$$A_d = (1-w)A_k + wA_r \text{ dB}$$

A description of the method of weighting these estimators and calculating A_d and A_k is contained in Annex 3 to Ref. 6. The diffraction attenuation, A_d , is determined at two distances, d_3 and d_4 , in the far diffraction region, and a straight line through the points (A_3, d_3) and (A_4, d_4) is defined as

$$m_d = (A_4 - A_3)/(d_4 - d_3) \text{ dB/km} \quad (\text{slope})$$

and

$$A_{ed} = A_{fo} + A_4 - m_d d_4 \quad (\text{intercept})$$

where A_{fo} is a "clutter factor" (≤ 15 dB).

If the scatter attenuation is less than the diffraction attenuation, as is sometimes the case in trans-horizon paths where the distance d or the angular distance θ is large, then $A_{cr} = A_s$. When the product of d in kilometers and θ in radians is greater than 0.5, A_s is computed at large distances, d_5 and d_6 , and a straight line through the points (A_5, d_5) and (A_6, d_6) is defined as follows:

$$m_s = (A_6 - A_5) / (d_6 - d_5)$$

and

$$A_{es} = A_5 - m_5 d_5.$$

As before the reference attenuation then becomes

$$A_{cr} = A_s = A_{es} + m_s d \quad d \geq d_x$$

The quantity d_x is defined as the distance where the scatter attenuation is equal to the diffraction attenuation.

It can be seen from the above description and Ref. 6 that the actual determination of the output quantities is somewhat complex and for most applications the information contained in the graphs and tables describing path loss and signal strength is sufficient. Consequently the data presented in the next sub-section will primarily consist of derivations from those portions of the output. If the quantities in

Fig. 6 are important to the user it should be noted that for certain input combinations the format statements contained in the TROPOPLOT program will produce an all asterisk, "*****", printout indicating that the format statement governing that particular variable requires modification.

B. ACTUAL PATH LOSS MEASUREMENTS

1. Procedure

In order to obtain the proper input parameters for entry into TROPOPLOT certain preliminary measurements and calculations were required. The first step was to obtain charts of the path area¹ and from these determine the terrain profile over a great circle path between transmitter and receiver. The great circle path was approximated by a rhumb line for path lengths less than 70 kilometers and the availability of 7½' topographic charts for the longer paths enabled the use of straight lines over the chart area. This profile information was plotted on a curved earth's surface using the plotting program described in Appendix A. The value of the surface refractivity used in determining the effective earth's radius was the same as that used in the input to the

¹To obtain a catalogue for U.S. Charts write to

Denver Distribution Section
U.S. Geological Survey
Denver Federal Center, Building 41
Denver, Colorado 80255

program and can readily be obtained from Ref. 9 or from actual meteorological data. If the charts of Bean et al. (1960) are used this value must be converted from N_o to N_s by the equation

$$N_s = N_o \exp(-0.1057 h_s)$$

The value of h_s used depends on several factors most important of which is the mode of propagation. For most of the paths considered herein the value of h_s chosen was determined by the elevation of the lowest antenna. For trans-horizon paths a mean N_s is computed using heights at the obstacle horizons. As was previously noted the values of N_s for input can range from 250 to 400 N-units, so it is obvious that predictions of path loss for anomalous conditions are not readily obtained using TROPOPLOT which is designed for long-term and median input parameters. The effects of non-standard atmospheric conditions along these paths are considered in Section III.

After plotting the path profile the required input parameters were determined using the methods described in Appendix B and a number of parameters were varied to produce the results described below.

2. Results

The output of the path profile/routine for each path considered is shown in Figs. 8-19 while the corresponding input parameters used are contained in Table I. All the links were analyzed for path loss at both VHF and S-band to

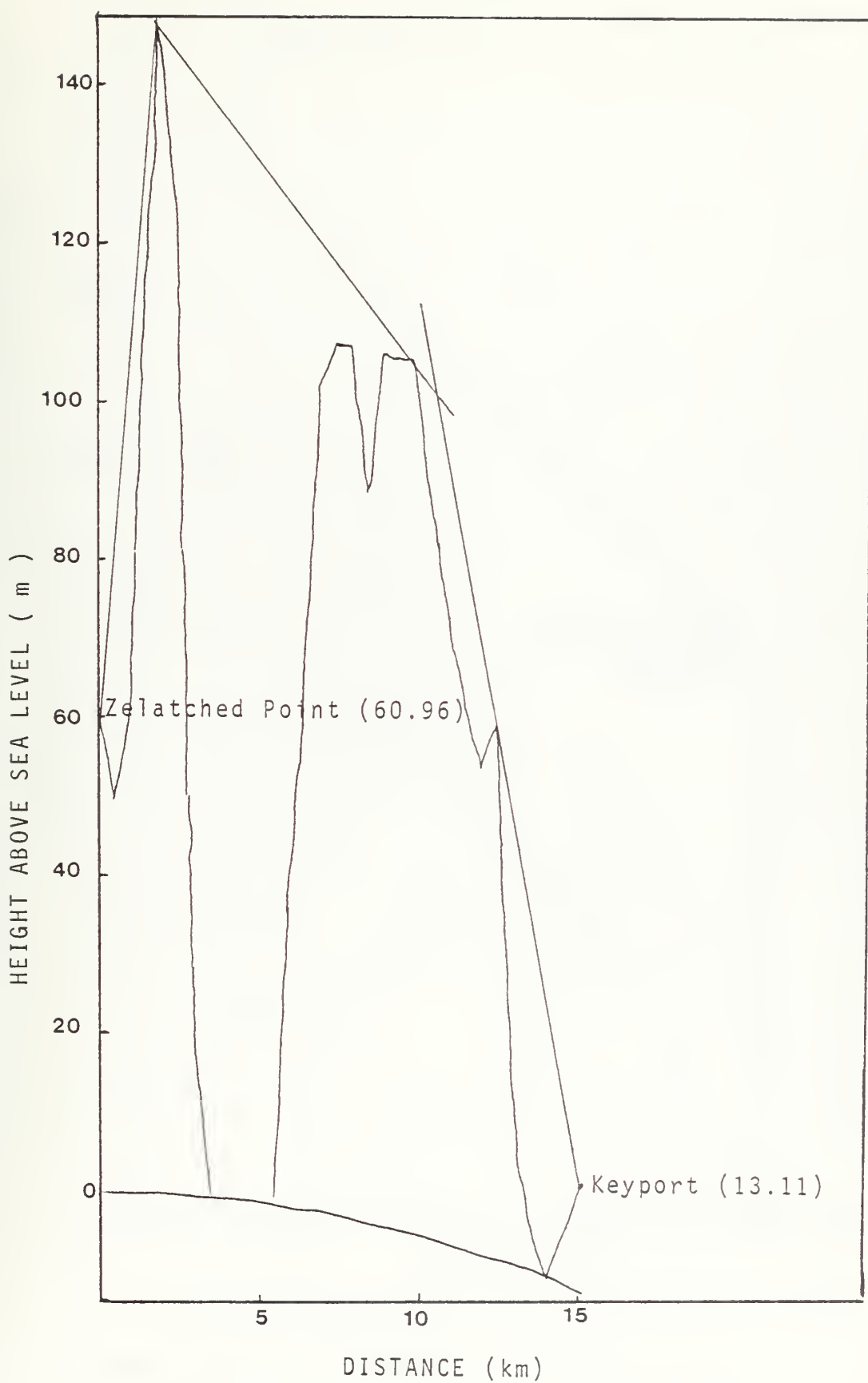


Figure 8

Terrain Profile for the Zelatched Point to Keyport Path

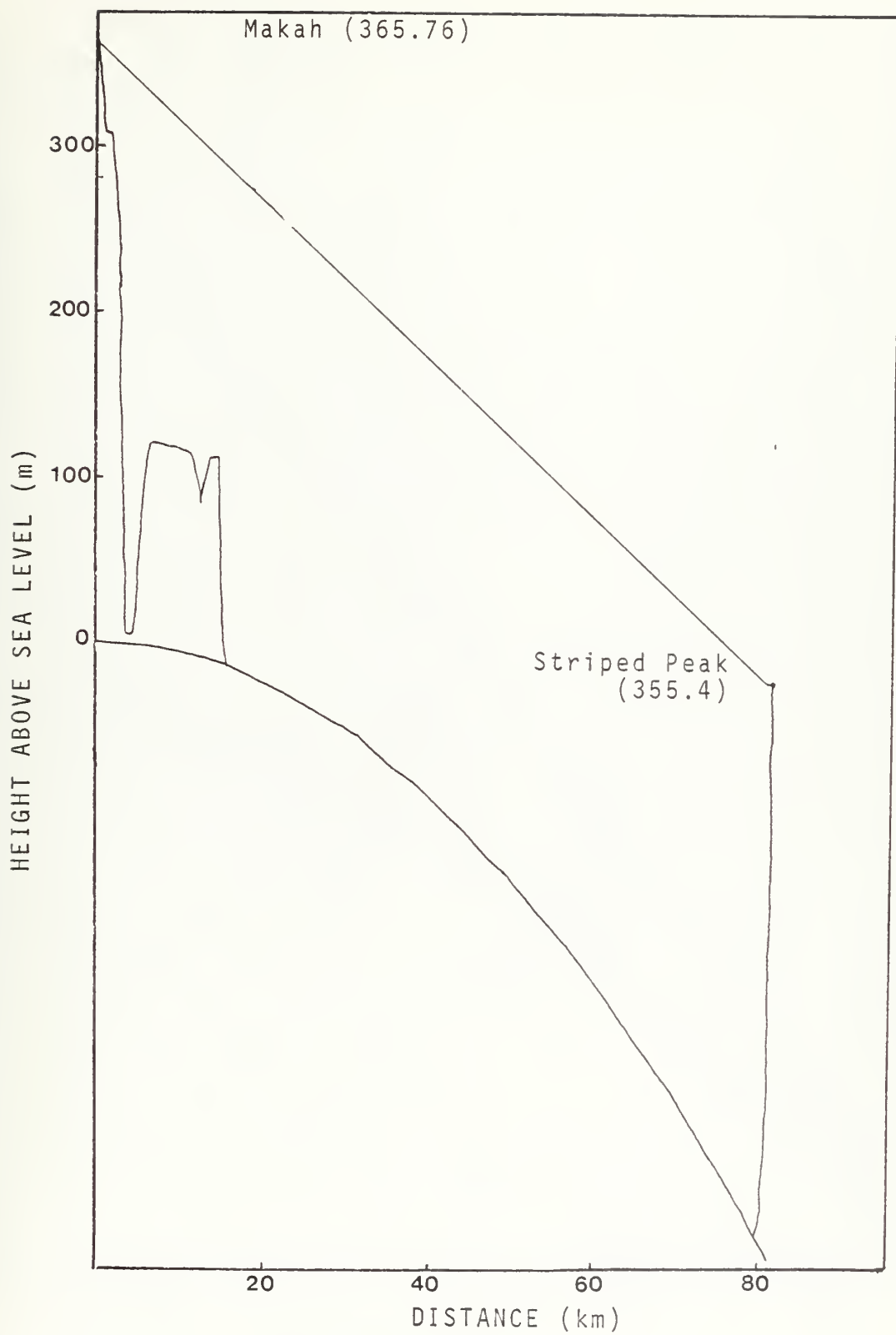


Figure 9

Terrain Profile for the Makah to Striped Peak Path

HEIGHT ABOVE SEA LEVEL (m)

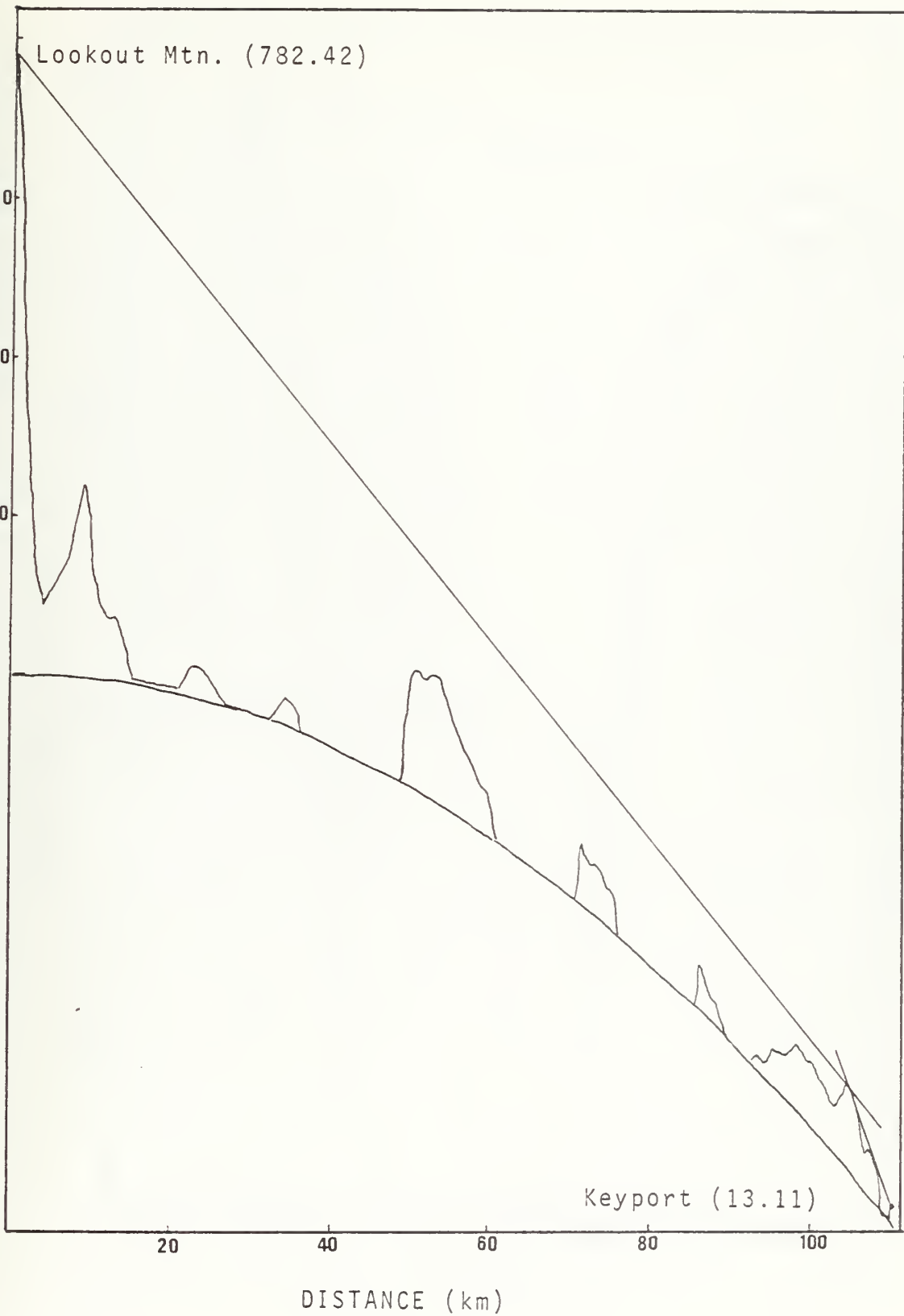


Figure 10

Terrain Profile for the Lookout Mt. to Keyport Path

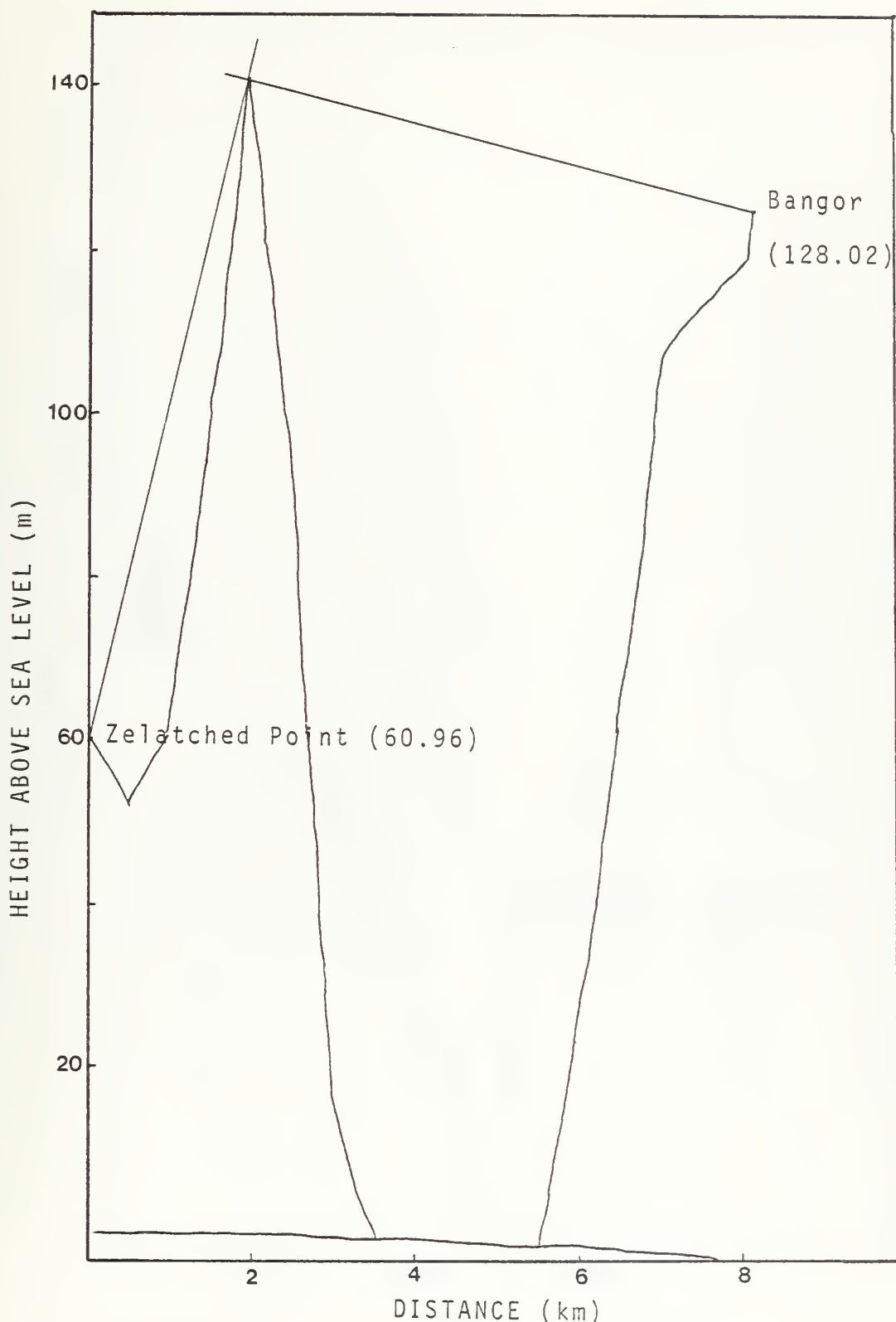


Figure 11
Terrain Profile for the Zelatched Point to
Bangor Path

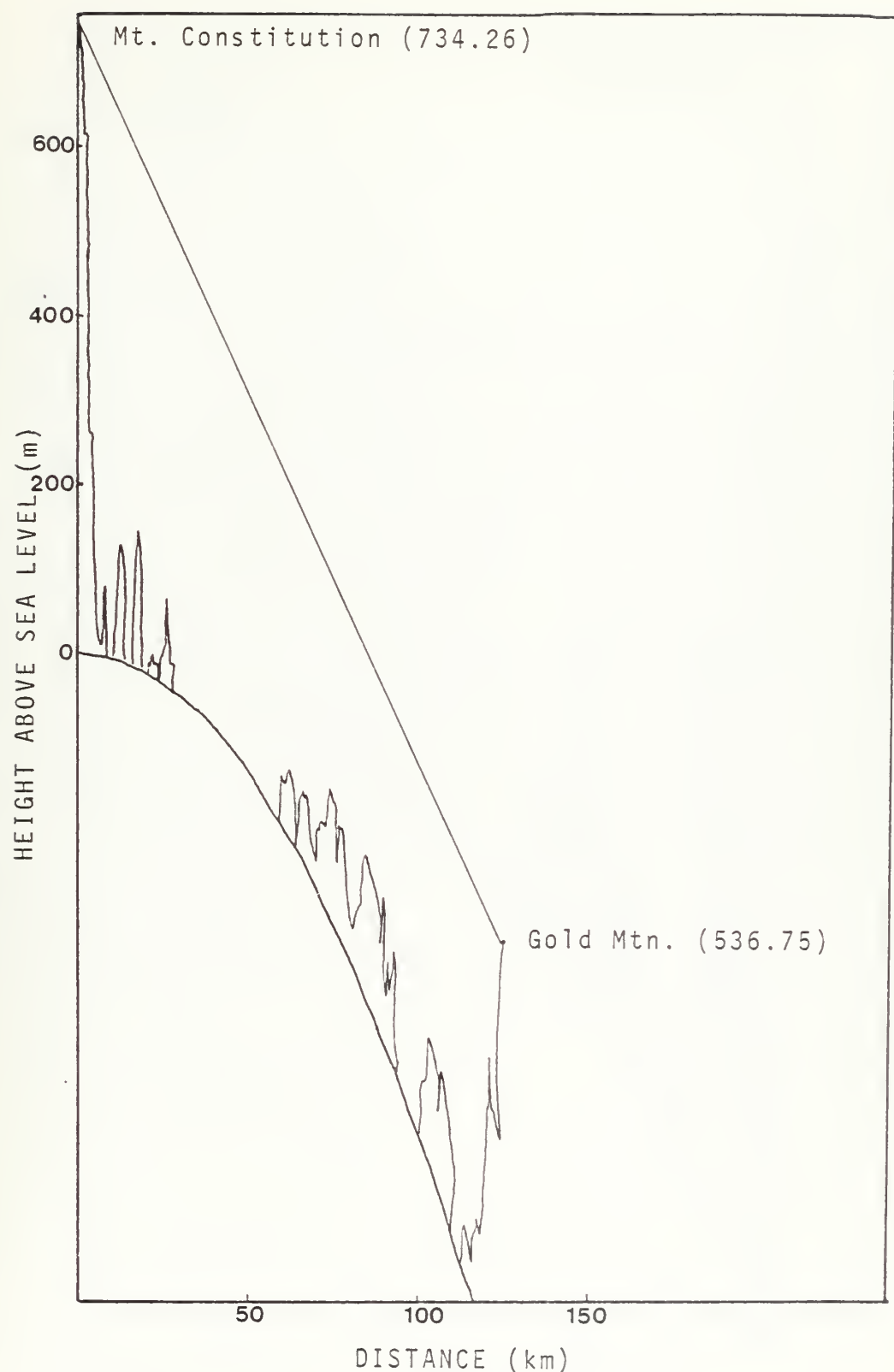


Figure 12
Terrain Profile for the Mt. Constitution to
Gold Mt. Path

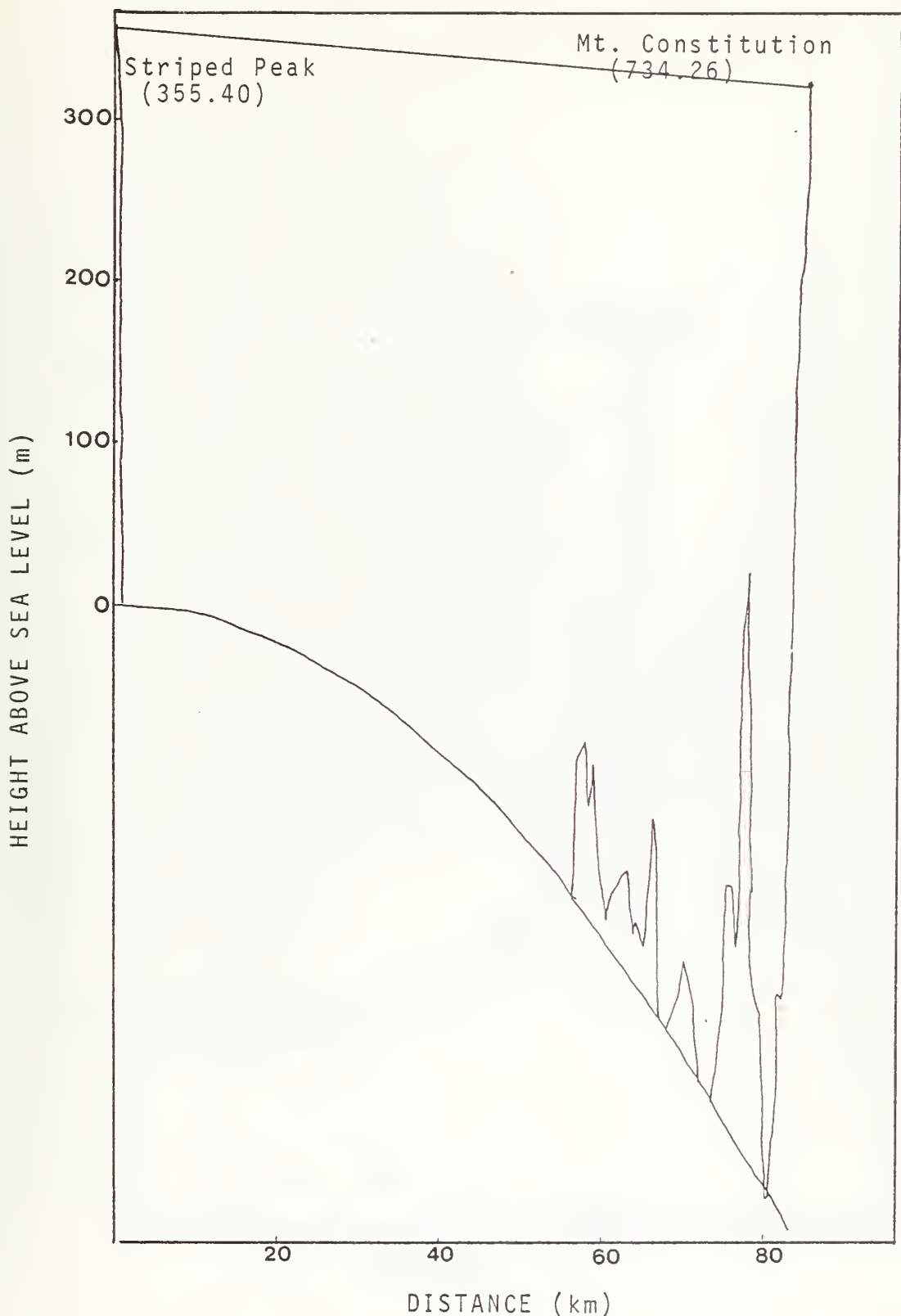


Figure 13
Terrain Profile for the Striped Peak to
Mt. Constitution Path

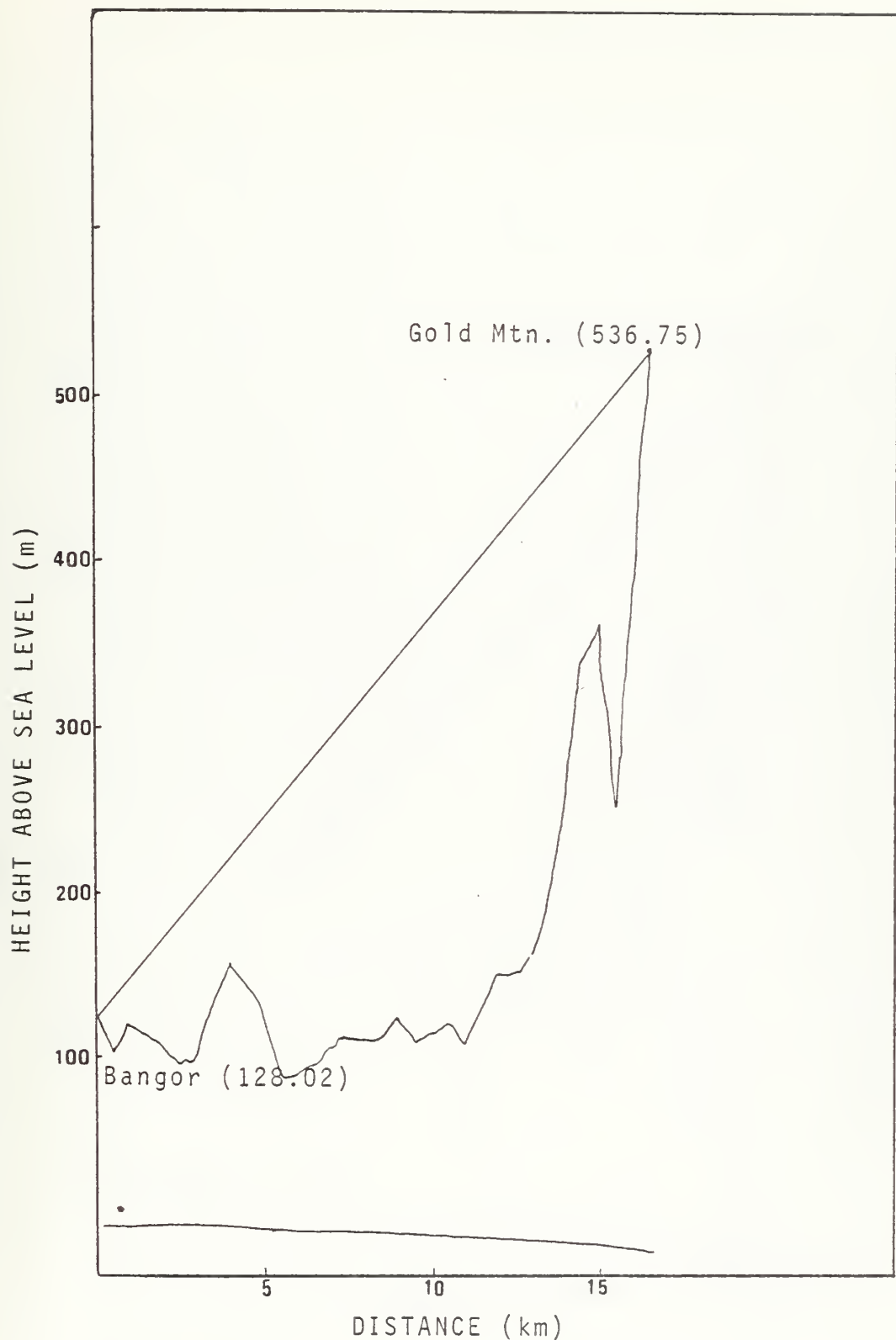


Figure 14
Terrain Profile for the Bangor to Gold Mt. Path

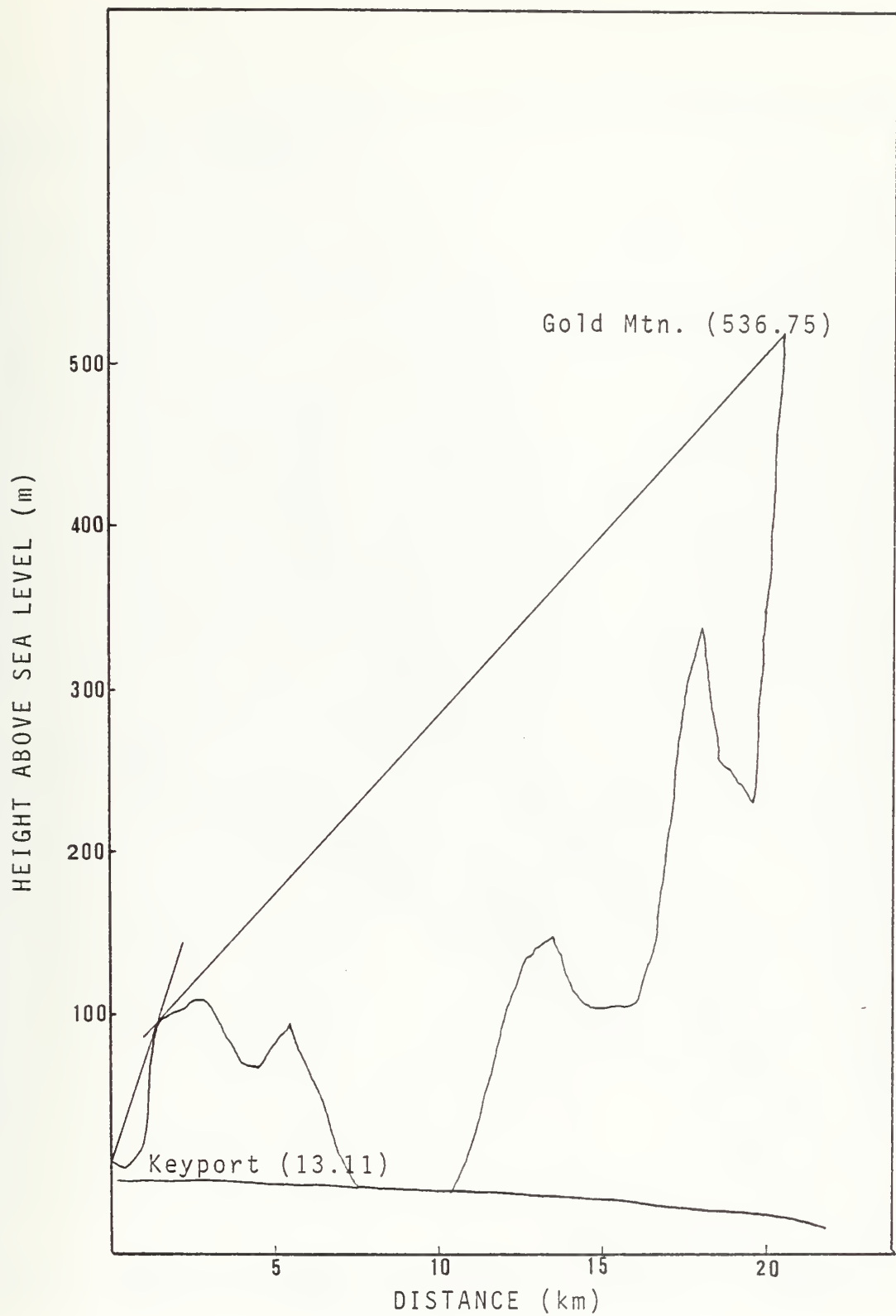


Figure 15
Terrain Profile for the Keyport to Gold Mt. Path

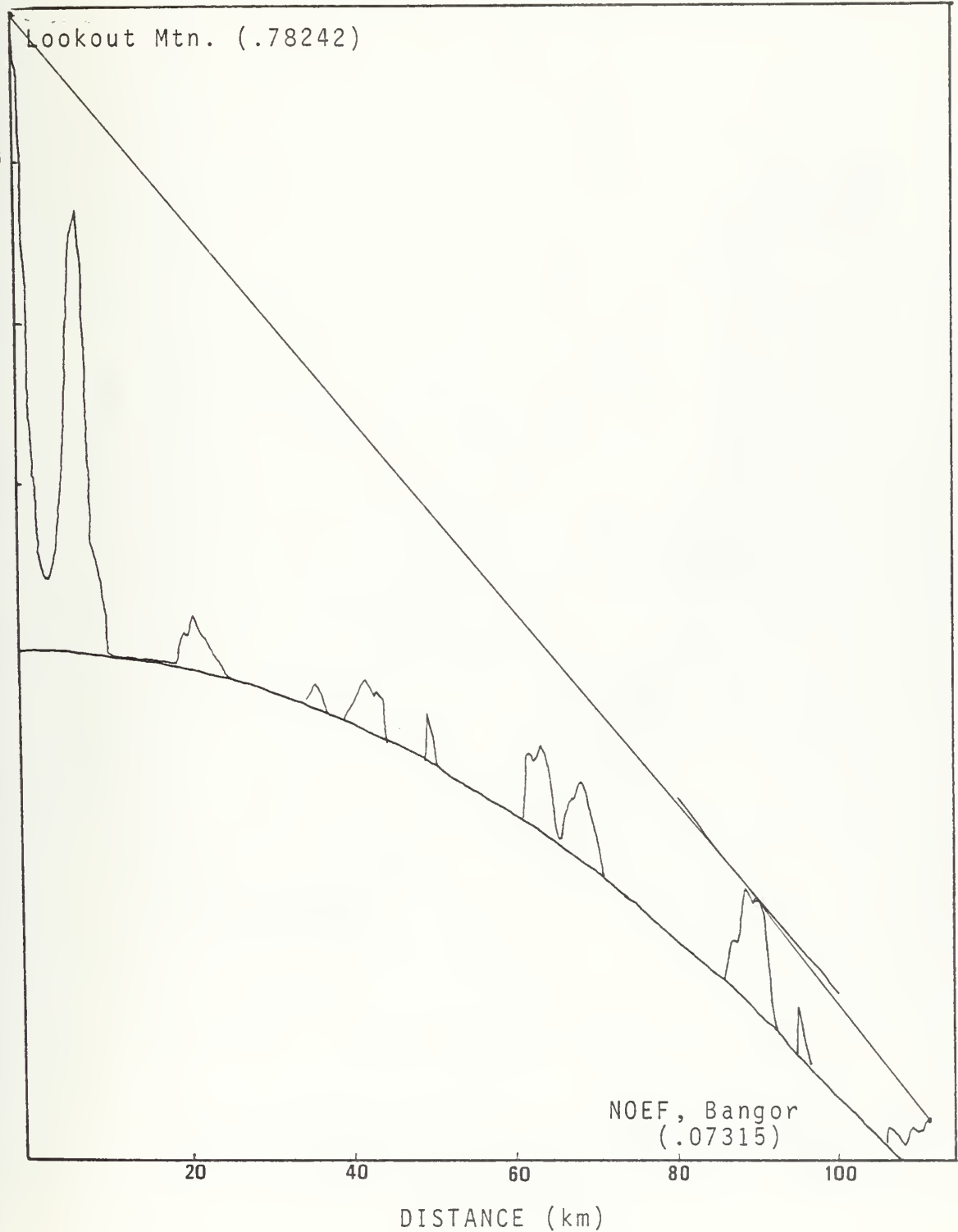


Figure 16
Terrain Profile for the Lookout Mt. to NOEF,
Bangor Path

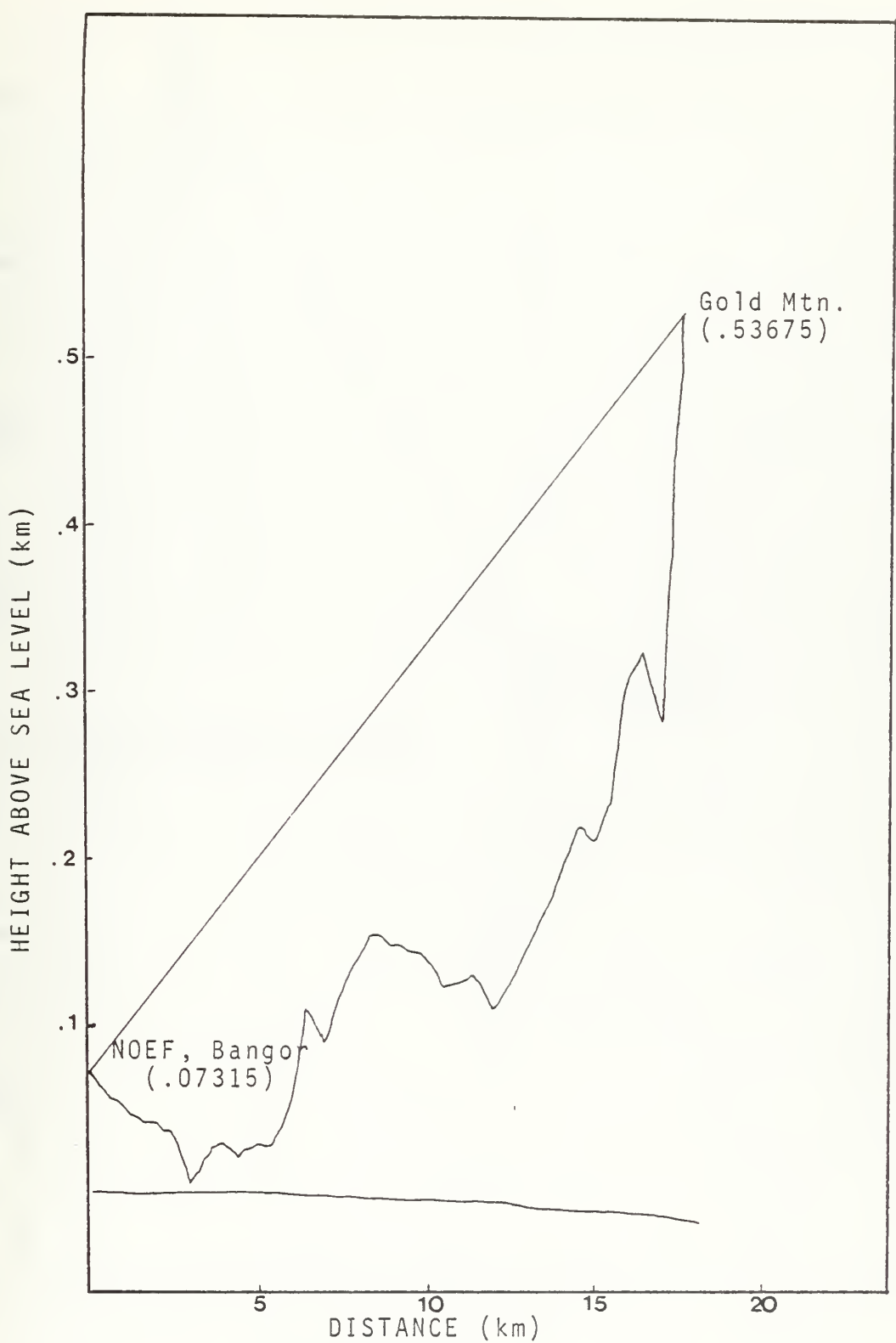


Figure 17

Terrain Profile for the NOEF, Bangor to Gold
Mt. Path

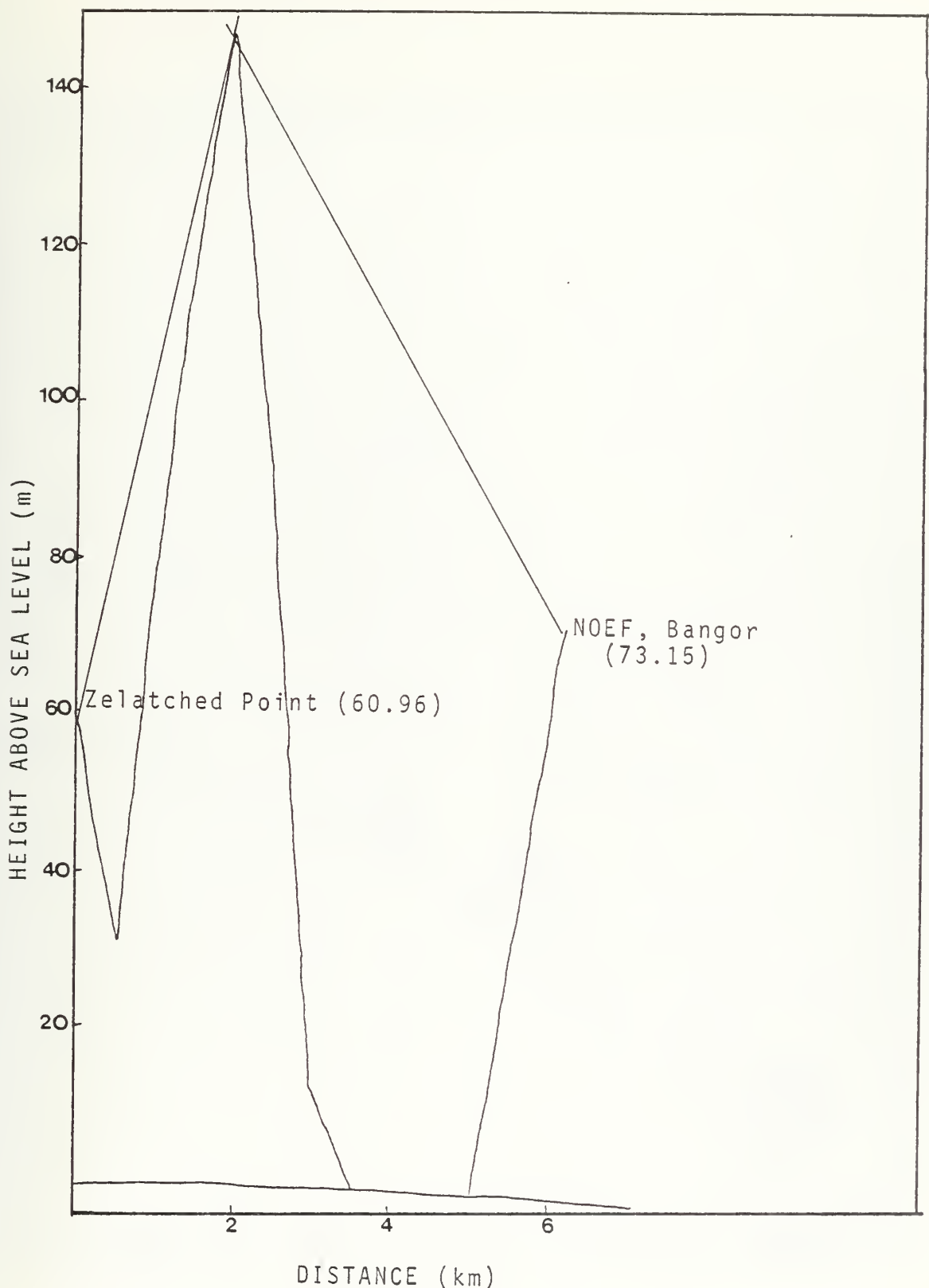


Figure 18

Terrain Profile for the Zelatched Point to NOEF,
Bangor Path

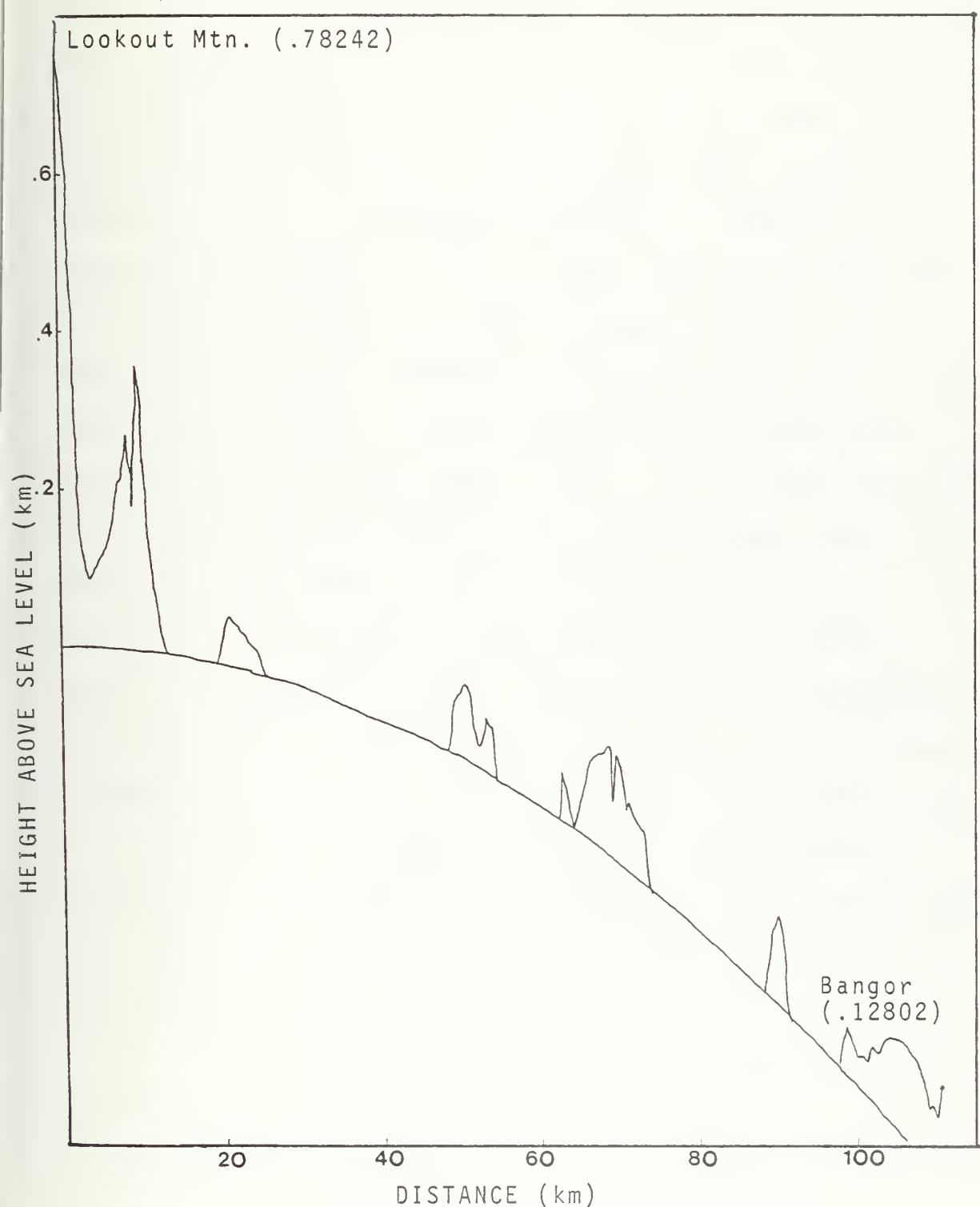


Figure 19
Terrain Profile for the Lookout Mt. to Bangor Path

illustrate the increase in path loss when frequency is increased. The results are shown in Figs. 20-31. The quantities (referred to in an above sub-section) which required interpretation as to the precise value to be used in detailed terrain studies are varied for a single path so that the effects of this variation can be shown. A sample path (Lookout Mt. to Keyport) was selected for this purpose and the effects of several different antenna heights in an unmodified version of TROPOPLOT are shown in Fig. 32. These same antenna heights are then entered into the modified program and the results shown in Fig. 33. To show the effects of variations in conductivity and permittivity σ and ϵ are varied over the same path with the results shown in Fig. 34. The effect of variations in the value of Δh is shown in Fig. 35. The quantity $\bar{\Delta h}$ was computed by taking the mean value of Δh over all the paths considered, Δh_t is the tabulated estimation of terrain irregularity found in both Ref. 6 and Ref. 7, Δh_r is the parameter computed by the methods of Appendix B. This comparison is intended to show the degree of precision required in choosing a parameter when uncertainty over the means of selection is present.

The importance of detailed path profile information is pointed up in the Zelatched Pt. to Keyport path (Fig. 8). If TROPOPLOT is used without modification, errors in prediction can occur at 2000 MHz the results of which are shown in Fig. 20. Note that this output predicts free space attenuation,

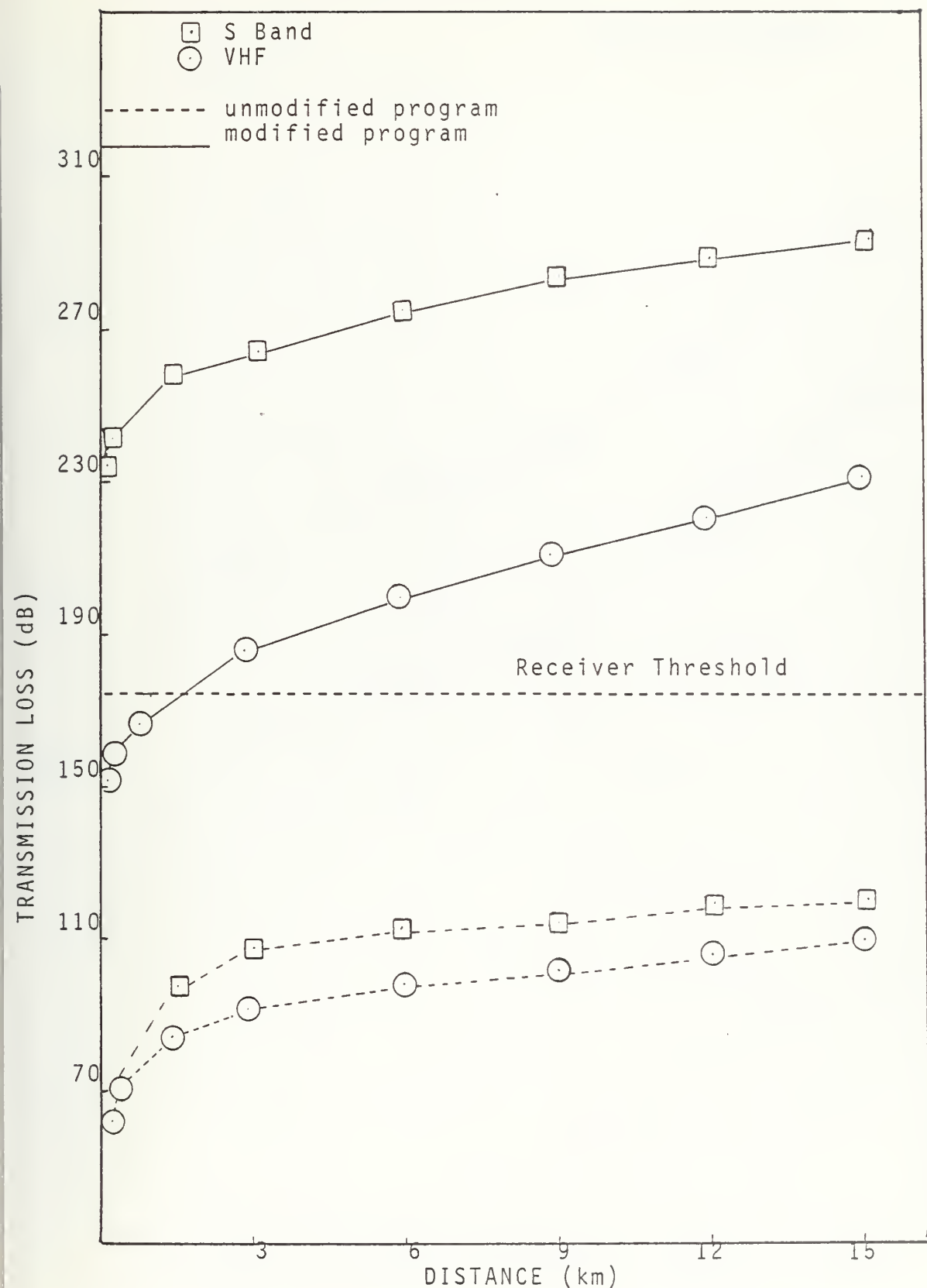


Figure 20
Transmission Loss vs. Distance for the Zelatched
Pt. to Keyport Path

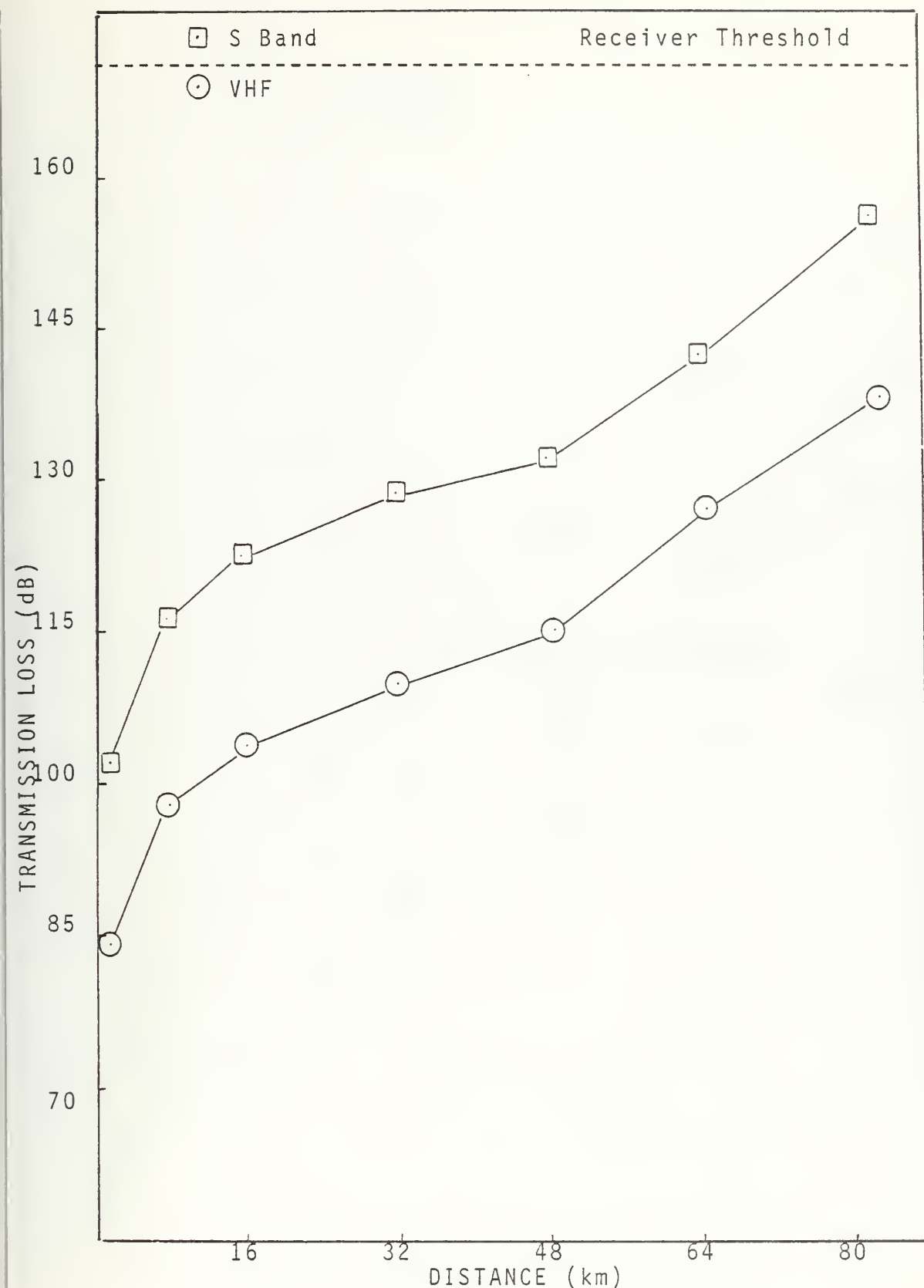


Figure 21

Transmission Loss vs. Distance for the Makah to
Striped Peak Path

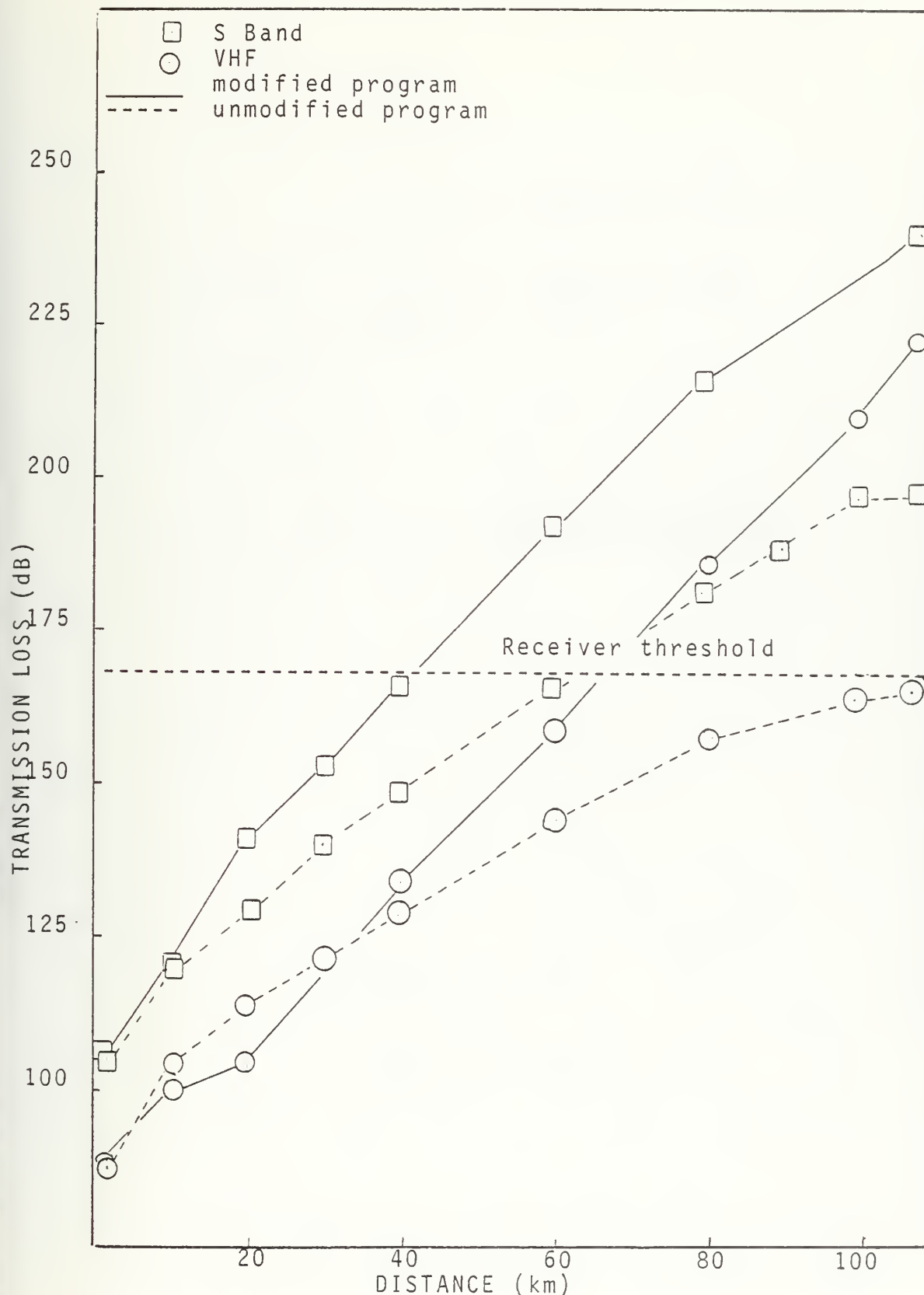


Figure 22
Transmission Loss vs. Distance for the Lookout Mt.
to Keyport Path

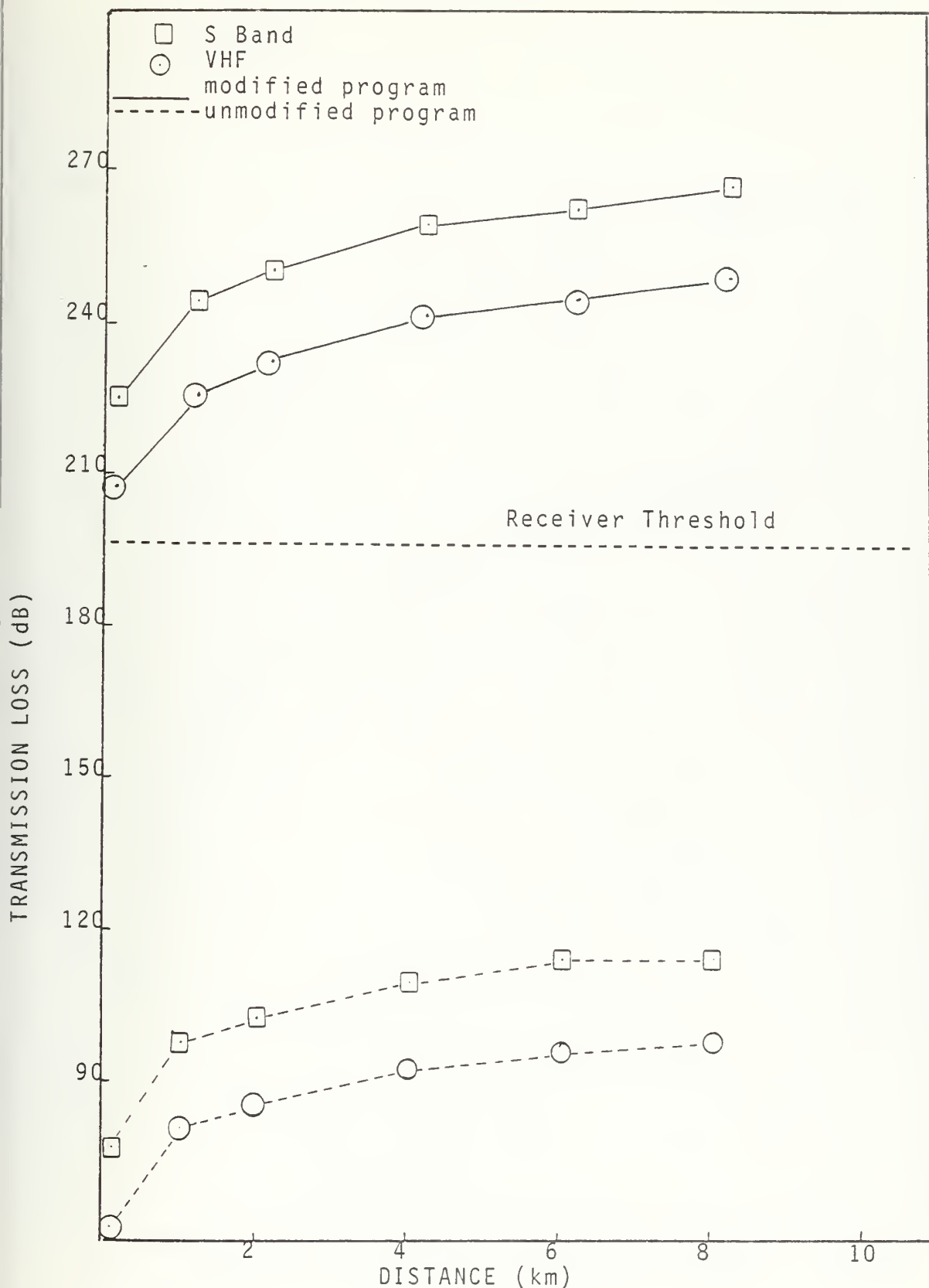


Figure 23

Transmission Loss vs. Distance for the Zelatched Point to Bangor Path

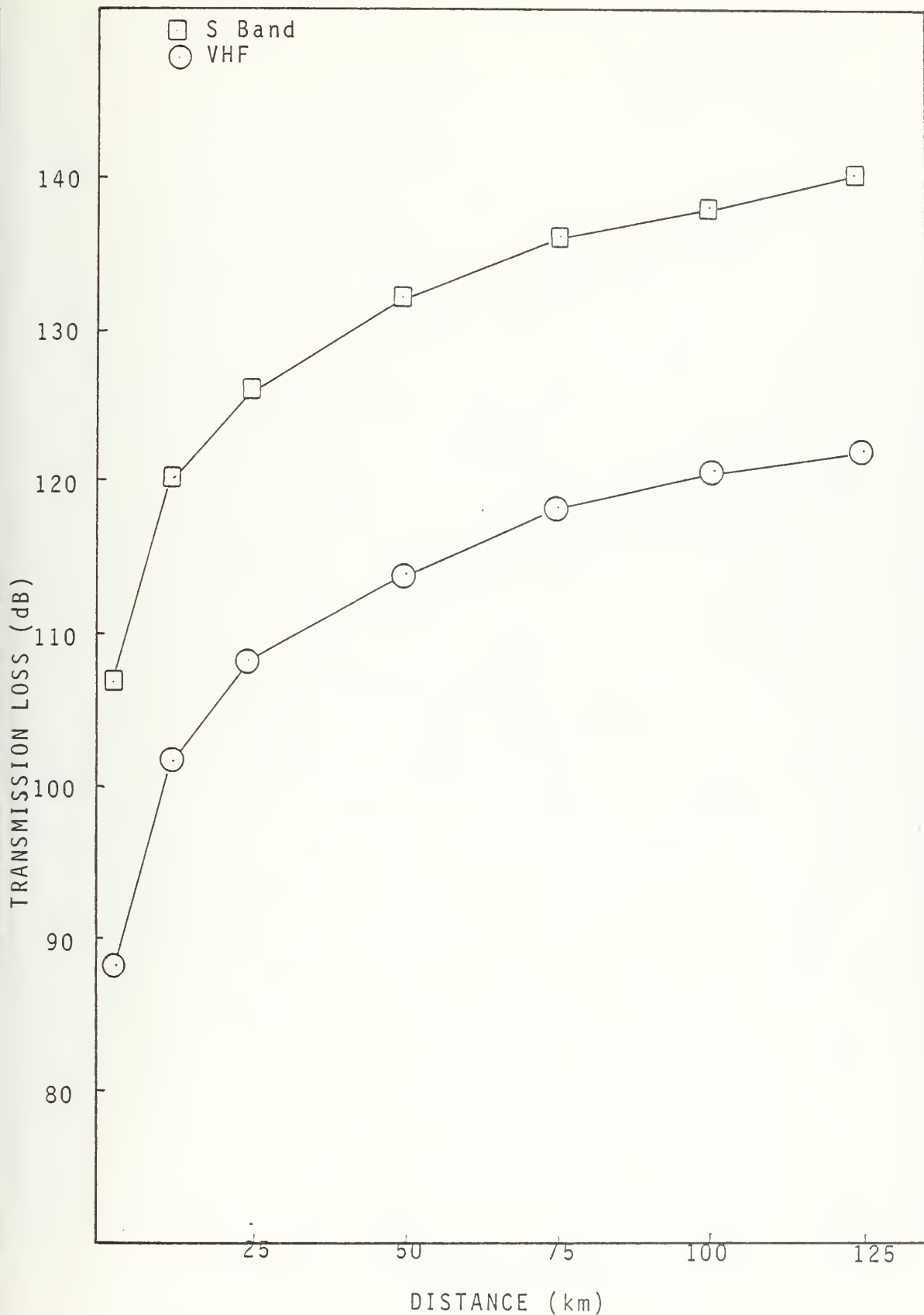


Figure 24

Transmission Loss vs. Distance for the Mt. Constitution
to Gold Mt. Path

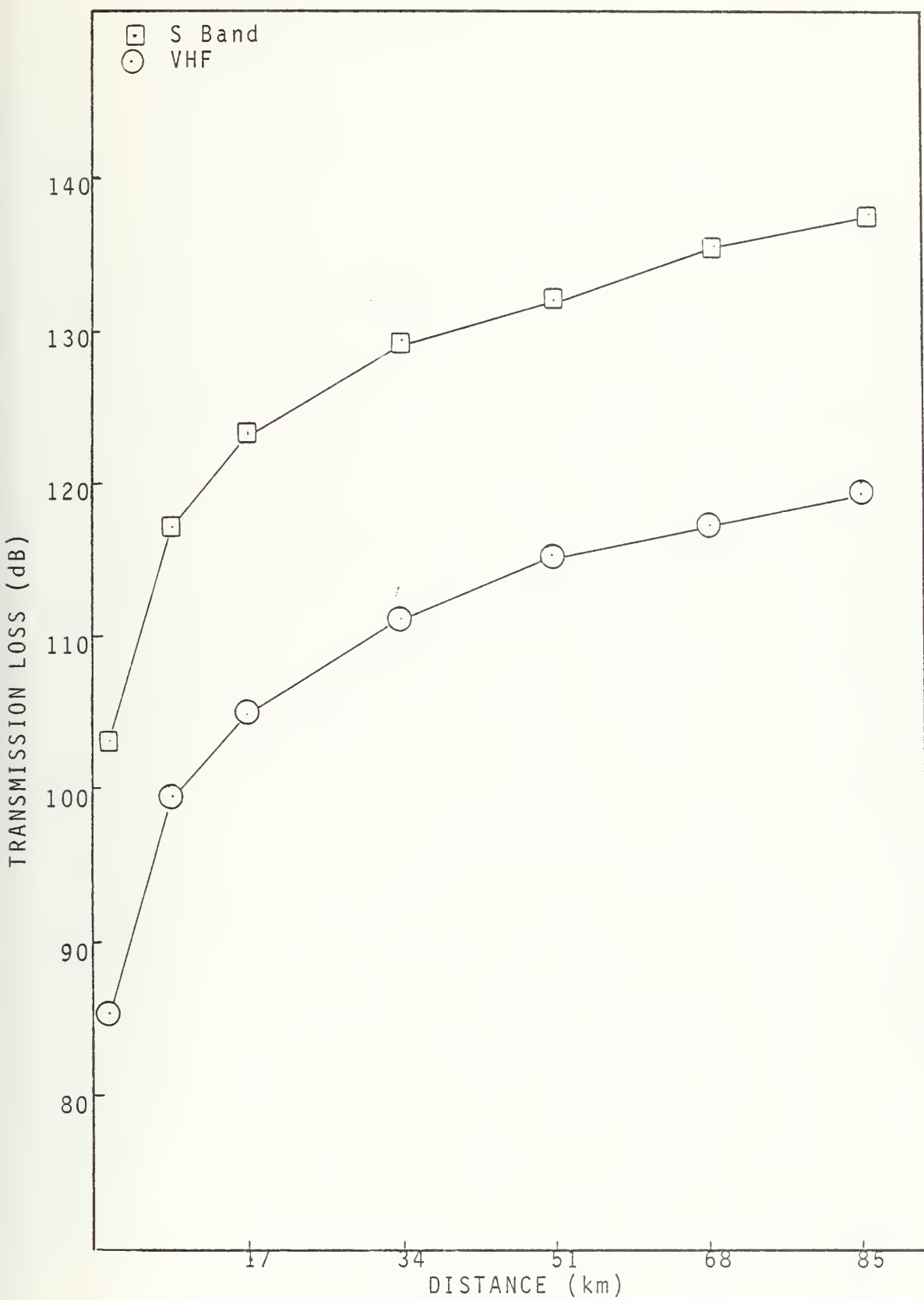


Figure 25

Transmission Loss vs. Distance for the Striped Peak to Mt. Constitution Path

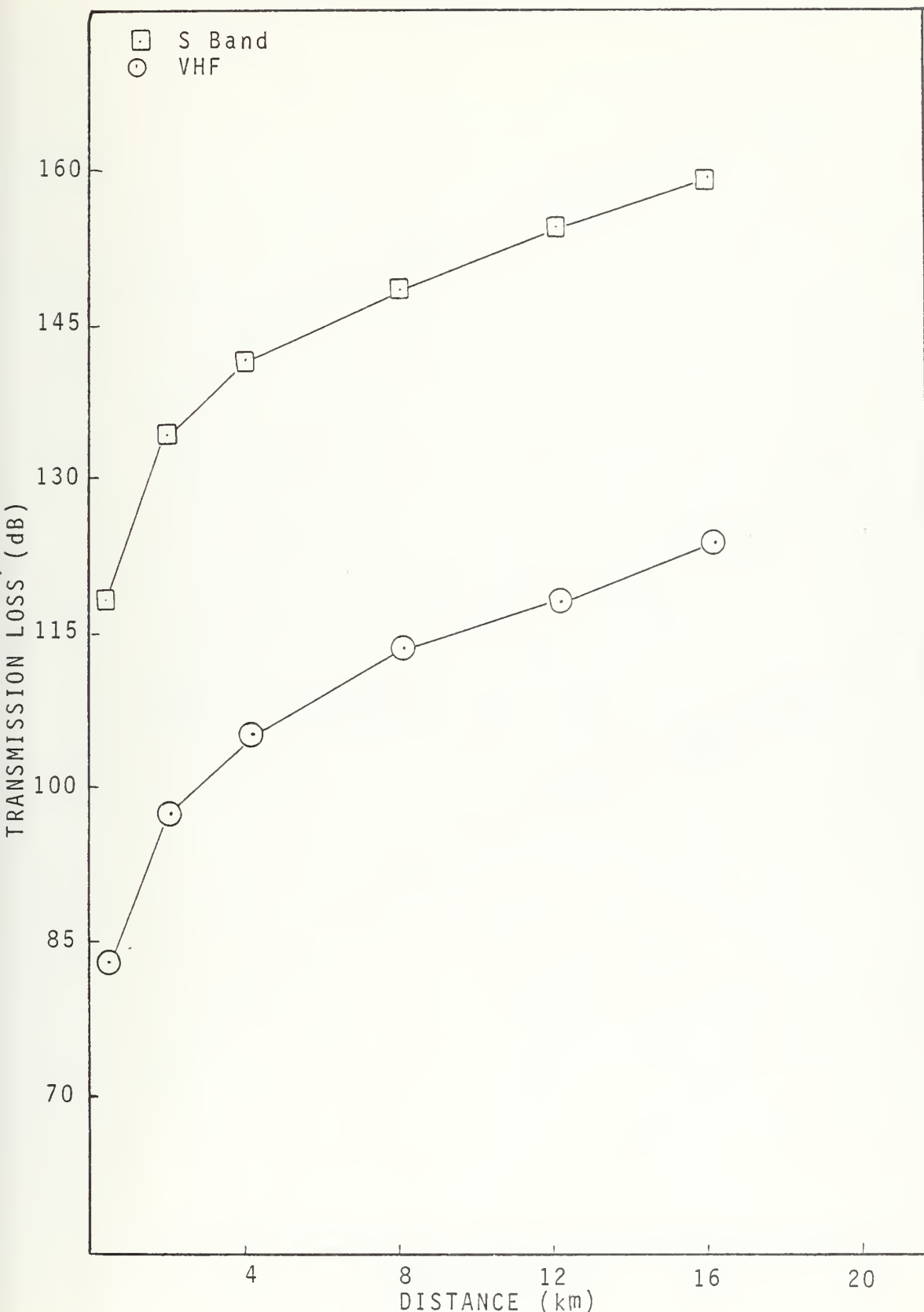


Figure 26

Transmission Loss vs. Distance for the Bangor to
Gold Mt. Path

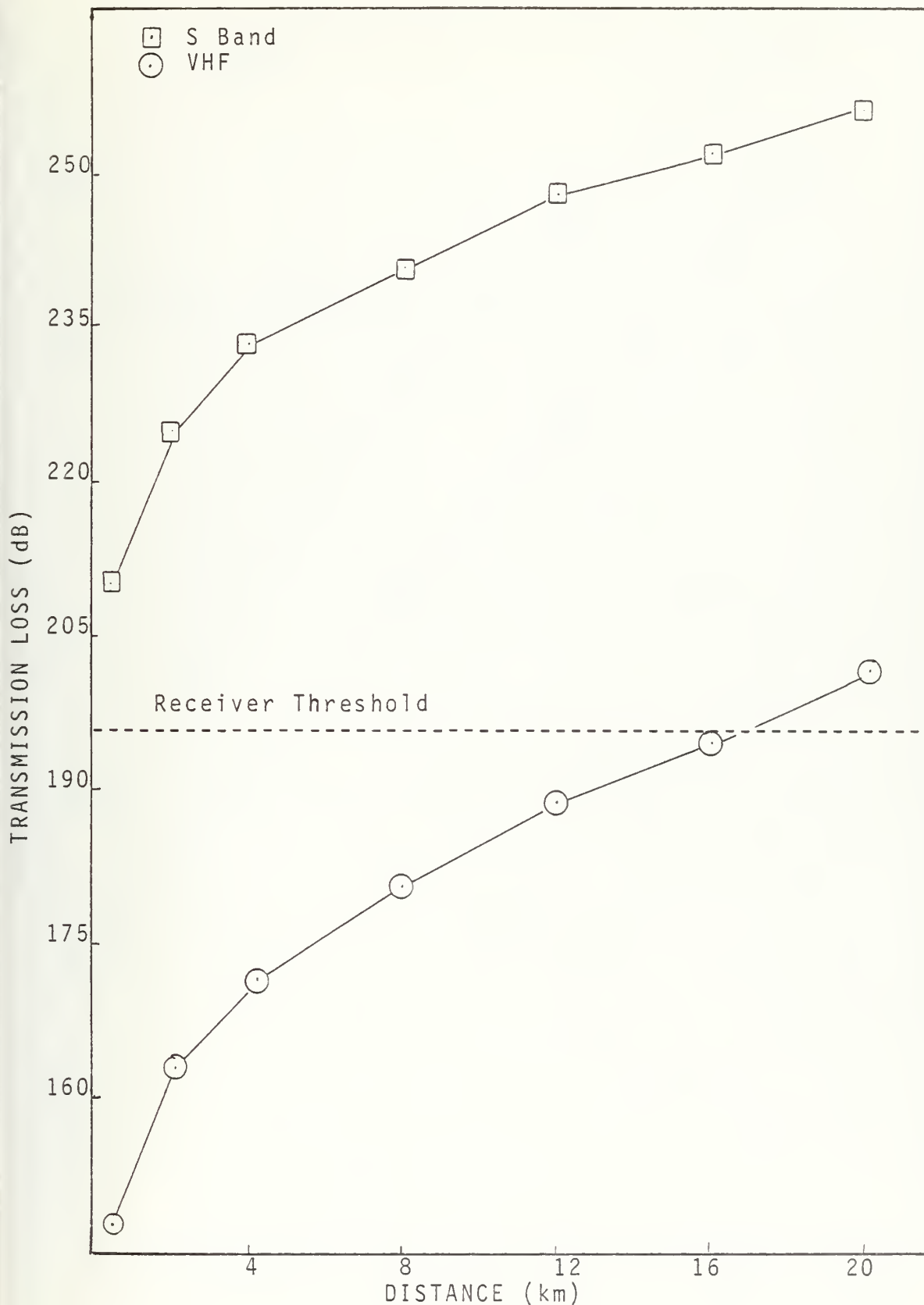


Figure 27

Transmission Loss vs. Distance for the Keyport
to Gold Mt. Path

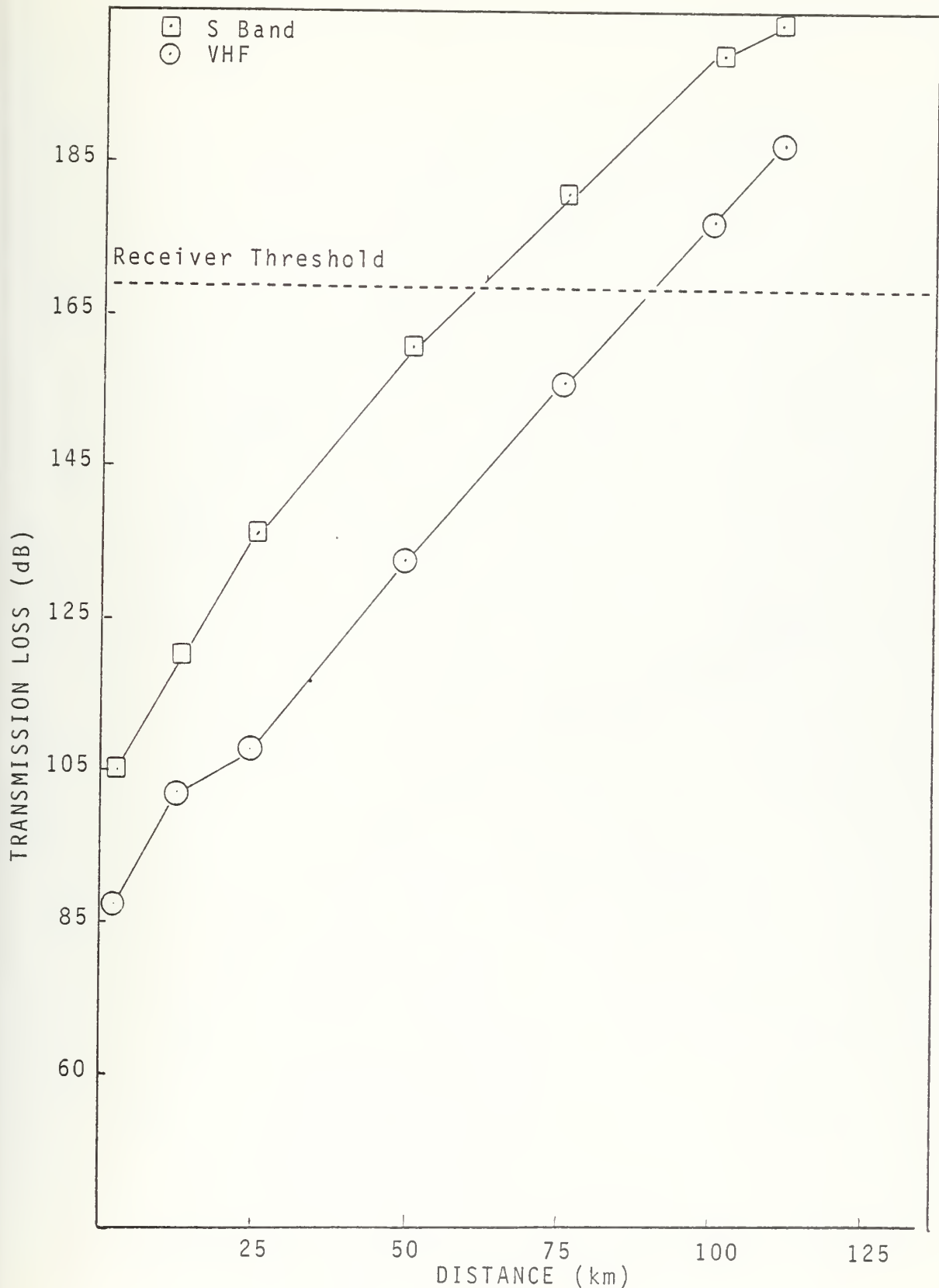


Figure 28

Transmission Loss vs. Distance for the Lookout Mt.
to NOEF, Bangor Path

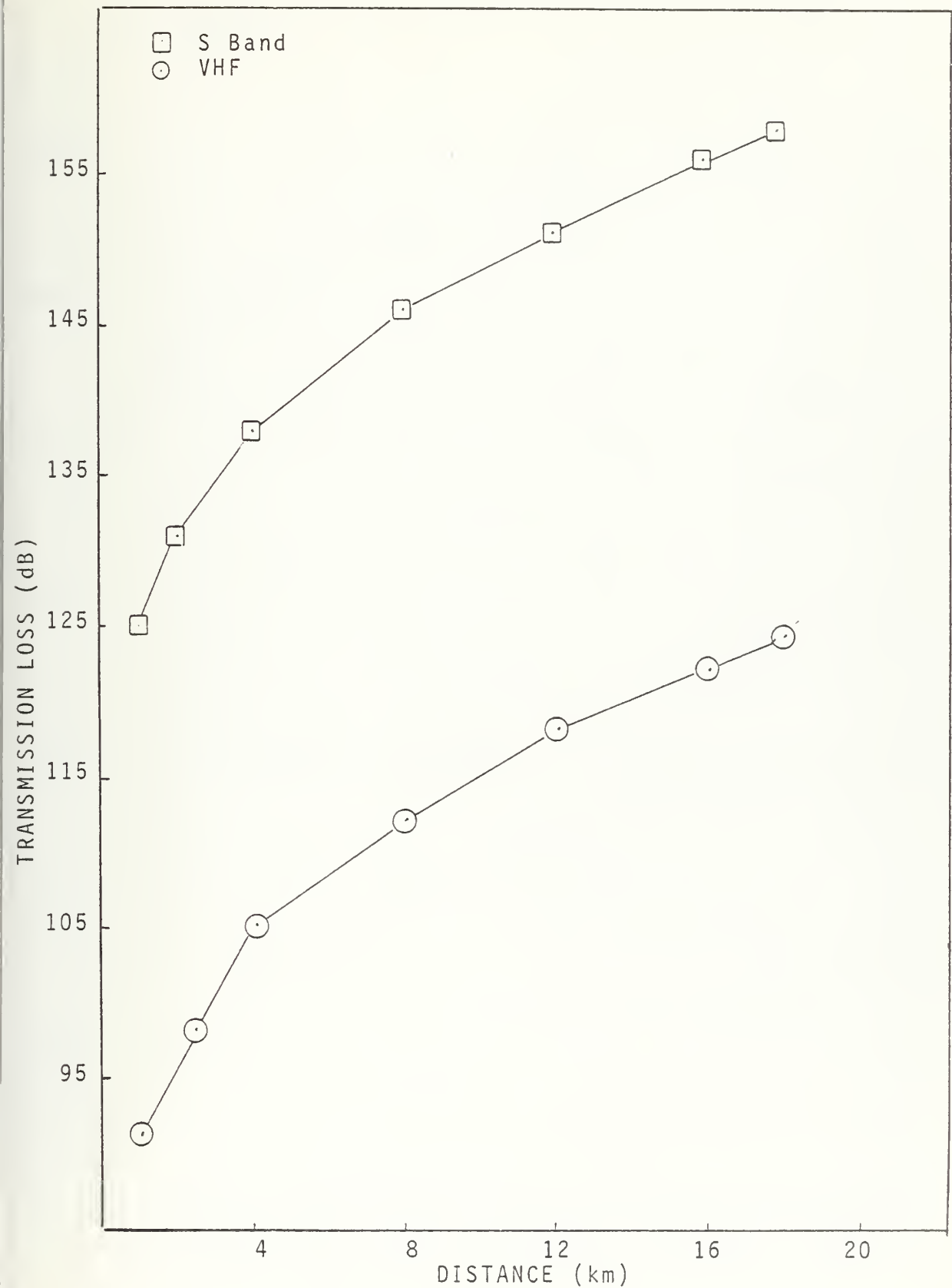


Figure 29

Transmission Loss vs. Distance for the NOEF,
Bangor to Gold Mt. Path

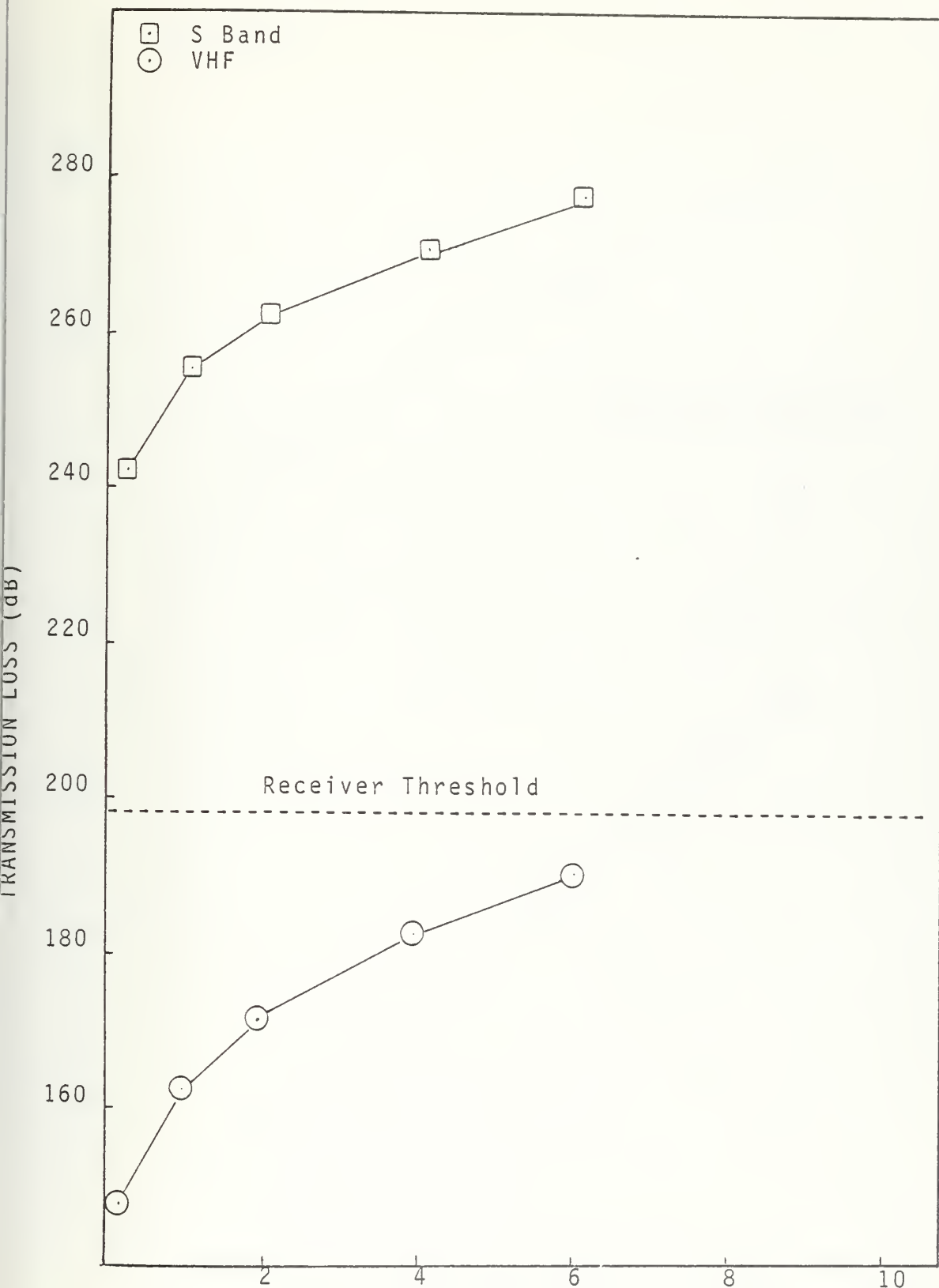


Figure 30

Transmission Loss vs. Distance for the Zelatched Point
to NOEF, Bangor Path

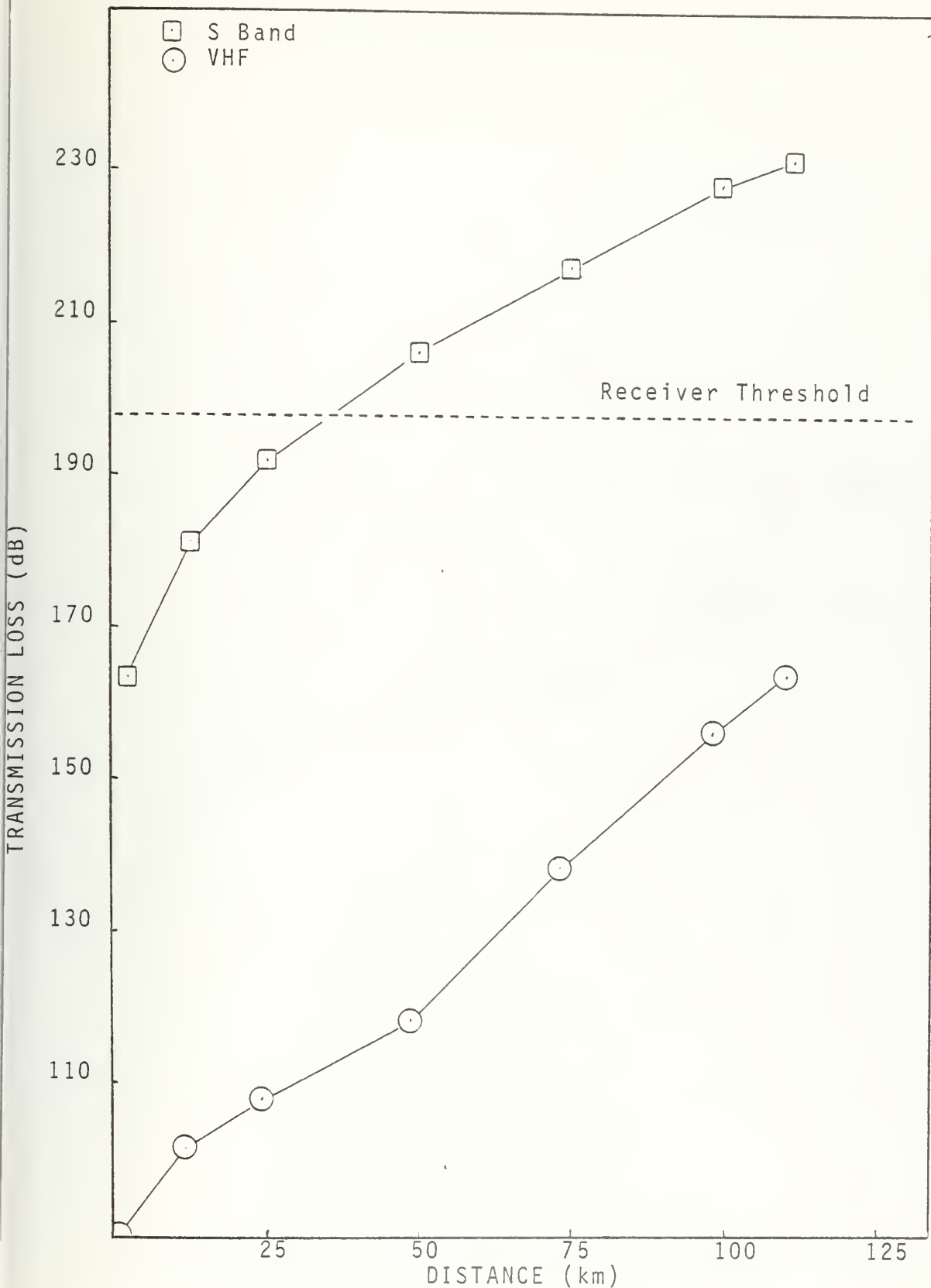


Figure 31
Transmission Loss vs. Distance the Lookout Mt.
to Bangor Path

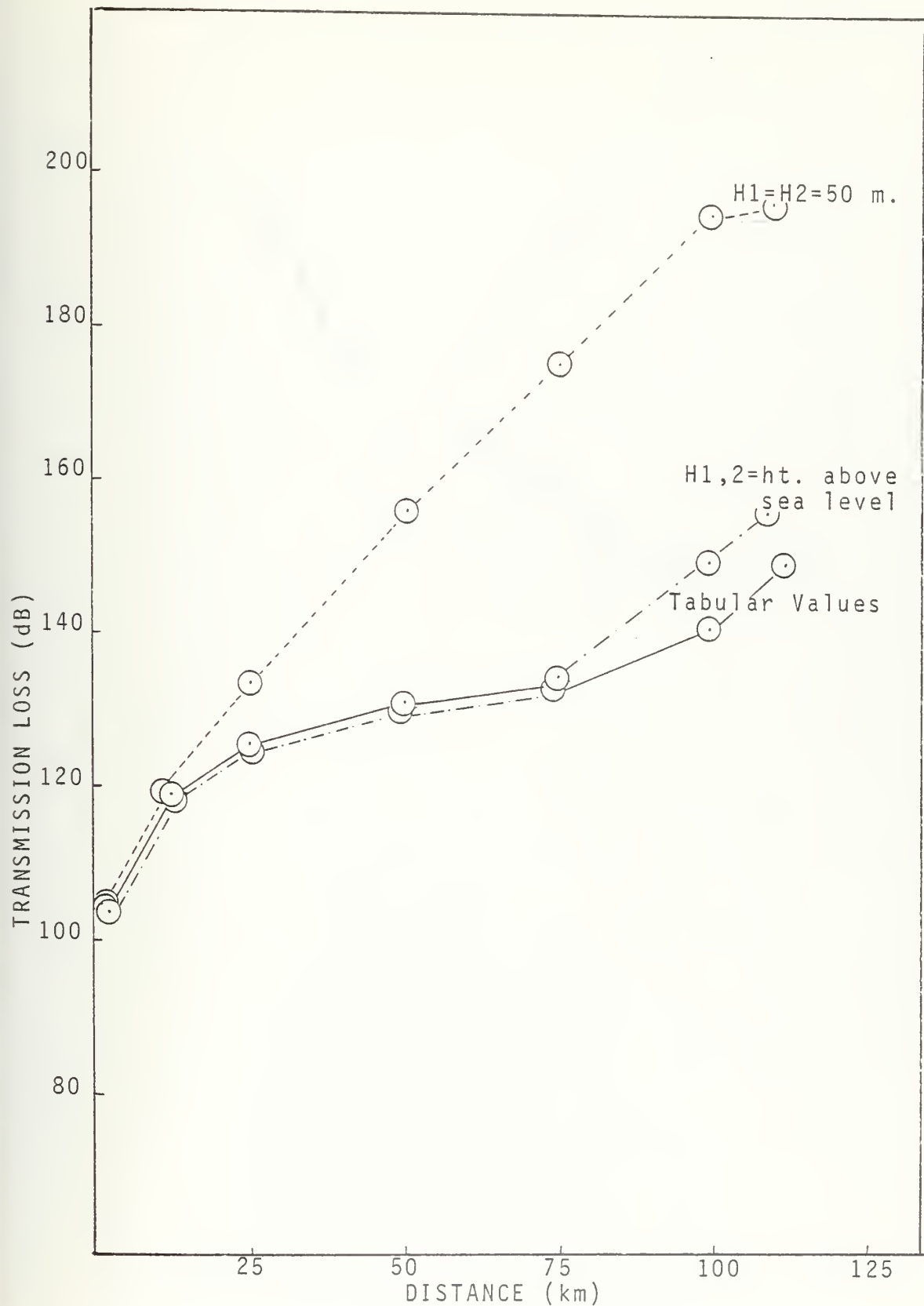


Figure 32

Antenna Height Variation for an Unmodified Version of TROPOPLOT
Transmission Loss vs. Distance

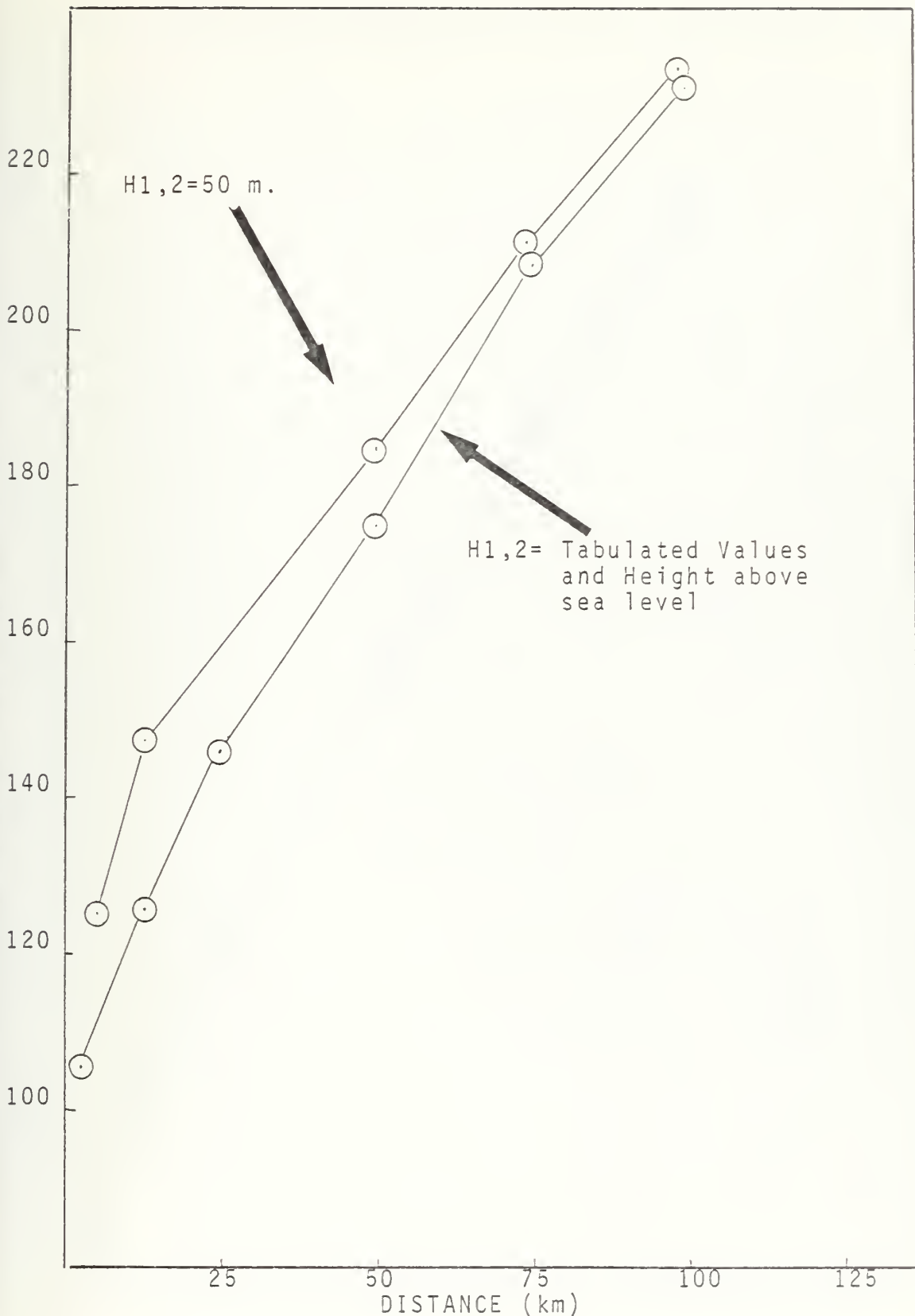


Figure 33

Antenna Height Variation for the Modified Version of TROPOPLOT
Transmission Loss vs. Distance

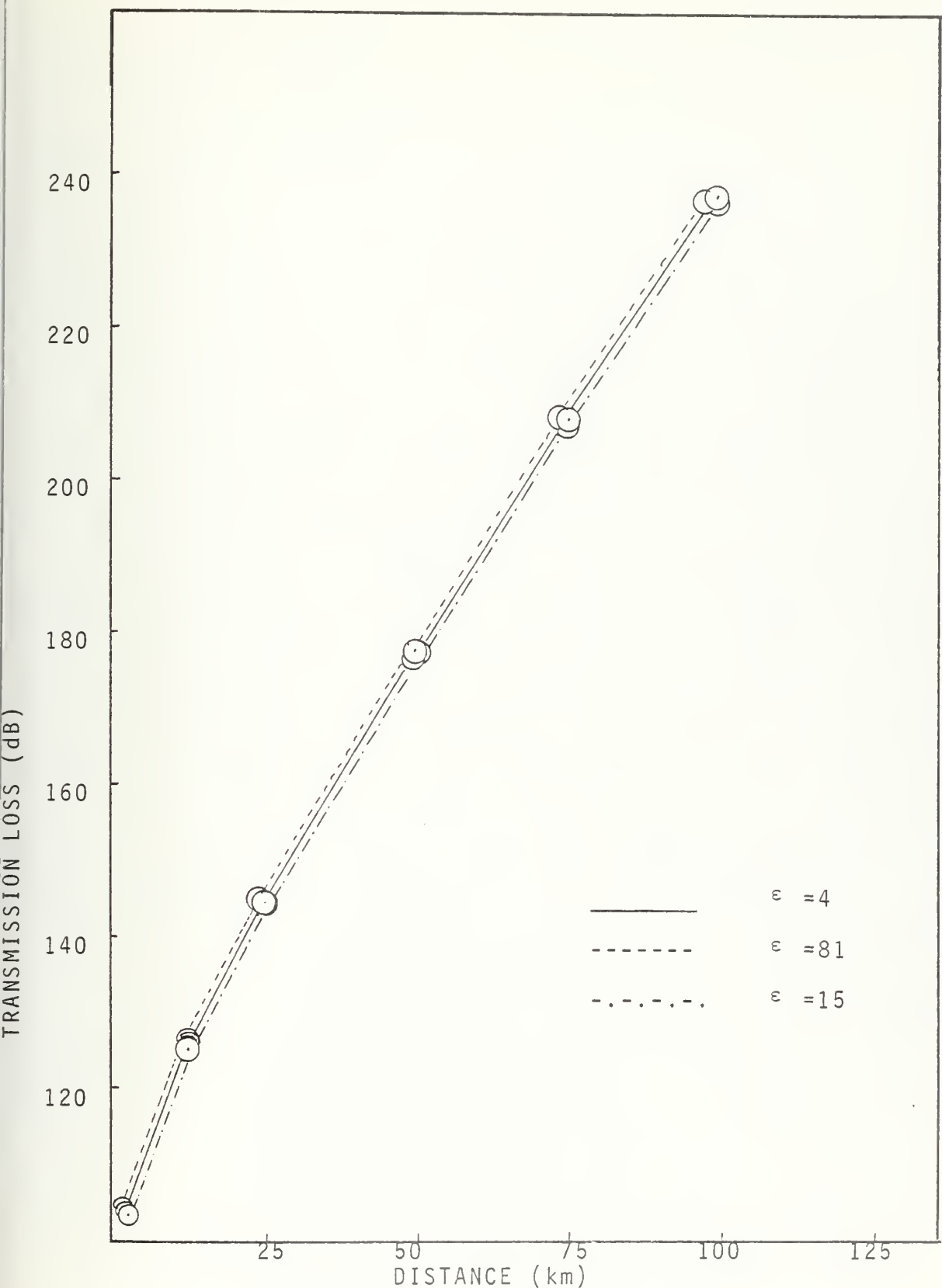


Figure 34

Variation in ϵ and σ for the Lookout to Keyport Path
Transmission Loss vs. Distance

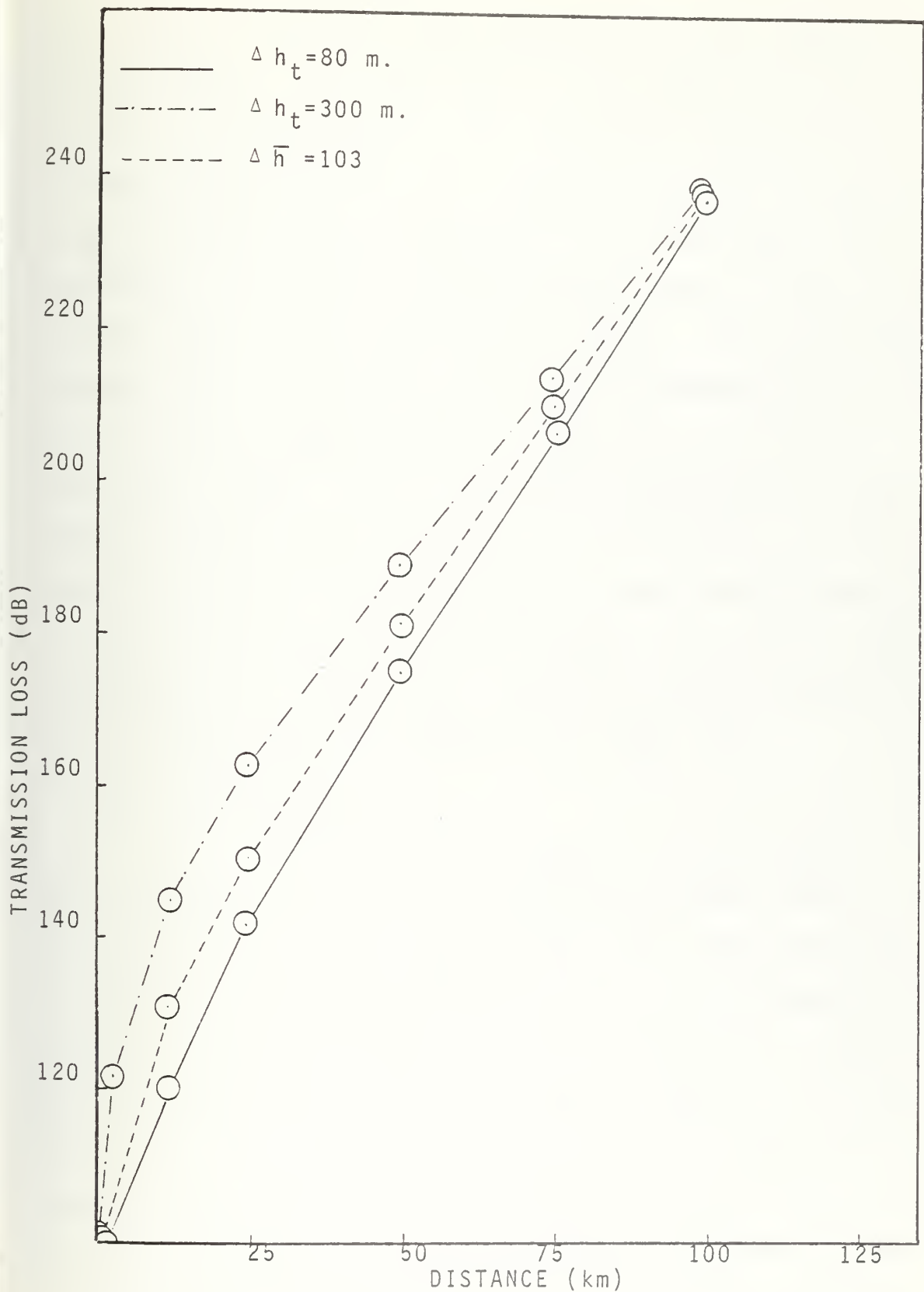


Figure 35

Variation in Δh for the Lookout Mt. to Keyport Path
Transmission Loss vs. Distance

when there is clearly a large attenuation of the signal by path obstacles. The same error can occur when the modified program is used; primarily due to the fact that the terrain is represented statistically. Large deviations from the range of terrain heights occurring in mid-path may not be considered as an obstacle by the program when in fact it is a major factor in the attenuation process. These smoothing effects can be alleviated somewhat by examining the terrain profile and performing graphical analysis, such as is described in Refs. 1-5, to check the effectiveness of the computer routine when its output is questionable. Another possible source of error can occur in short paths where only a single knife edge obstacle is present. In this case the predicted value of path loss is too high since a non-LOS path loss is calculated for a double knife edge case.

3. Conclusions

It is obvious that the quality of the output of this tropospheric propagation prediction program depends on which of several possible assumptions were made concerning the choice of input parameters. Clearly, if information is desired concerning a particular path or path area a path profile should be drawn and the ray path checked to insure that the values of the corresponding angles of elevation (depression) fall within the program constraints. As previously stated, if these values exceed the limits then TROPOPLOT must be modified and a detailed terrain profile obtained.

The effect of the variations of several of the parameters shown above allow some inferences to be drawn concerning the care with which the input variables must be chosen. It would seem from the path studied that variations of σ and ϵ have the least effect on path loss (<1 db), variations in Δh have only a small effect, particularly for longer distances, and variations in antenna height have the greatest effect on path loss. The unmodified version of the program appears more susceptible to these changes than the version modified to accept detailed profile information. The sensitivity of the transmission loss to antenna height value variation was alluded to in an earlier section and thus the suggestion that care be exercised in selecting these values is well taken if any degree of precision is desired. The detailed computation of Δh , on the other hand, is not necessary. By using the tabulated values corresponding to a particular type of terrain [Ref. 6] similar results can be obtained.

The transmission loss predictions seem to be accurate, or at least within an expected range of values except for short diffraction paths. In order to assess the goodness of the prediction, comparison with empirical data for these paths should be accomplished in a later study.

III. PROPAGATION IN A NON-STANDARD ATMOSPHERE

The computer analysis conducted in the previous section produced a long-term median attenuation value as output and consequently required that standard atmospheric conditions be assumed. In providing input under this assumption, the "standard" atmosphere for the locations under consideration was characterized by the median value of minimum monthly surface refractivity at sea level (N_0) corrected to emitter elevation. This element of the prediction routine could, in some cases, lead to an over-optimistic expectation of link performance, particularly in a locale where anomalous conditions frequently occur. One method of avoiding this potential source of error is to examine the statistical occurrence of these conditions and the severities of the effect of the anomalies on the link in question. For the purposes of this study the non-standard conditions dealt with involved the super-refractive, subrefractive and ducting cases. The statistics used in this determination were derived from IREPS output and the effects of non-standard refractivity were modeled by assuming certain values of effective earth's radius for corresponding conditions. Prior to the presentation of these results the theory involved in the anomalous propagation problem is reviewed.

A. THEORY

The primary medium through which electro-magnetic waves with wavelengths less than 1 or 2 meters propagate is the troposphere. This region, bounded below by the earth's surface and above by the tropopause, is approximately 10 km thick and is characterized by a general decrease in temperature with height up to a zone of constant temperature called the tropopause. The tropopause is not a static boundary, but has a height which is variable with both time and latitude.

The troposphere is usually assumed to be a lossless dielectric with $\mu = 1$ and $\sigma = 0$. The index of refraction, n , is then

$$n = \sqrt{\epsilon_r} \text{ atm.}$$

At the earth's surface n has been found to equal approximately 1.0003. Since air with a higher water vapor content has a larger value of permittivity, that is,

$$\epsilon_{\text{wet air}} > \epsilon_{\text{dry air}}$$

and since the lower atmosphere usually has the higher water vapor content, the permittivity of the atmosphere exhibits a decrease with height to a value of unity. This effect causes the refractive index to similarly decrease with height. It has been ascertained [Ref. 3] that for temperate climates the average variation near the ground is

$$\frac{dn}{dh} = -0.039 \times 10^{-6} \text{ per meter}$$

In order to avoid the use of such small numerical quantities a variable, N , designated as the refractivity or co-index of refraction, has been defined as

$$N = (n-1) \times 10^6 \quad N\text{-units}$$

and so within one kilometer of the earth's surface

$$\frac{dN}{dh} = -39 \text{ N-units/meter}$$

A standard atmosphere is then defined in Refs. 11 and 12 as follows:

$$1. \quad \varepsilon = 1; \\ n = 1$$

$$2. \quad \frac{dT}{dh} = \frac{1}{150} \text{ } ^\circ\text{C/m}$$

$$3. \quad N = \frac{77.6}{T} (p + 4810 \frac{e}{T}) \quad p = \text{pressure (mb)} \\ T = \text{absolute temp. } (\text{°K}) \\ e = \text{vapor pressure (mb)}$$

By assuming a linear refractivity gradient it is possible to define an effective earth radius as was done in an earlier part of this report. This allows the rays representing the radio wave to be drawn as straight lines over a curved earth. An alternative representation which enables the effect of several different values of effective earth radius to be shown on the same profile is to show the rays as curves from transmitter to receiver over a plane earth. Details of constructing this sort of representation are presented in Refs. 3 and 13.

Non-standard propagation can occur when the above conditions are not met. This is manifested by the manner in which the radio wave path is curved. Under normal conditions the decrease of the refractive index with height causes a downward bending of the wave path. Changes in the refractive index super-refraction or in certain cases an upward bending of the ray which is termed subrefraction. If the refractive effects are severe enough, the formation of ducts occurs in which the majority of radio wave energy is trapped within a narrow region.

Ducting can occur as a result of a number of different atmospheric conditions. The primary requirement in producing this phenomena is that the curvature of the radio wave must be greater than that of the earth. This is produced by a rapid change in N with height which is caused by a sharp decrease in moisture with height (abnormal moisture lapse rate) and/or a sharp increase in temperature with height (temperature inversion). The formation of a ground- or surface-based duct can occur when warm dry air flows from land over water. Moisture evaporates from the water into the lower layers of air cooling the air and producing an increased moisture lapse rate and a temperature inversion. The downward motion of warm dry air is frequently associated with the clear weather found on the eastern side of vast high pressure regions in the lower and middle atmosphere. Subsidence such as this can also result in elevated ducts which are found to be strongest and

lowest in fair weather and highest and weakest near storms. Surface ducts are also formed in certain regions by nocturnal cooling but unlike the evaporation duct this sort of anomaly if found over land, particularly desert regions.

The opposite effect to super-refractive ducting is the upward bending of radio waves caused by an increase in refractivity with height. This condition typically occurs in moist and cloudy regions.

- The determining factor in all the above cases is the refractivity gradient. Table II below, found in Ref. 11, shows the range of refractivity gradients over which anomalous conditions prevail.

Table II. Range of refractive index gradient for differing types of propagation conditions.

P (mb)	h (km)	Sub- Refractive	Unstratified	Super- Refractive
1000-850	0-1.46	$-dn/dh \leq 0$	$20 \leq -dn/dh \leq 60$	$100 \leq -dn/dh$
850-700	1.46-3.01	$-dn/dh \leq 0$	$20 \leq -dn/dh \leq 50$	$80 \leq -dn/dh$
700-600	3.01-4.20	$-dh/dh \leq 0$	$20 \leq -dn/dh \leq 40$	$70 \leq -dn/dh$
600-500	4.20-5.57	$-dh/dh \leq 0$	$20 \leq -dn/dh \leq 30$	$50 \leq -dn/dh$
500-400	5.57-7.18	$-dn/dh \leq 0$	$20 \leq -dn/dh \leq 25$	$40 \leq -dn/dh$

The refractivity gradient can be related to the effective earth radius and the resulting ray trace when drawn on the terrain profile corresponding to this radius, will show the effect of the anomaly on a particular path.

The following holds for most conditions [Ref. 3]:

$$\text{effective radius} = k = \frac{1}{1 + 6.4 \times 10^{-3} dN/dh}$$

From this relationship it can be seen that for the standard refractivity gradient, which was defined as -39 N-units/km, the effective earth radius would be equal to 4/3. The presence of anomalous conditions thus cause an effective earth radius greater or less than 4/3. The interrelationship of the refractivity gradient, the radius of curvature of the wavefront, the effective radius, and the associated types of refraction are shown in Table III [Ref. 3].

Note that there is some difference in the exact gradient value which defines super-refraction. The super-refractivity gradient referred to in Table II includes both the extended range and the ducting conditions, while that referred to in Table III includes only the ducting case.

In the actual paths under study several values of effective earth radius were used to simulate the effect of anomalous conditions. Table IV [Ref. 15] provides a guide to the use of k as an estimate of propagation conditions for 99.9%-99.99% path reliability.

Table III. Relationship of Refractive Gradient to Various Propagation Variables.

$\frac{dN}{dh}$	N-units km	Curvature (in km)	ρ	K	Atmospheric Refraction	Virtual Earth	Horizontally Launched Ray
> 0		Upward		< 1			
= 0		Nil	∞				
0 > $\frac{dN}{dh}$ > -39							
- 39							
- 39 > $\frac{dN}{dh}$ > -157							
- 157							
< -157							

Moves Away
from earth

Actual Earth

Less Convex
than Actual
Earth

Normal

Above Normal

$a = 6350$
 $= \rho$

Plane

Remains
parallel to
Earth

Draws Closer
to Earth

Table IV. K Factor Guide.

	Propagation Conditions				
	Perfect	Ideal	Average	Difficult	Bad
Weather	Standard atmosphere	No surface layer or fog	Substandard light fog	Surface layers, ground fog	Fog moisture over water
Typical	Temperate zone, no fog, no ducting, good atmospheric mix day and night	Dry, mountainous, no fog	Flat, temperate, some fog	Coastal	Coastal, water, tropical
K Factor	1.33	1-1.33	0.66-1.0	0.66-0.5	0.5-0.4

The path profiles from Keyport to Gold Mt., Keyport to Lookout Mt., and Bangor to Lookout Mt. are shown for two values of K; 0.5 which represents the difficult case as either when one antenna is inside a duct and the other outside, or the subrefractive condition, and -3.57 which represents a subrefractive gradient of -200 N-units/km. The effect of the change in earth radius shown in Figs. 36-41 is most noticeable in the Keyport to Lookout Mt. path. Using graphical methods of analysis found in Refs. 1 and 3 the approximate degradation in link performance can be estimated. While little change is observed in the Keyport to Gold Mt. link due to the shortness of the path length, the Keyport to Lookout Mt. path with $K = \frac{1}{2}$ exhibits an additional loss of up to 60 db over that found in

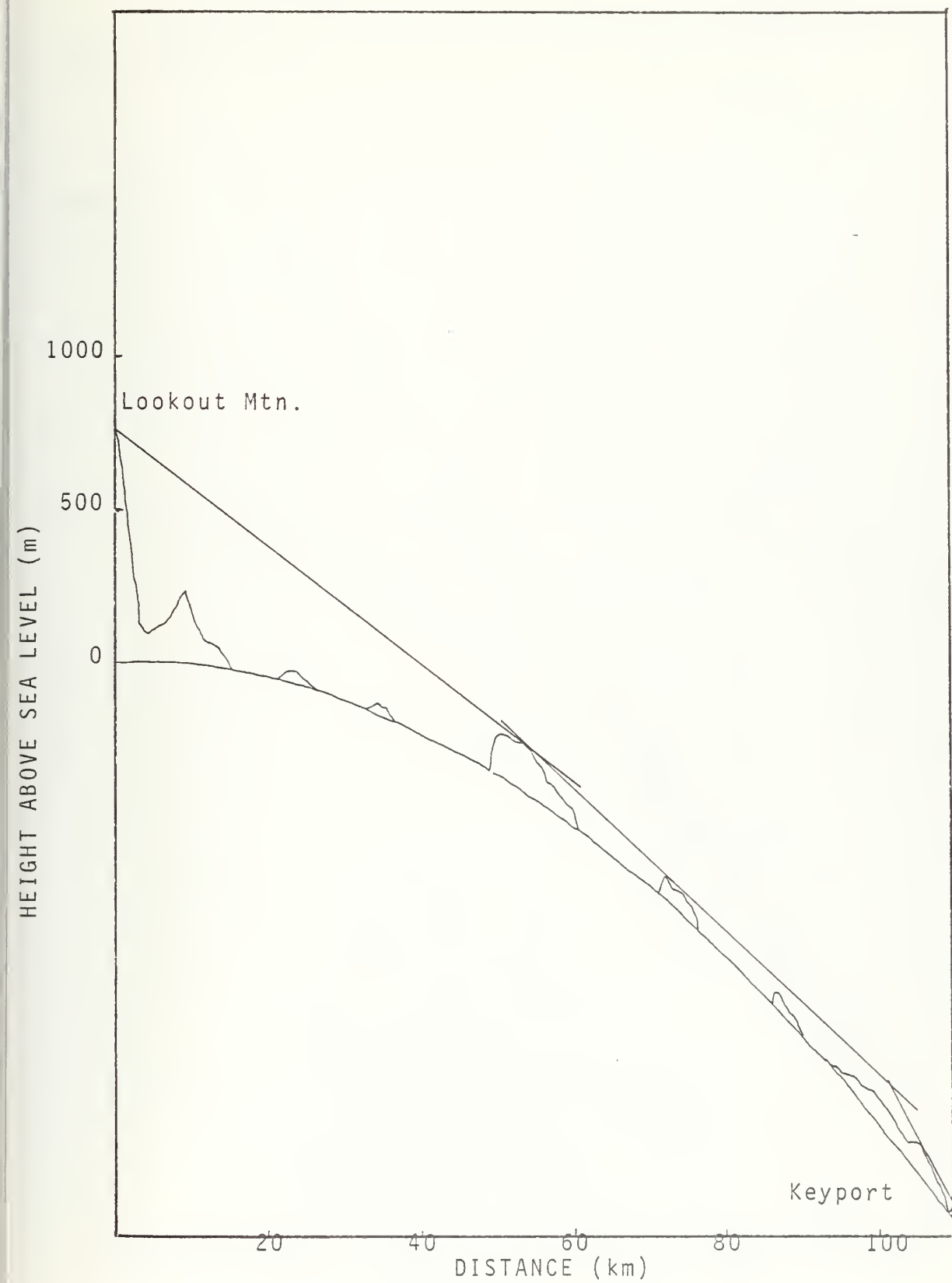


Figure 36
Path Profile for Lookout Mt. to Keyport ($K=1/2$)

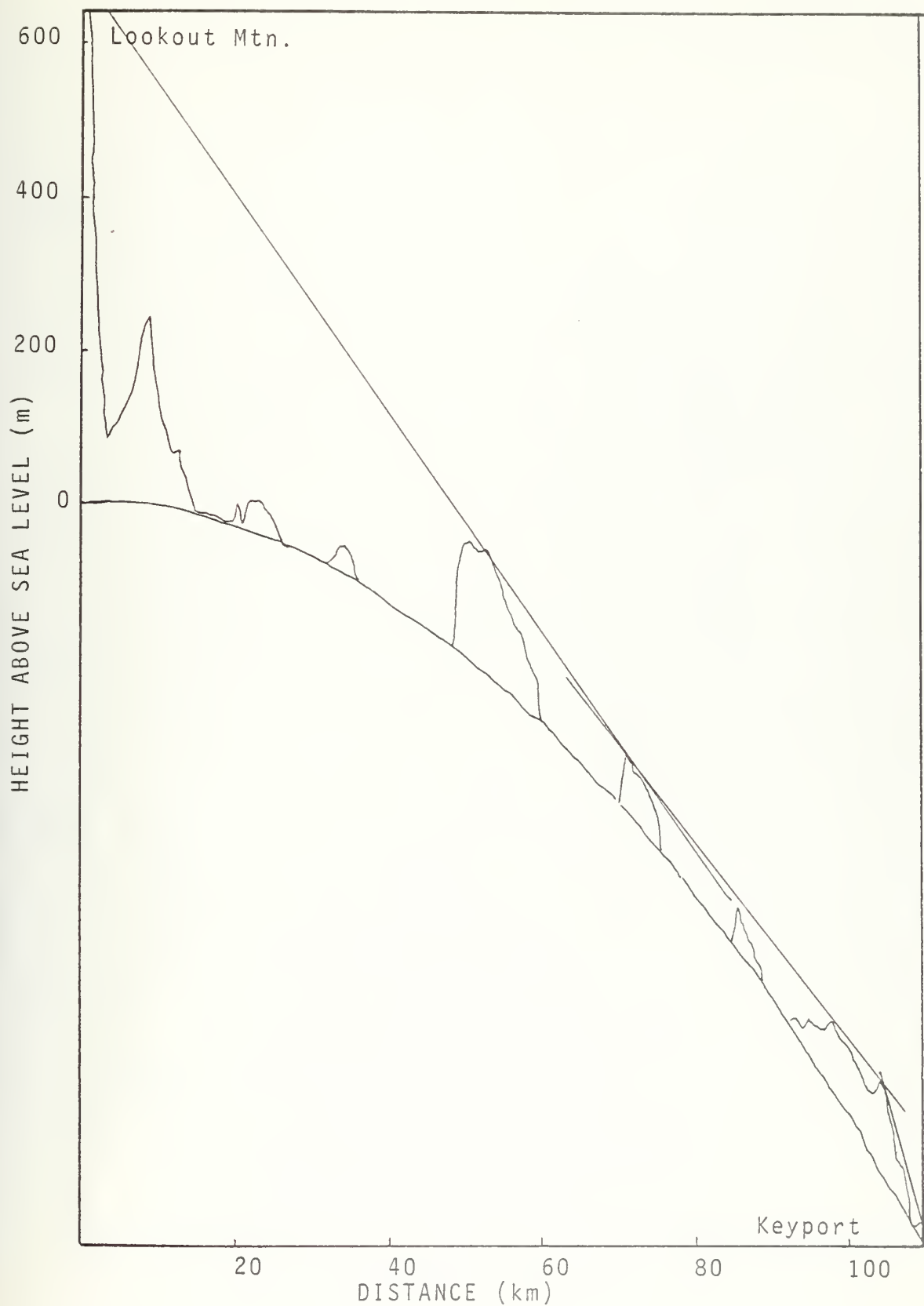


Figure 37
Path Profile for Lookout Mt. to Keyport (K=1)

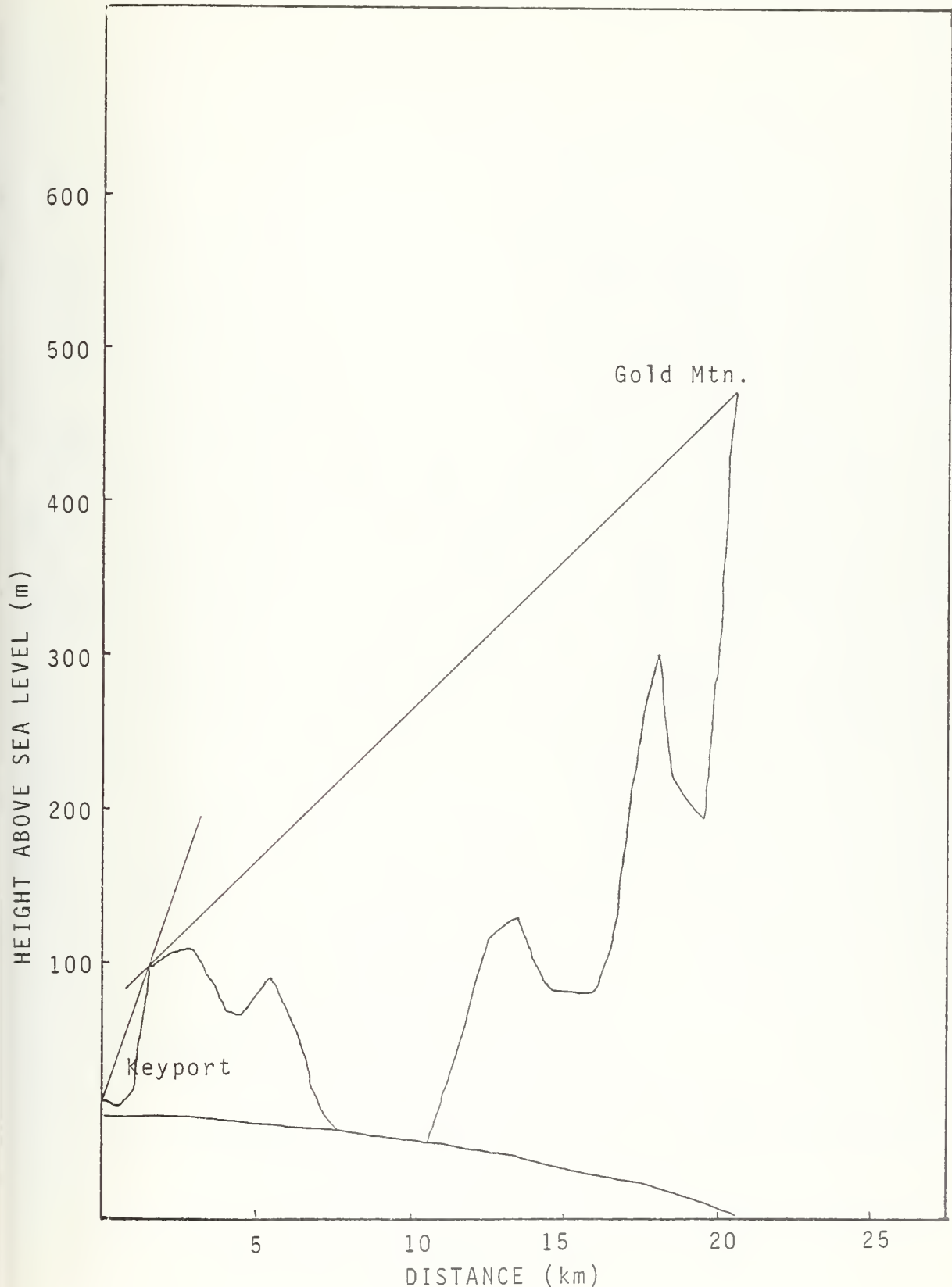


Figure 38
Path Profile for Keyport to Gold Mt. ($K=1/2$)

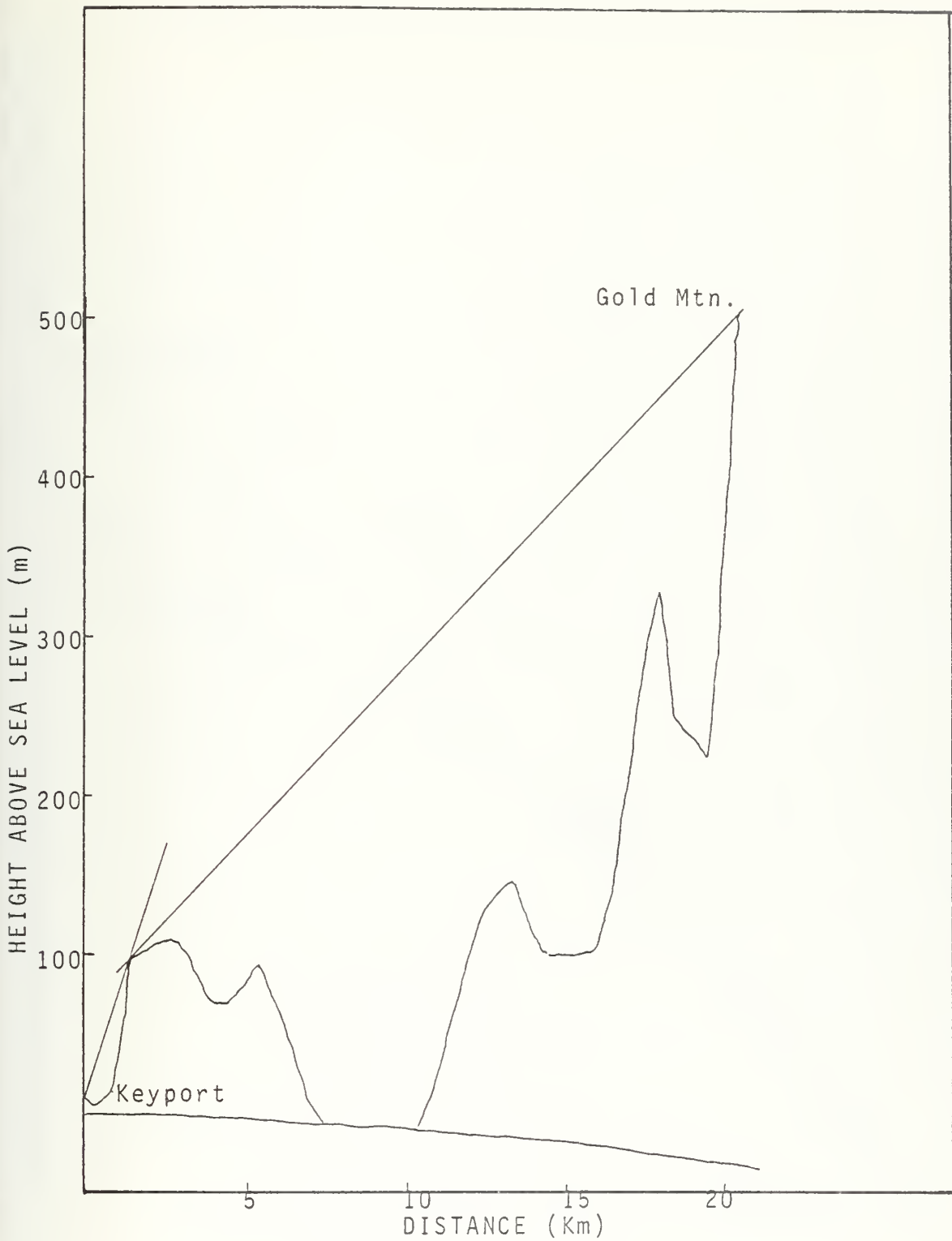


Figure 39

Path Profile for Keyport to Gold Mt. (K=1)

ELEVATION PROFILE (m)

1000

500

0

Lookout Mtn.

Bangor

20

40

60

80

100

DISTANCE (km)

Figure 40

Path Profile for Lookout Mt. to Bangor ($K=1/2$)

ELEVATION ABOVE SEA LEVEL (ft.)

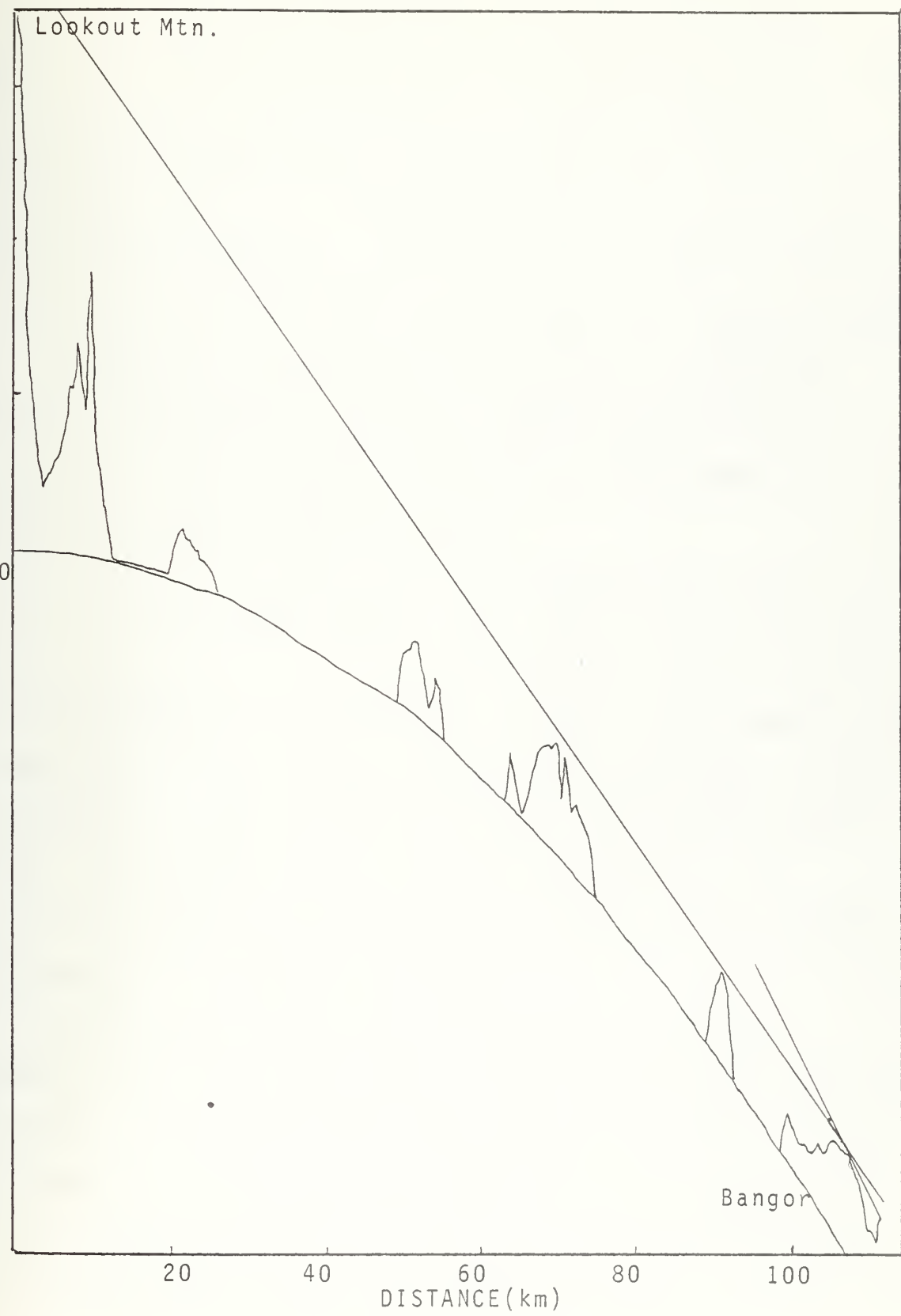


Figure 41
Path Profile Lookout Mt. to Bangor ($K=1$)

standard atmospheric conditions. This same path however suffers no apparent degradation for $K = 1$ as the Fresnel zone clearance remains greater than .6. The Lookout Mt. to Bangor path degradation was found to be 12-30 db for $K = \frac{1}{2}$ and 6-15 db for $K = 1$. From these results it can be seen that changes in effective earth radius can have a significant effect on path loss, particularly as the path length increases.

The profile representation using N data is the most commonly used in the literature, however the depiction of ducting or trapping types of profiles is often done with modified or M-unit profiles where

$$M = N + \frac{(a)}{h} \times 10^6 \quad \begin{aligned} a &= \text{actual earth radius} \\ h &= \text{height above sea level} \end{aligned}$$

This adjustment to the N-profile is used in the anomalous case since straight rays above a curved earth now become curved rays above a planar earth and the duct can be more clearly shown. The variability of M curves corresponding to a particular propagation condition is shown in Table V which was derived from Ref. 16.

The M-curve is thus a transformation in which the relative curvature between the normal of the electro-magnetic wavefront and the surface of the earth is unchanged. A duct is formed whenever the M curve has a relative minimum. The base of an elevated duct is the height on the M curve below the minimum that has the same M value as the relative minimum.

When no such height exists, the base of the duct is at the ground and a so-called ground based duct exists [Ref. 12]. The main disadvantage in the use of M data is that above the duct N is grossly overcorrected.

Table V. Variability of M curves with type of transmission conditions.

<u>M</u>	<u>M-Curve</u>	<u>Type of Transmission</u>
Increases linearly	Straight line, with positive slope	Standard
	Slope decreases near earth surface with rays curving up	Substandard
	Slope increases near surface with less upward curve	Superstandard
	Vertical, no curve	Very great coverage
Decreases with height	Slope linear and negative rays curve down	Trapping or ducting

Having demonstrated the effect of anomalous conditions on several propagation paths and considered the theory involved the next step is to determine the frequency with which these conditions occur. The method chosen to accomplish this was to access the IREPS historical file for the geographical area in question as described in the following section.

B. INTEGRATED REFRACTIVE EFFECTS PREDICTION SYSTEM (IREPS)²

IREPS is an experimental system ultimately designed to provide the capability for on-board assessment of the effect of atmospheric anomalies on sensor performance. The hardware portion of the system consists of a mini-computer with an interactive graphics terminal on which the required inputs are entered and the results displayed in an easily understood graphic format. The information stored in the systems memory includes a refractivity library containing long-term meteorological statistics on the occurrence of ducting conditions as a function of location. This library data is obtained from radiosonde stations throughout the world and can be augmented by on-scene refractometer or radiosonde data input in order to tailor the output to a particular location. In the case of the Washington paths, there were only two upper air sounding stations in the vicinity of the sites. One is located at Tatoosh Island ($48^{\circ}24'N$, $124^{\circ}42'W$) and the other at Quillayute ($48^{\circ}00'N$, $124^{\circ}36'W$). The historical propagation summaries for each location are shown in Figs. 42 and 43. Note that while the statistics generated are geared toward radar performance, the frequencies to be used in the link are included so that some information concerning potential anomalies can be derived. The historical meteorological data for each station, shown in Figs. 44 and 45, provides information concerning median conditions in the vicinity of the

²For a detailed description of the system see Ref. 10.

sounding station and shows the seasonal and diurnal variation in this data. Based on this data, the program then can generate a series of profiles. Figures 46 and 47 are M and N profiles in the vicinity of the two sounding stations. Also available in the program output capabilities is a ray trace diagram from a particular emitter. This is useful in a qualitative sense in that it shows potential areas of non-coverage which may be important in maintaining a ground to air communications link. The first set of traces demonstrates the effect on the ray trace diagram of selected sites for the median ducts found in the Tatoosh Island profile and are shown in Figs. 48-52. A second set of traces are shown in Figs. 54-57 exhibiting the effect of an elevated duct between 1100 and 1400 feet. The profile responsible for this condition is shown in Fig. 53. The third set of traces show a duct between 2300 and 2900 feet in Figs. 59 and 60 and the corresponding profile in Fig. 58.

Besides the above mentioned output format the IREPS program can also provide path loss information, with a detection threshold for a particular sensor superimposed on the distance vs. dB display and also a coverage diagram for a particular sensor. These two output diagrams were not produced for this study but an example of each is included in Figs. 61 and 62 [Ref. 10].

LOCATION 48 24 N 124 36 W
SEASON ALL YEAR
TIME DAY & NIGHT

SURFACE TO SURFACE:

6 %	PROBABILITY OF EXTENDED RANGES FOR FREQUENCIES	30 MHZ	TO 1 GHZ
6 %	PROBABILITY OF EXTENDED RANGES FOR FREQUENCIES	1 GHZ	TO 3 GHZ
7 %	PROBABILITY OF EXTENDED RANGES FOR FREQUENCIES	3 GHZ	TO 6 GHZ
19 %	PROBABILITY OF EXTENDED RANGES FOR FREQUENCIES	6 GHZ	TO 10 GHZ
42 %	PROBABILITY OF EXTENDED RANGES FOR FREQUENCIES ABOVE	10 GHZ	

SURFACE TO AIR:

2 % PROBABILITY FOR:
EXTENDED RANGES UP TO MEDIAN ALTITUDE OF 92. METERS
POSSIBLE HOLES ABOVE MEDIAN ALTITUDE OF 92. METERS

AIR TO AIR:

4 % PROBABILITY FOR:
EXTENDED RANGES FOR MEDIAN ALTITUDES BETWEEN 735. AND 816. METERS
POSSIBLE HOLES FOR MEDIAN ALTITUDES ABOVE 816. METERS

GENERATE PROFILE (STANDARD, ELEVATED, SURFACE, ALL, NONE)?

Figure 42

Historical Propagation Conditions for Tatoosh Island, Wash.

LOCATION 48° 00' N 124° 36' W
SEASON ALL YEAR
TIME DAY & NIGHT

SURFACE TO SURFACE:

11 %	PROBABILITY OF EXTENDED RANGES FOR FREQUENCIES 30 MHZ TO 1 GHZ
12 %	PROBABILITY OF EXTENDED RANGES FOR FREQUENCIES 1 GHZ TO 3 GHZ
13 %	PROBABILITY OF EXTENDED RANGES FOR FREQUENCIES 3 GHZ TO 6 GHZ
25 %	PROBABILITY OF EXTENDED RANGES FOR FREQUENCIES 6 GHZ TO 10 GHZ
47 %	PROBABILITY OF EXTENDED RANGES FOR FREQUENCIES ABOVE 10 GHZ

SURFACE TO AIR:

8 % PROBABILITY FOR EXTENDED RANGES UP TO MEDIAN ALTITUDE OF 68 METERS POSSIBLE HOLES ABOVE MEDIAN ALTITUDE OF 68 METERS

AIR TO AIR:

15 % PROBABILITY FOR EXTENDED RANGES FOR MEDIAN ALTITUDES BETWEEN 1090 AND 1187 METERS POSSIBLE HOLES FOR MEDIAN ALTITUDES ABOVE 1187 METERS

GENERATE PROFILE (STANDARD, ELEVATED, SURFACE, ALL, NONE) ?

Figure 43

Historical Propagation Conditions for Quillayute, Wash.

HISTORICAL METEOROLOGICAL DATA FOR LIGHTNING TIME: 48-54¹¹-15¹¹-30^W
ALL YEAR DAY & NIGHT

UPPER AIR PROFILE SOURCE: TATOSH
EVAPORATION DUCT SOURCE: MARSDEN
MEDIAN SURFACE DUCT: INTENSITY 332.
MEDIAN SURFACE DUCT: INTENSITY 1.
MEDIAN ELEVATED DUCT: INTENSITY 2.

MEDIAN SURFACE N UNITS:	MEDIAN N UNITS		UNIT GRADIENT:	-53.0 (N/KM)				
	1. MUNITS, TOP 92 MTRS	2. MUNITS, TOP 816 MTRS, BASE 735 MTRS						
YEARLY AUG	WINTER DAY	NIGHT	SPRING DAY	NIGHT	SUMMER DAY	NIGHT	AUTUMN DAY	NIGHT
	0.0	0.0	10.3	11.3	5.3	1.0	0.0	0.0
% SURFACE DUCTS	2 2	0.0	5.0	14.0	5.3	9.0	0.0	0.0
% ELEVATED DUCTS	4 2	0.0	0.0	0.0				
EVAPORATION DUCTS								
% 0 TO 3 METERS	23.6	26.4	26.1	29.3	27.9	24.4	21.3	16.9
% 3 TO 6 METERS	22.1	22.0	26.5	23.1	29.4	18.0	23.7	15.5
% 6 TO 9 METERS	21.9	23.1	25.4	18.9	22.0	17.2	24.5	19.8
% 9 TO 12 METERS	15.2	16.1	14.2	11.7	12.1	13.7	13.6	20.0
% 12 TO 15 METERS	7.2	5.7	4.7	5.1	3.6	7.4	7.3	12.4
% 15 TO 18 METERS	3.2	2.4	1.2	2.2	1.4	4.1	3.0	6.4
% 18 TO 21 METERS	1.5	1.0	0.6	1.1	0.6	2.2	1.6	2.9
% 21 TO 24 METERS	0.6	0.1	0.2	0.7	0.2	1.5	0.6	1.0
% 24 TO 27 METERS	0.5	0.5	0.2	0.6	0.3	0.9	0.6	0.6
% 27 TO 30 METERS	0.3	0.3	0.0	0.4	0.1	0.6	0.5	0.3
% > 30 METERS	3.8	2.4	0.8	6.7	2.5	9.9	3.4	3.6
MEAN DUCT HT MTRS	8.7	7.6	6.4	9.2	6.9	12.0	8.5	10.3
MEAN WIND SP M/S	7.1	9.3	9.3	6.2	6.2	5.7	5.7	7.2

GENERATE PROFILE (STANDARD, ELEVATED, SURFACE, ALL, NONE)?

Figure 44

Historical Meteorological Data for Tatoosh Island, Wash.

HISTORICAL METEOROLOGICAL DATA FOR LOCATION: 48° 00' N 124° 36' W
TIME: ALL YEAR DAY & NIGHT

UPPER AIR PROFILE SOURCE: QUILAYUT WASH, USA
EVAPORATION DUCT SOURCE: MARSDEN SQ 159

MEDIAN SURFACE N UNITS: 324.
MEDIAN SURFACE DUCT: INTENSITY 3.
MEDIAN ELEVATED DUCT: INTENSITY 3.

MEDIAN N UNIT GRADIENT: -44.0 (N/KM)

3. MUNITS, TOP 68 MTRS

3. MUNITS, TOP 1187 MTRS, BASE 1090 MTRS

YEARLY AUG.	WINTER		SPRING		SUMMER		AUTUMN	
	DAY	NIGHT	DAY	NIGHT	DAY	NIGHT	DAY	NIGHT
SURFACE DUCTS	7.6	4.7	4.0	21.3	1.0	18.7	5.0	3.3
ELEVATED DUCTS	14.6	5.3	4.7	9.7	23.3	19.7	34.3	6.7

EVAPORATION DUCTS	SUMMER		AUTUMN		WINTER		SPRING		SUMMER		AUTUMN	
	DAY	NIGHT										
< 0 TO 3 METERS	23.6	26.4	26.1	29.3	27.9	24.4	21.3	16.9	21.3	16.7	23.7	15.5
3 TO 6 METERS	22.1	22.0	26.5	23.1	29.4	18.0	24.5	19.8	24.5	18.2	24.3	20.0
6 TO 9 METERS	21.9	23.1	25.4	18.9	22.0	17.2	13.6	13.7	13.6	20.0	20.0	20.0
9 TO 12 METERS	21.2	16.1	14.2	11.7	12.1	13.7	7.3	7.4	7.3	12.4	11.2	11.2
12 TO 15 METERS	15.2	7.2	5.7	4.7	5.1	3.6	4.1	4.1	4.1	6.4	5.2	5.2
15 TO 18 METERS	7.2	3.2	2.4	1.2	2.2	1.4	3.0	3.0	3.0	2.9	1.9	1.9
18 TO 21 METERS	5.7	1.5	1.0	0.6	1.1	0.6	2.2	2.2	2.2	1.6	0.6	0.6
21 TO 24 METERS	3.2	0.6	0.1	0.2	0.7	0.2	1.5	1.5	1.5	0.9	0.9	0.9
24 TO 27 METERS	1.5	0.5	0.5	0.2	0.6	0.3	0.6	0.6	0.6	0.6	0.6	0.6
27 TO 30 METERS	0.5	0.3	0.3	0.0	0.4	0.1	0.6	0.6	0.6	0.5	0.5	0.5
> 30 METERS	0.3	0.8	2.4	0.8	6.7	2.5	9.9	9.9	9.9	3.4	3.6	3.6
MEAN DUCT HT MTRS	8.7	7.6	6.4	9.2	6.9	12.0	8.5	10.3	8.5	10.3	8.7	8.7
MEAN WIND SP M/S	7.1	9.3	9.3	6.2	6.2	5.7	5.7	7.2	5.7	7.2	7.2	7.2

GENERATE PROFILE (STANDARD, ELEVATED, SURFACE, ALL, NONE)?

Figure 45

Historical Meteorological Data for Quillayute, Wash.

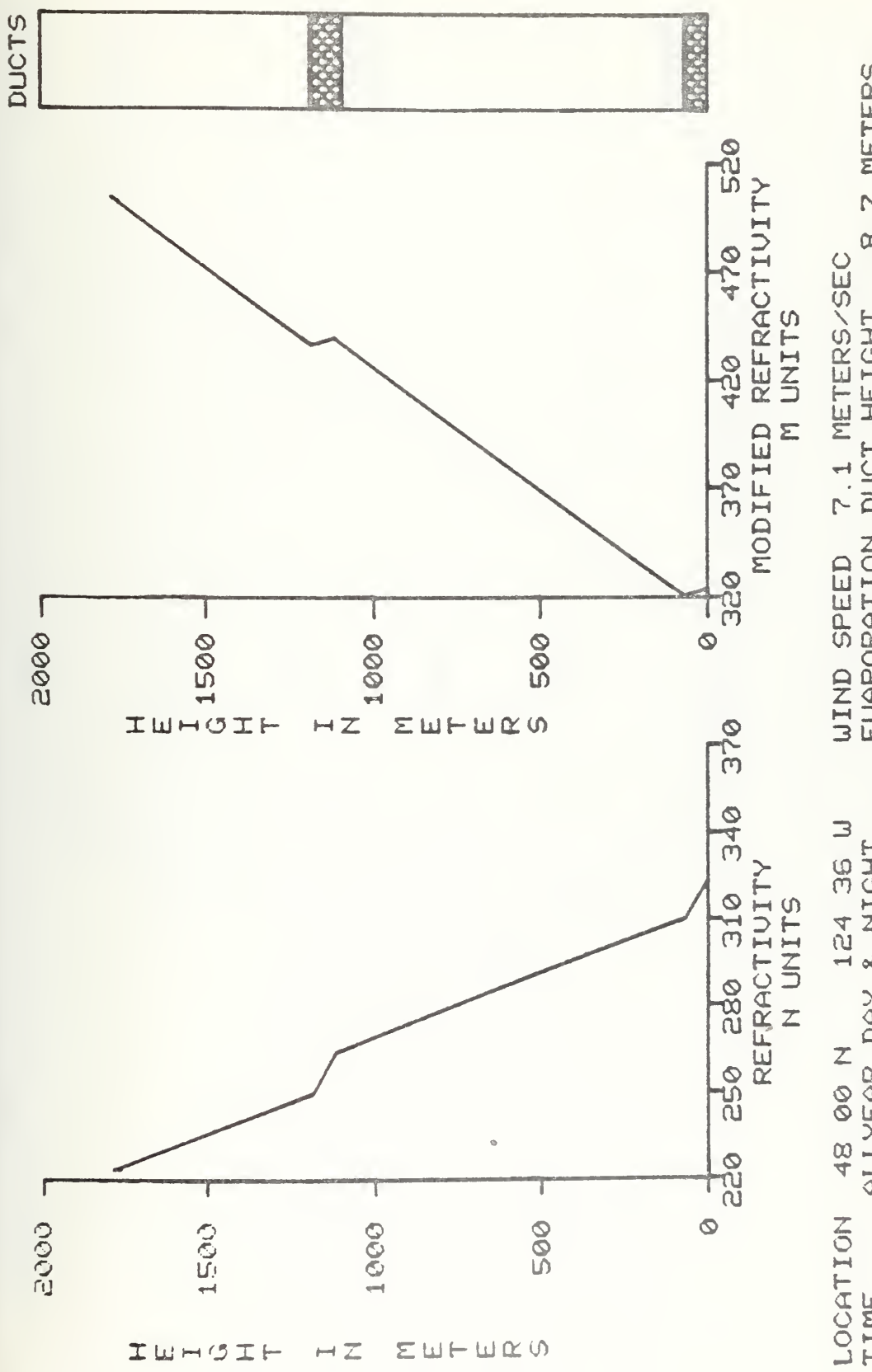


Figure 46
Median Profiles for Quillayute, Wash.

DUCTS

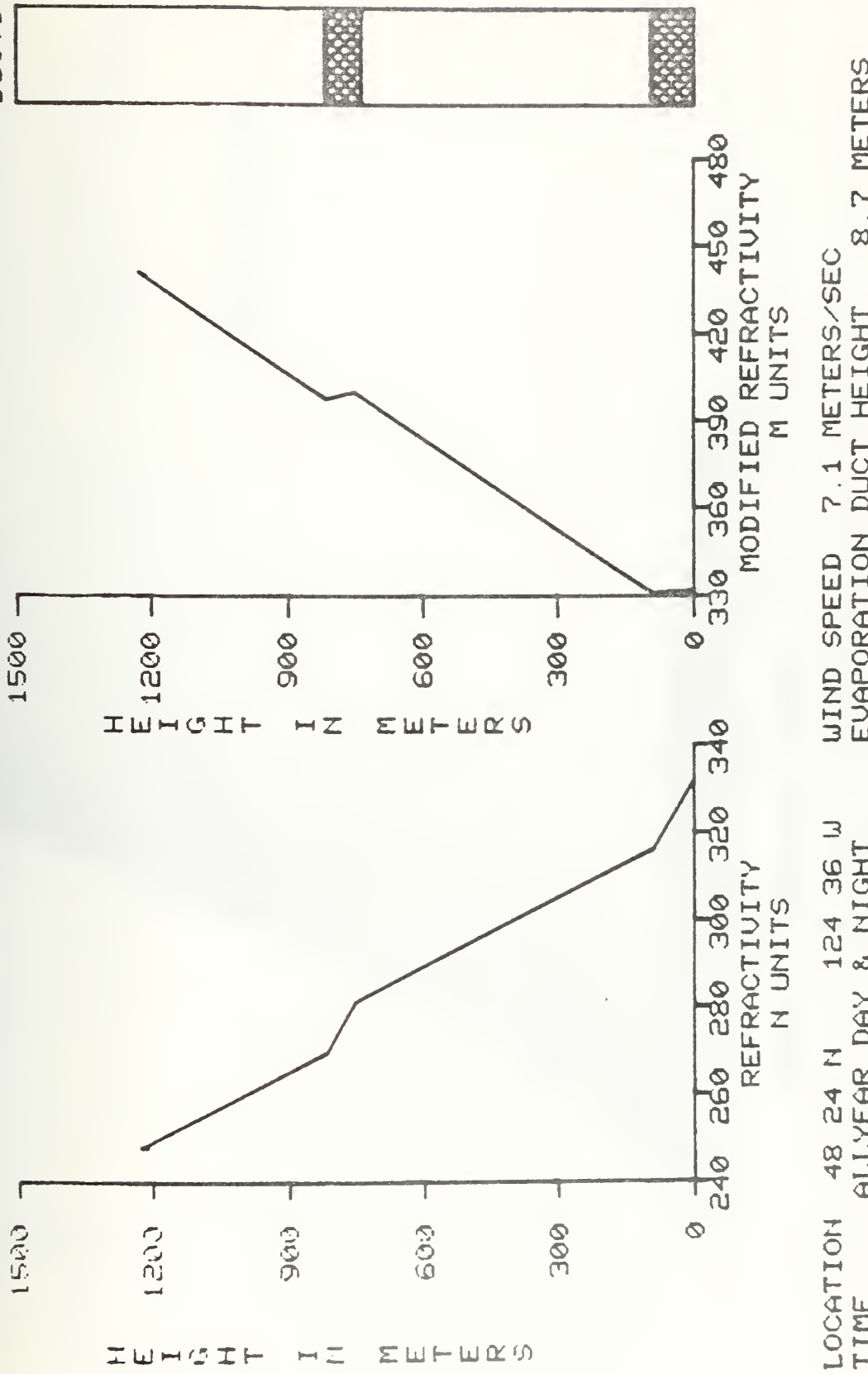


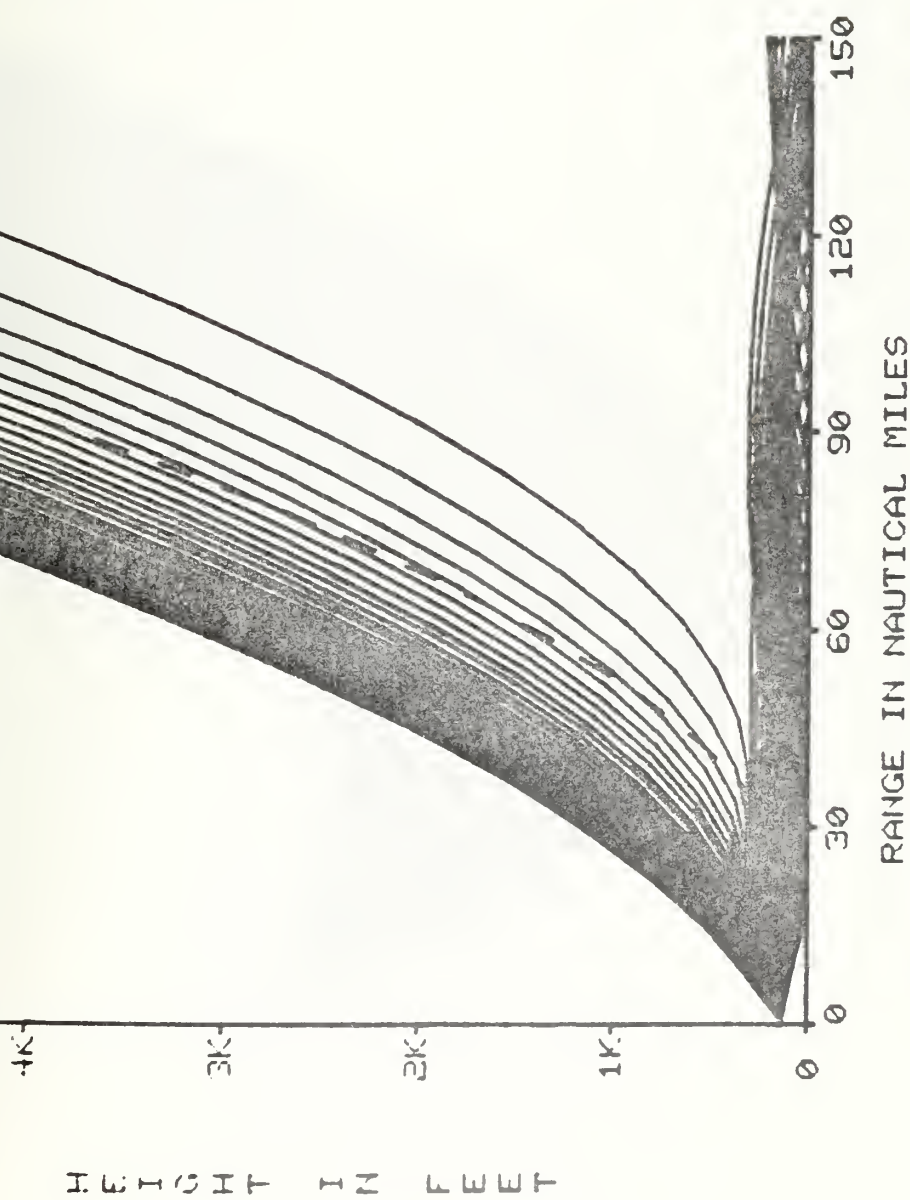
Figure 47

Median Profiles for Tatoosh Island

WINCHELSEA

TRANSMITTER/RADAR
HEIGHT 129.0 FT

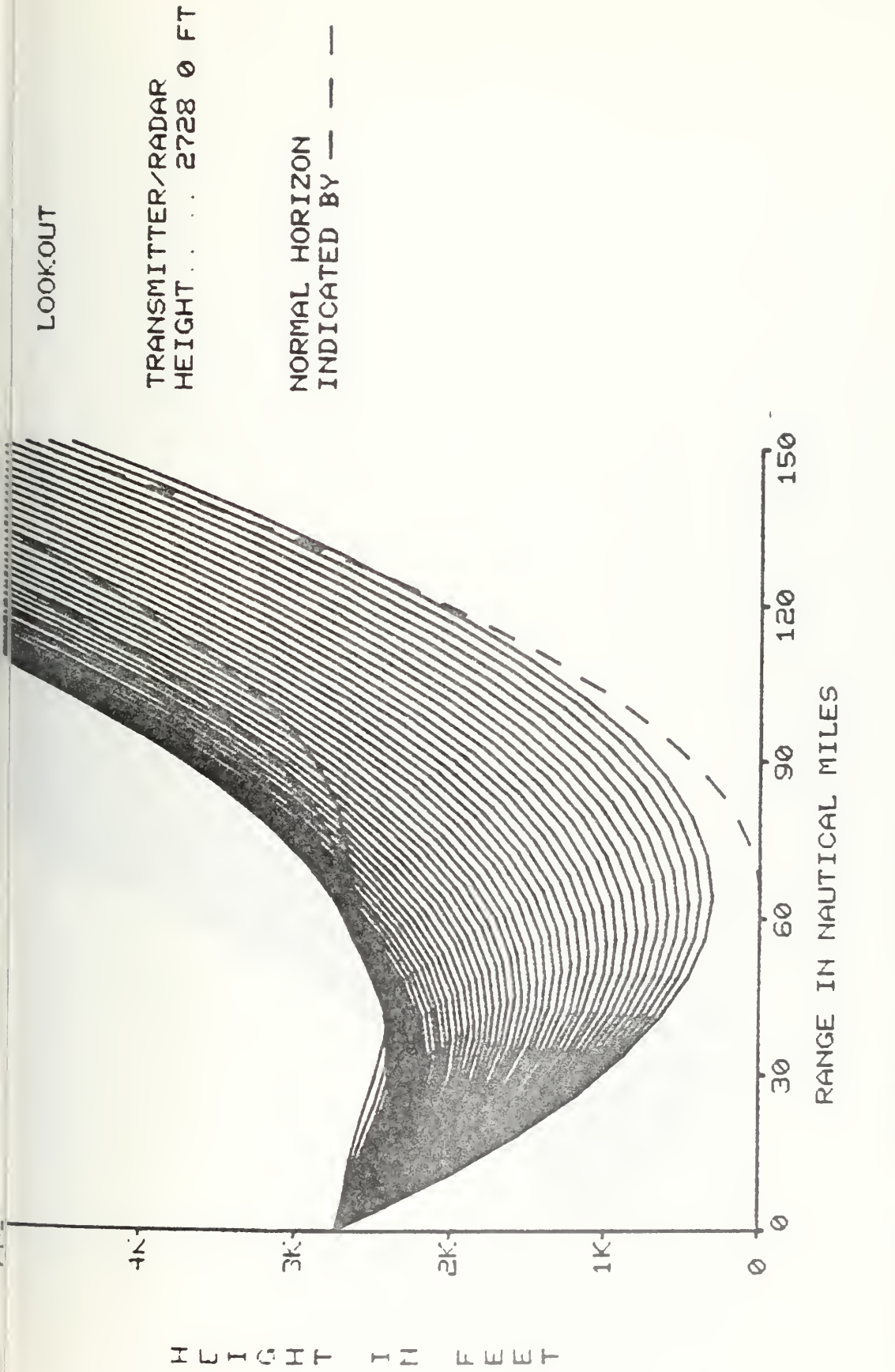
NORMAL HORIZON
INDICATED BY - - -



LOCATION: 48 24 N 124 36 W
TIME: ALL YEAR DAY & NIGHT
(PLOT, EDIT, LIST, SUMRY, RAYS, LOSS, COVER, END)?

Figure 48

Winchelsea Island Ray Trace for Median Conditions



LOCATION: 48 24 N 124 36 W
 TIME: ALL YEAR DAY & NIGHT
 (PLOT, EDIT, LIST, SUMRY, RAYS, LOSS, COVER, END)?

Figure 49

Lookout Mt. Ray Trace for Median Conditions

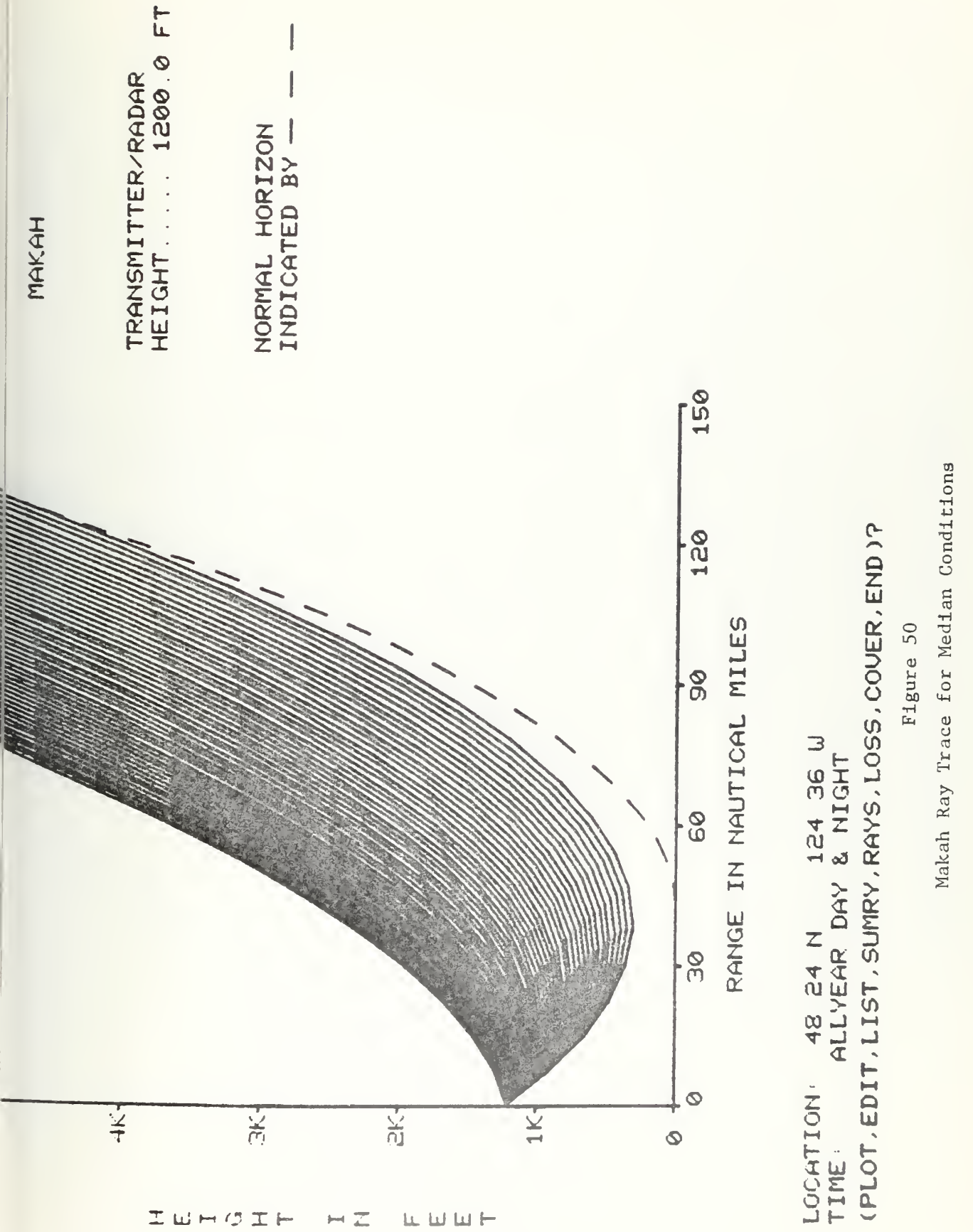


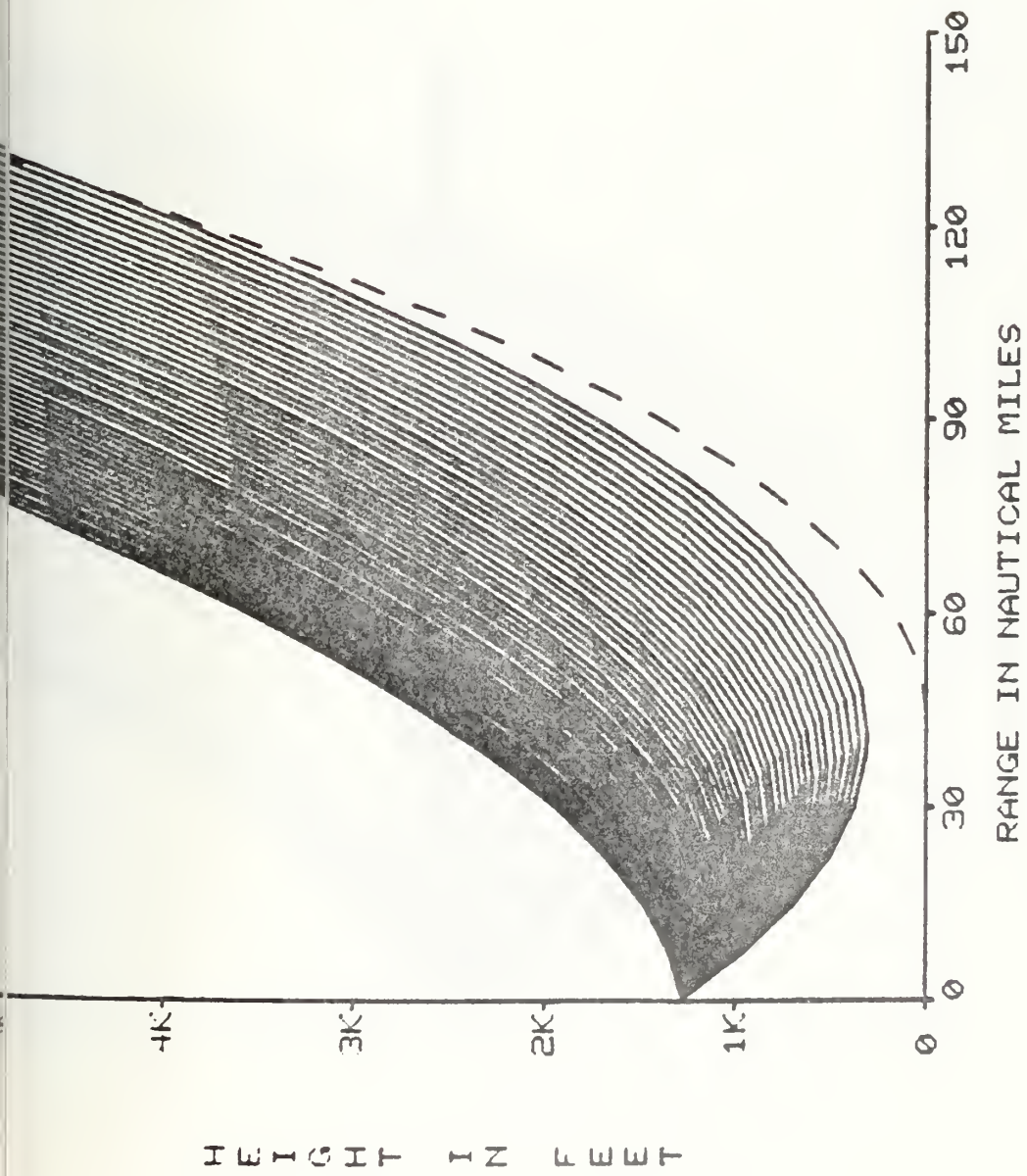
Figure 50

Makah Ray Trace for Median Conditions

STRIPED PK

TRANSMITTER/RADAR
HEIGHT 1266.0 FT

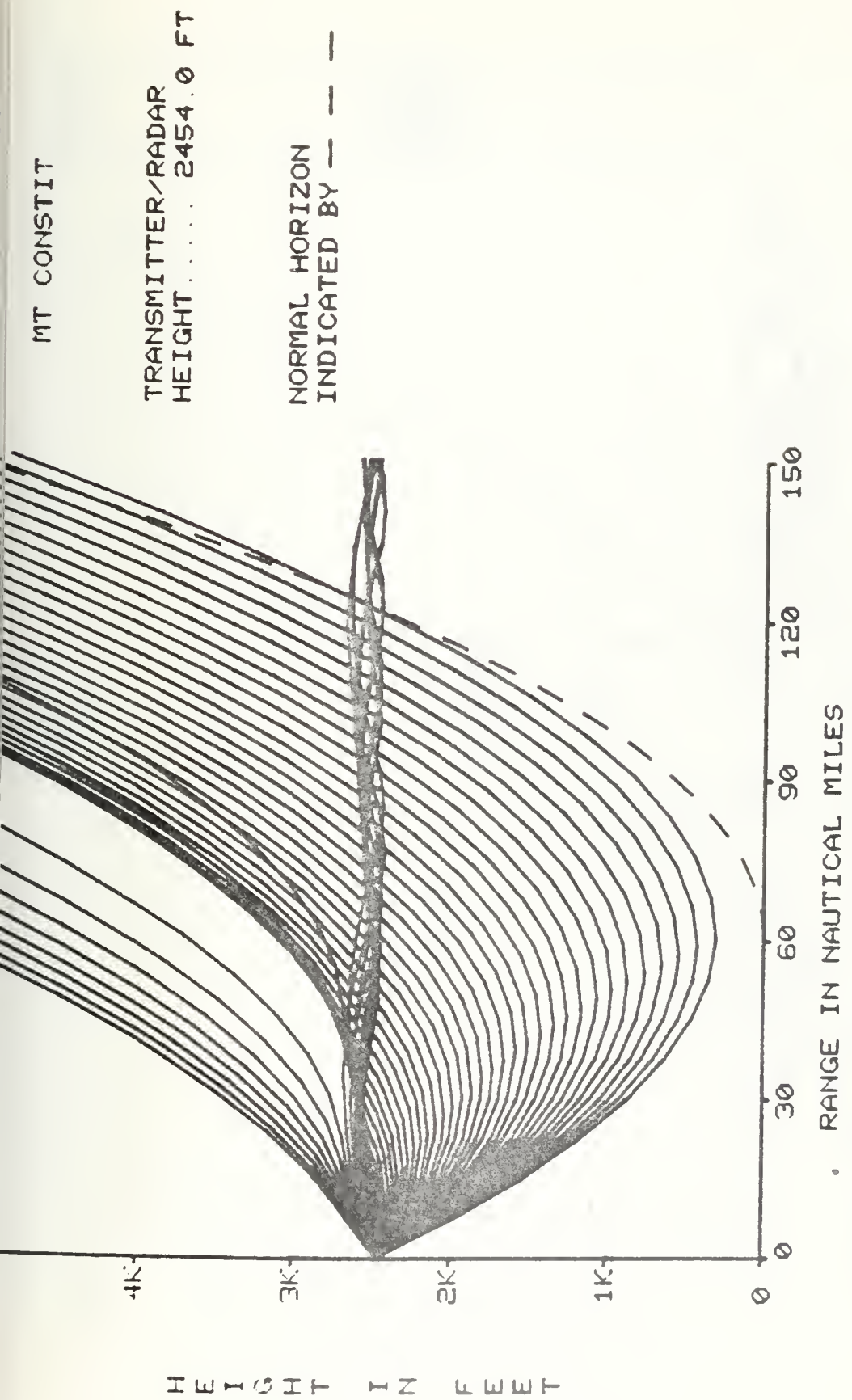
NORMAL HORIZON
INDICATED BY - - -



LOCATION: 48 24 N 124 36 W
TIME: ALL YEAR DAY & NIGHT
(PLOT, EDIT, LIST, SUMRY, RAYS, LOSS, COVER, END) ?

Figure 51

Striped Peak Ray Trace for Median Conditions



LOCATION: 48 24 N 124 36 W
 TIME: ALL YEAR DAY & NIGHT
 (PLOT, EDIT, LIST, SUMMARY, RAYS, LOSS, COVER, END)?

Figure 52

Mt. Constitution Ray Trace for Median Conditions

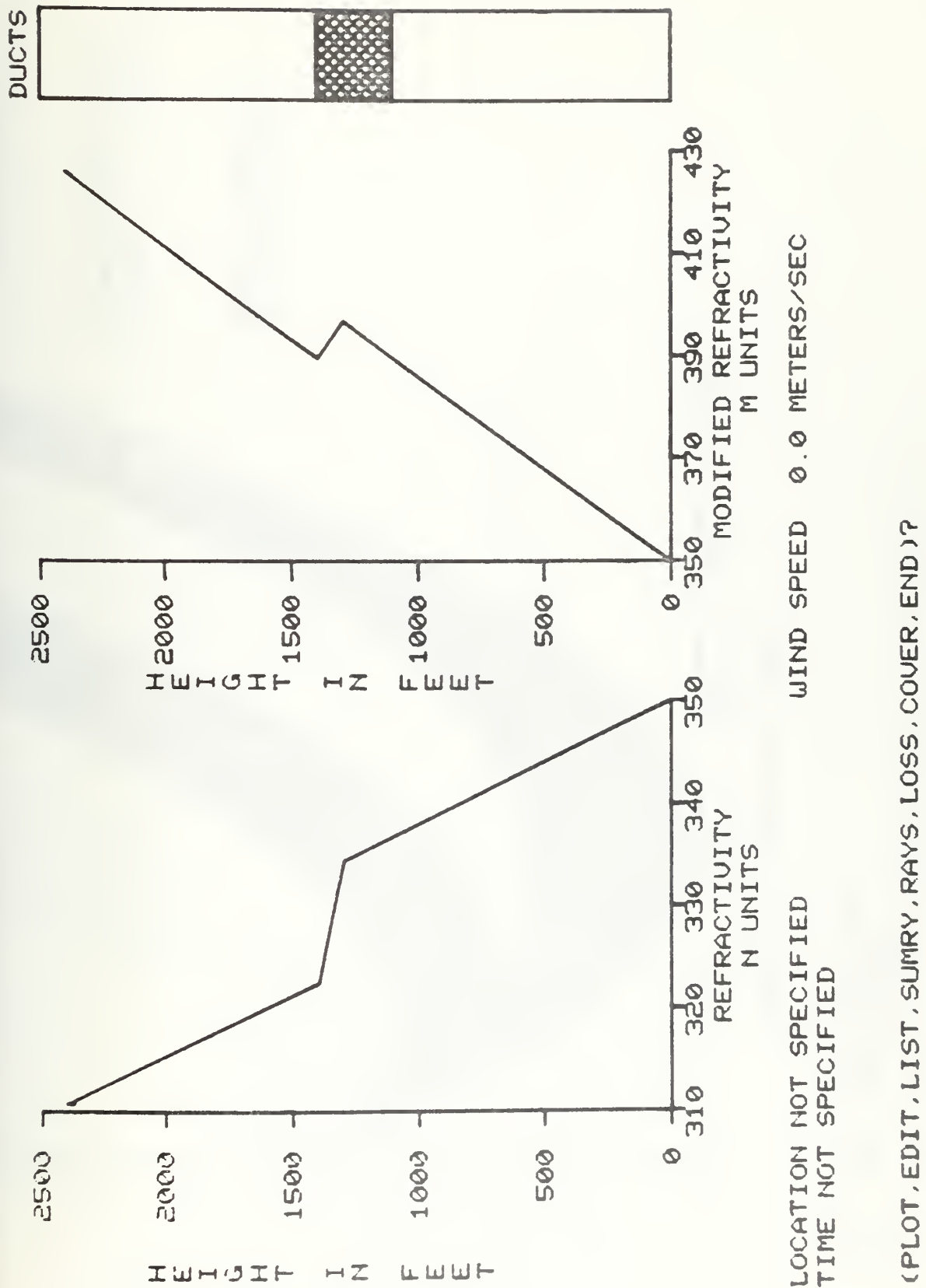


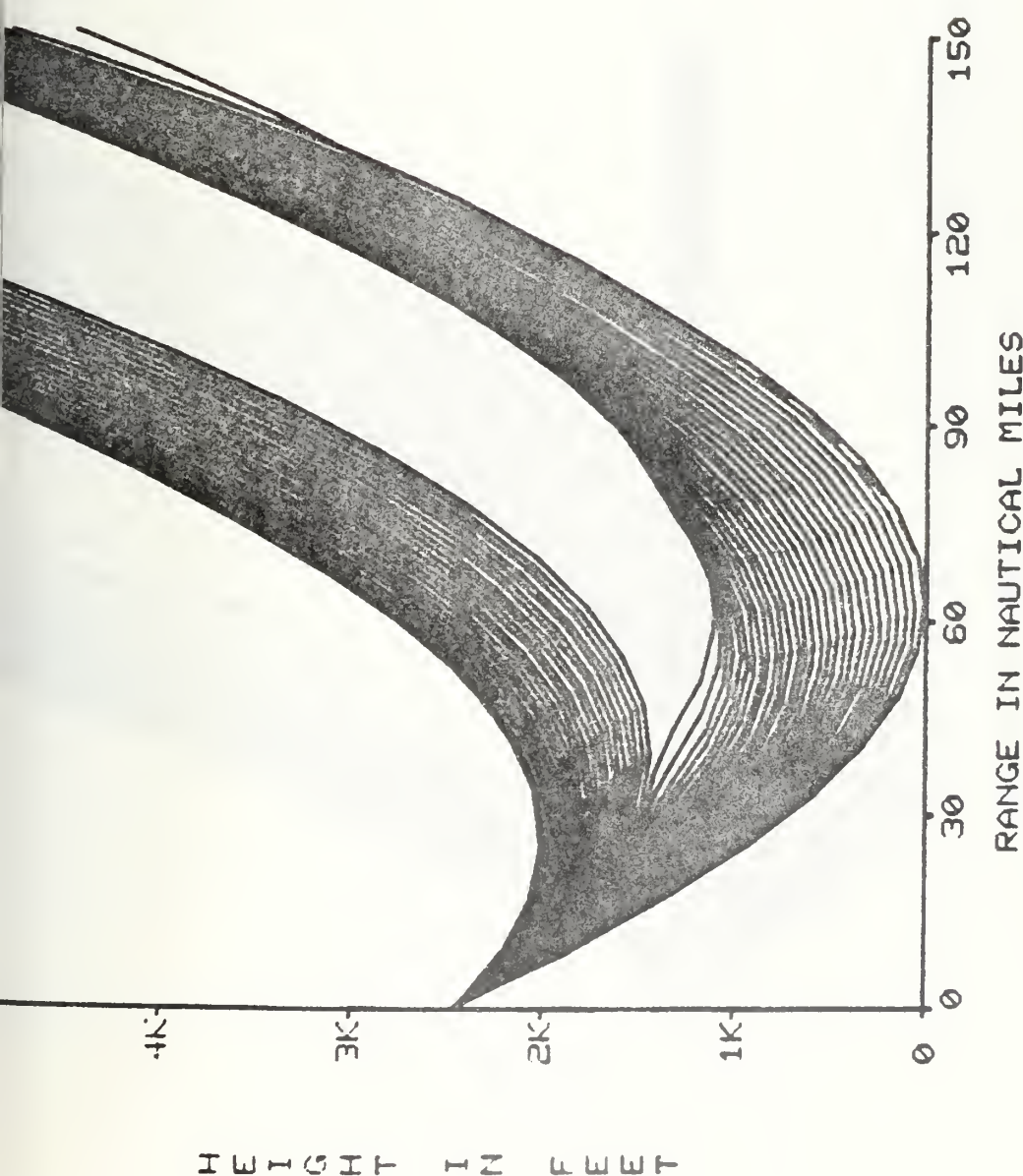
Figure 53

Profiles Required to Produce an Elevated Duct Between 1100-1400 Feet

MT CONSTIT

TRANSMITTER/RADAR
HEIGHT . . . 2454.0 FT

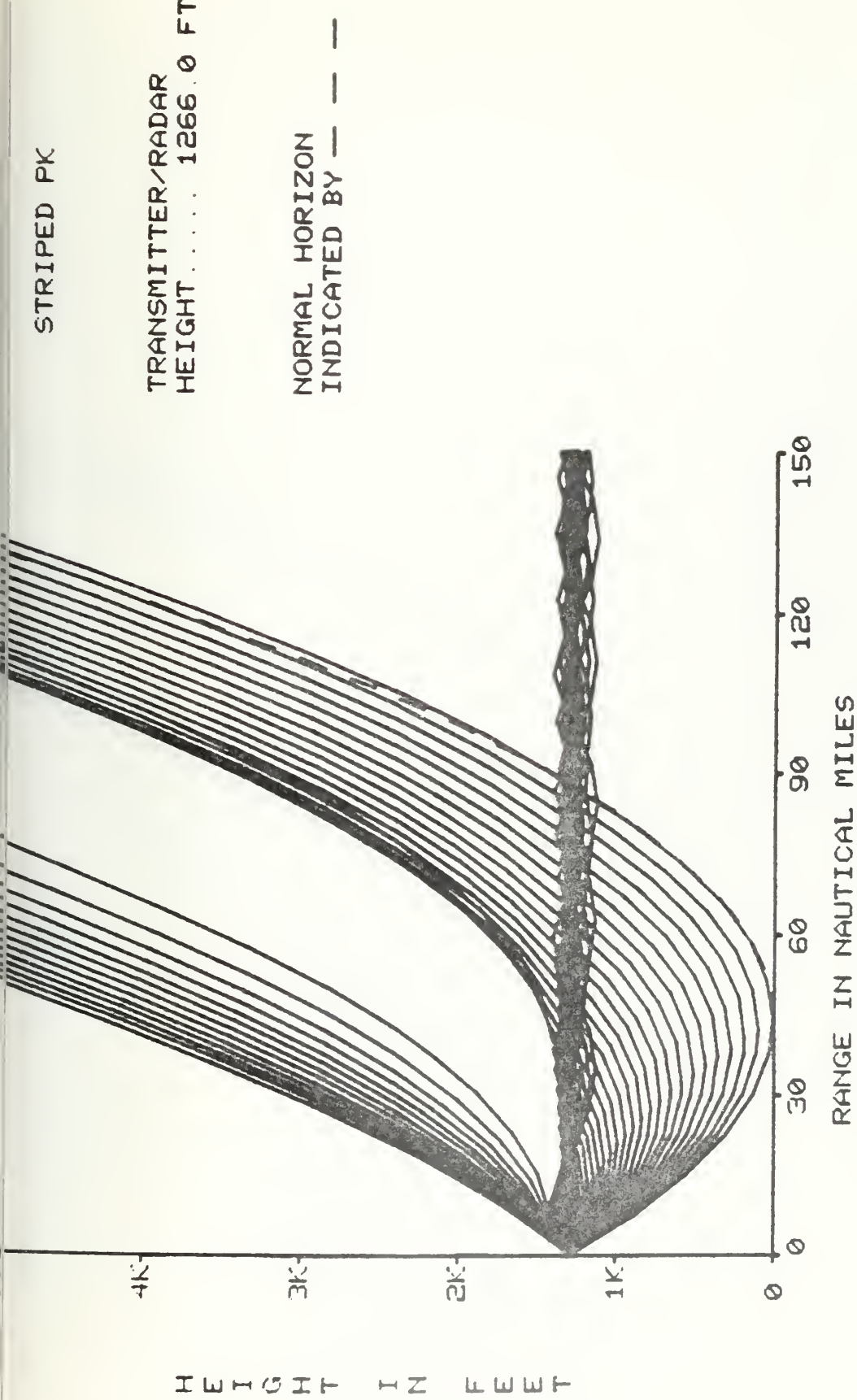
NORMAL HORIZON
INDICATED BY — — —



LOCATION: NOT SPECIFIED
TIME: NOT SPECIFIED
(PLOT, EDIT, LIST, SUMMARY, RAYS, LOSS, COVER, END)?

Figure 54

Ray Trace from Mt. Constitution for an Elevated Duct



LOCATION: NOT SPECIFIED
TIME: NOT SPECIFIED
(PLOT.EDIT.LIST.SUMRY.RAYSLOSS.COVER.END)?

Figure 55

Ray Trace from Striped Peak for an Elevated Duct

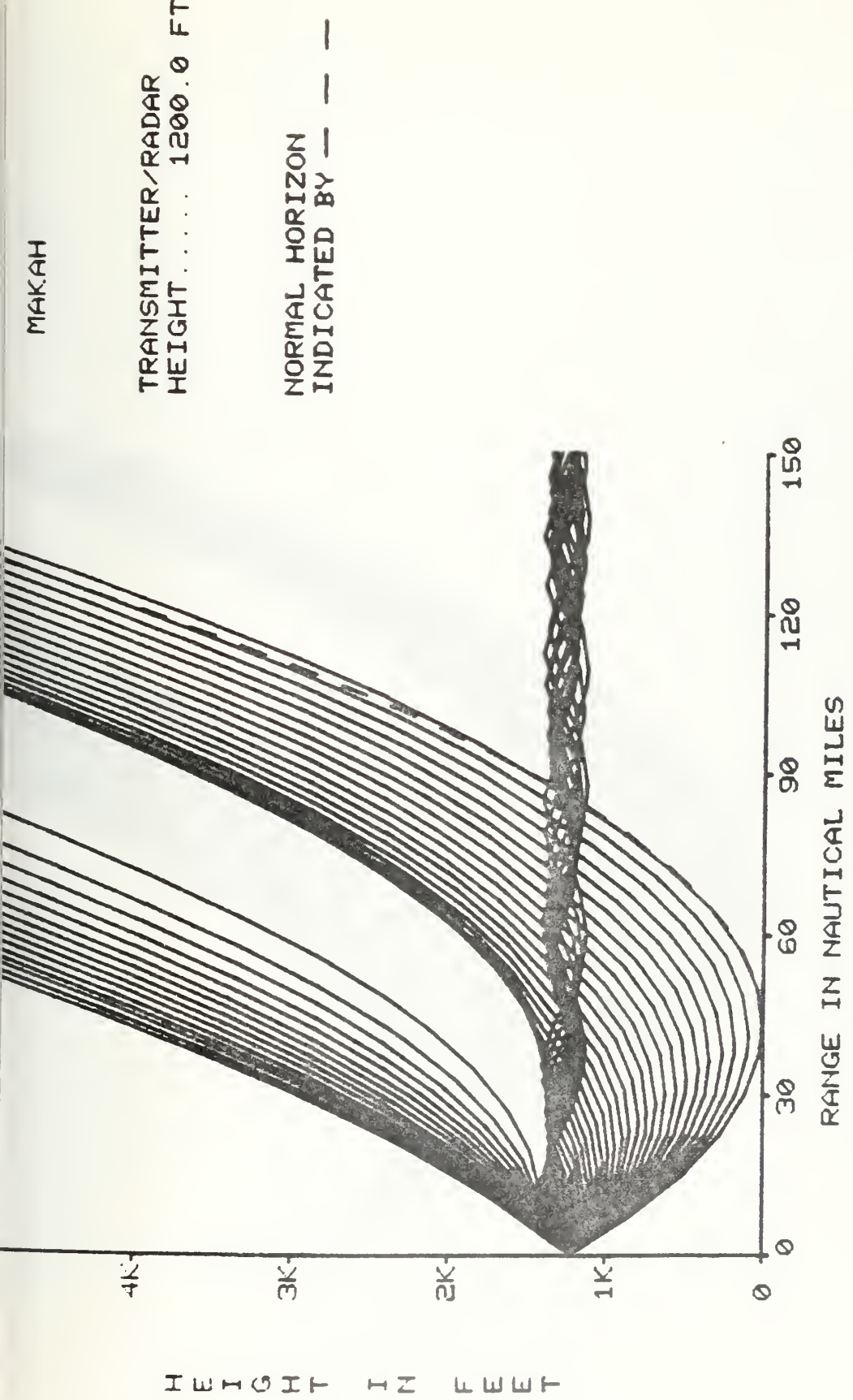
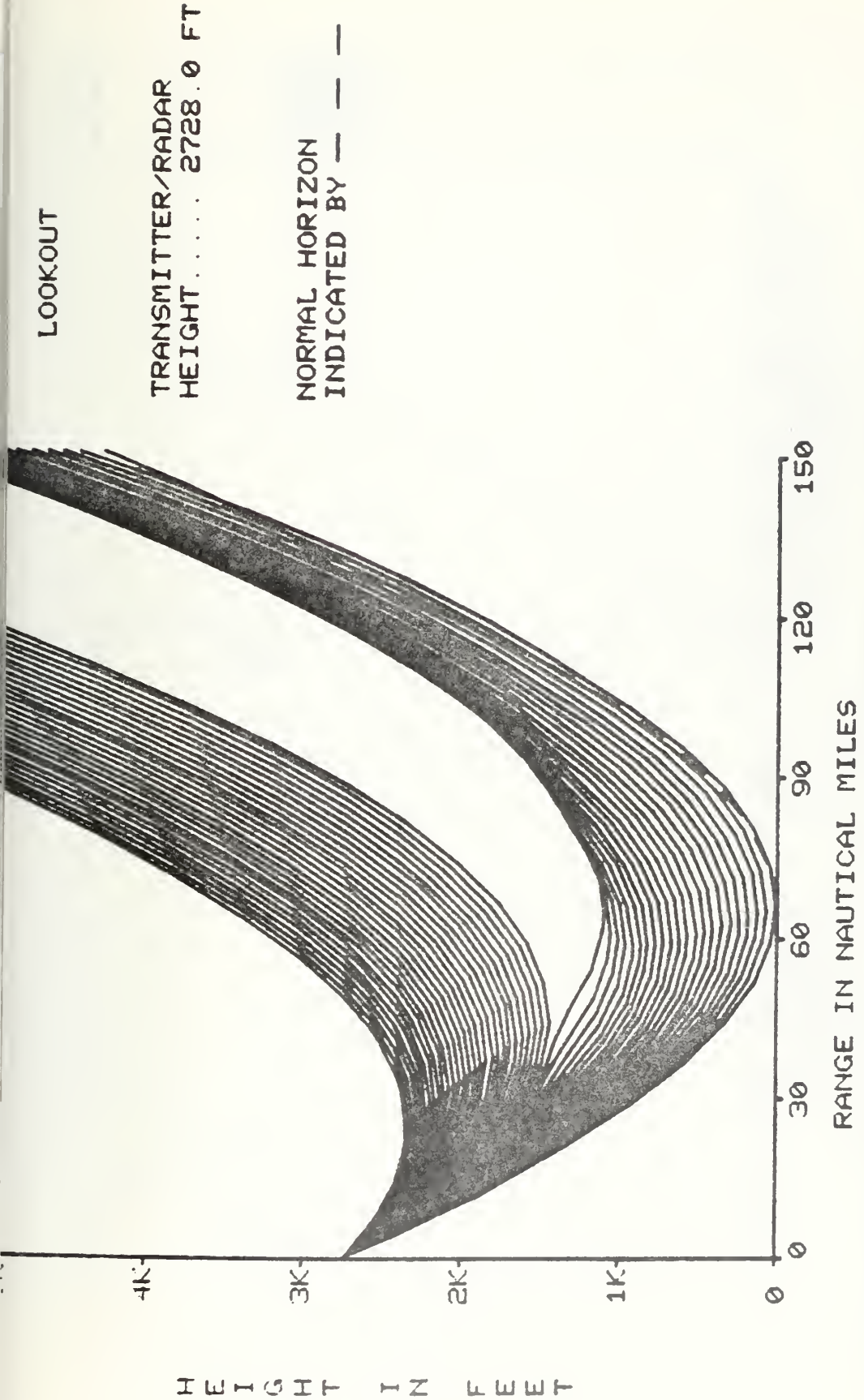


Figure 56
 Ray Trace from Makah for an Elevated Duct

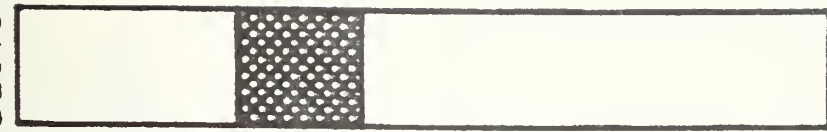


LOCATION: NOT SPECIFIED
TIME: NOT SPECIFIED
(PLOT, EDIT, LIST, SUMMARY, RAYS, LOSS, COVER, END)?

Figure 57

Ray Trace from Lookout Mt. for an Elevated Duct

DUCT'S



4K

3K

2K

1K

H E I G H T I N F E E T

4K

3K

2K

1K

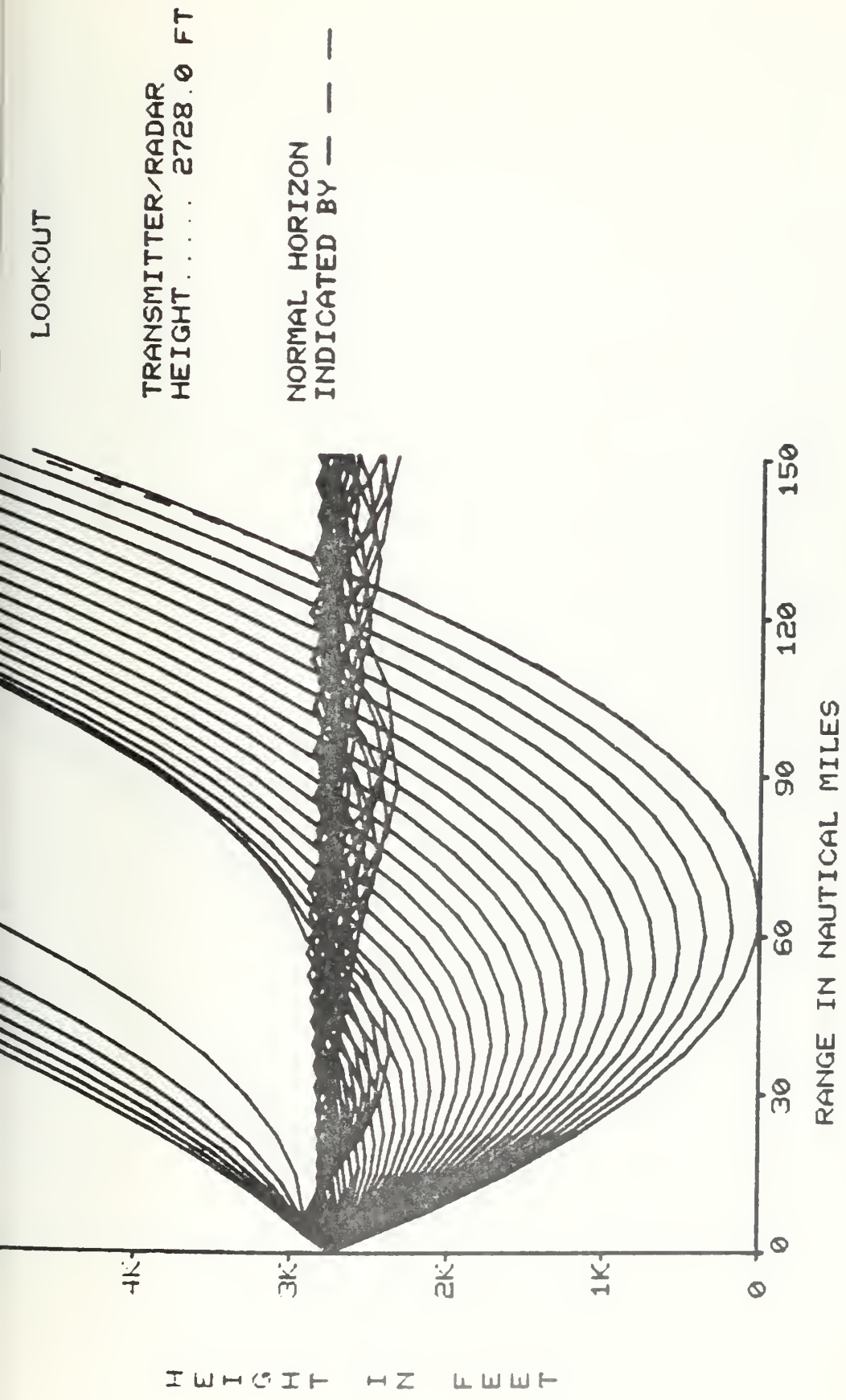
H E I G H T I N F E E T

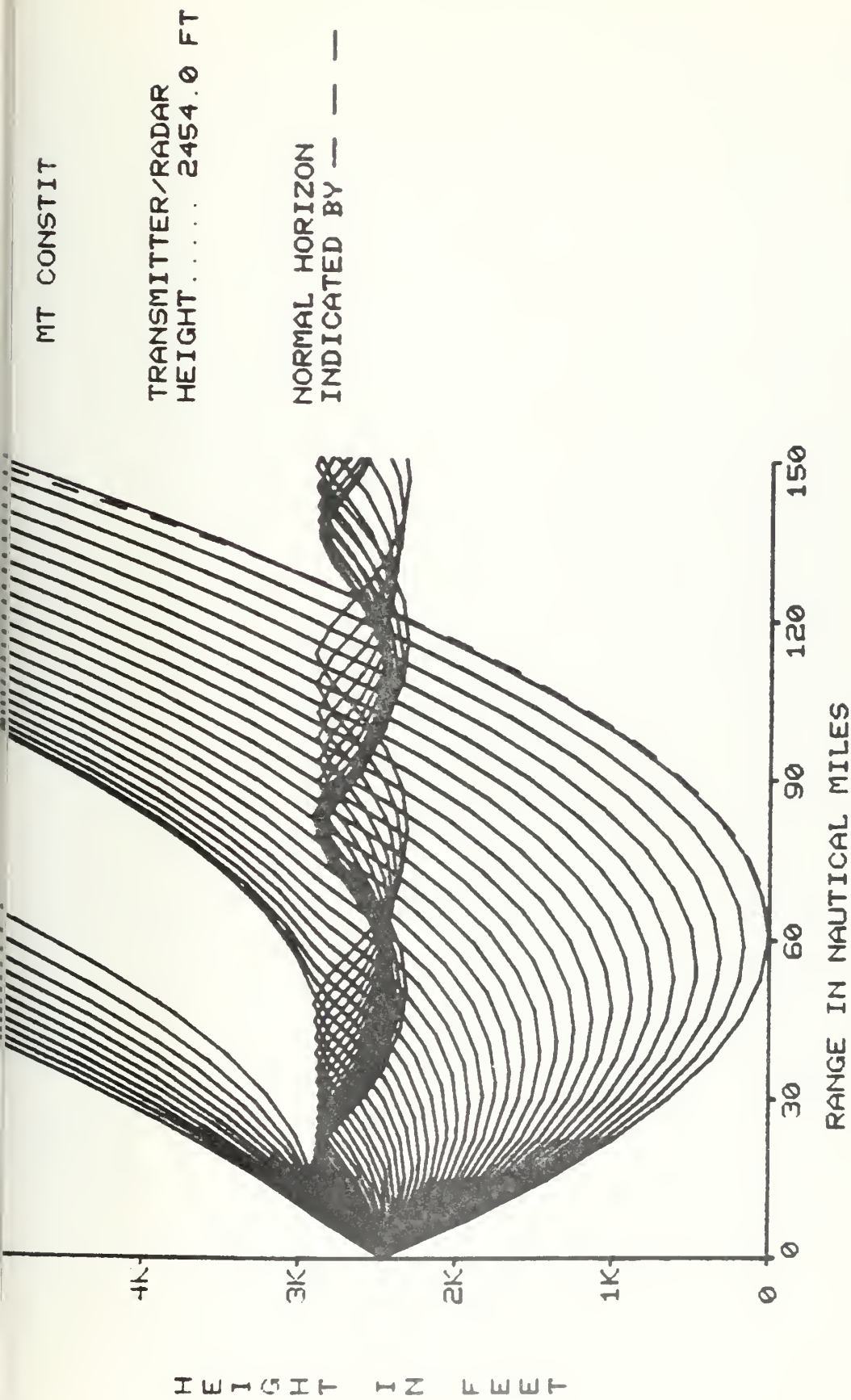


(PLOT, EDIT, LIST, SUMMARY, RAYS, LOSS, COVER, END)?

Figure 58

Profiles Required to Produce an Elevated Duct Between 2300-2900 Feet



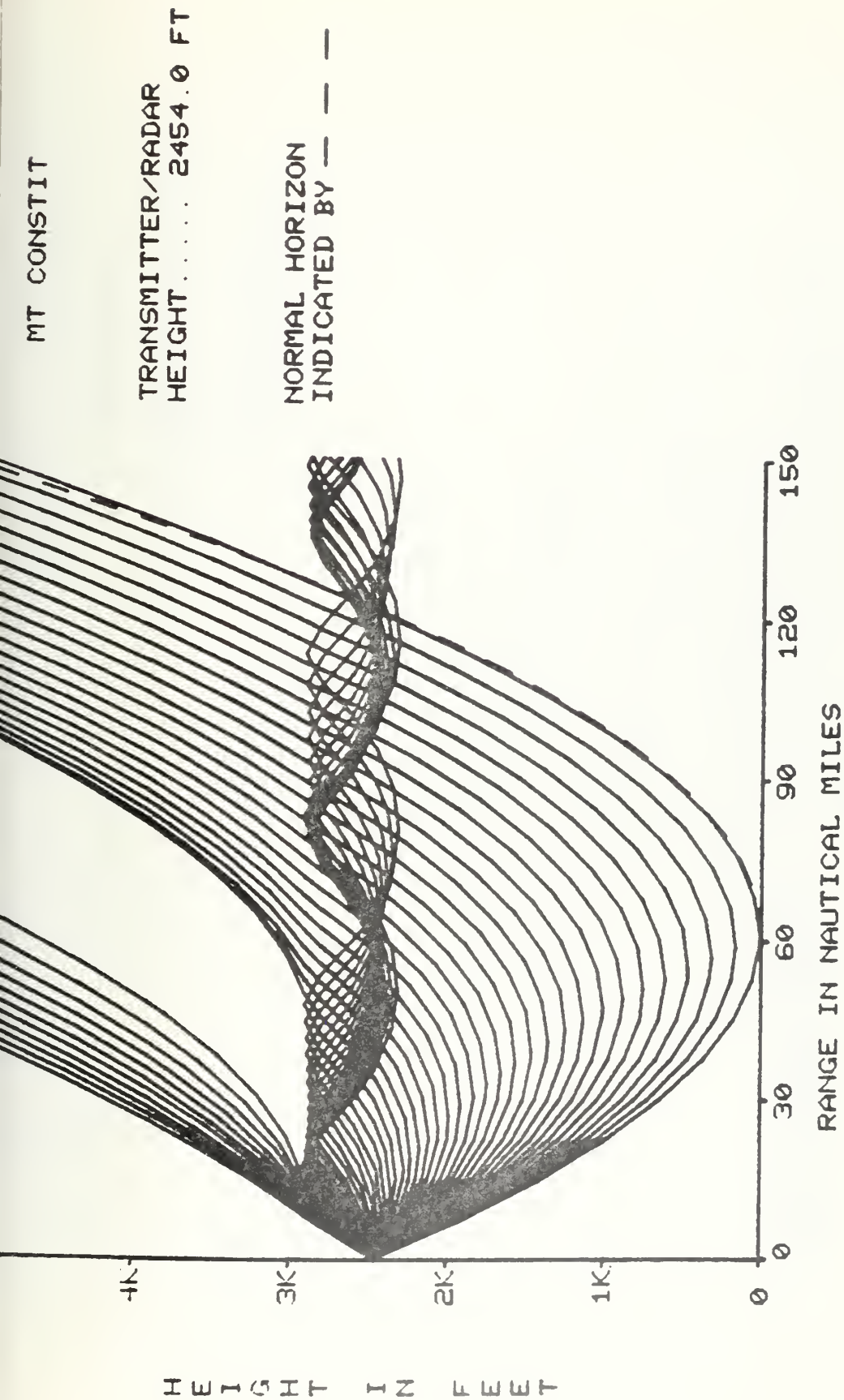


LOCATION: NOT SPECIFIED
TIME: NOT SPECIFIED
(PLOT, EDIT, LIST, SUMMARY, RAYS, LOSS, COVER, END)?

Figure 60

Ray Trace from Mt. Constitution for an Elevated Duct

MT CONSTIT



LOCATION: NOT SPECIFIED
TIME: NOT SPECIFIED
(PLOT, EDIT, LIST, SUMMARY, RAYS, LOSS, COVER, END)?

Figure 60

Ray Trace from Mt. Constitution for an Elevated Duct

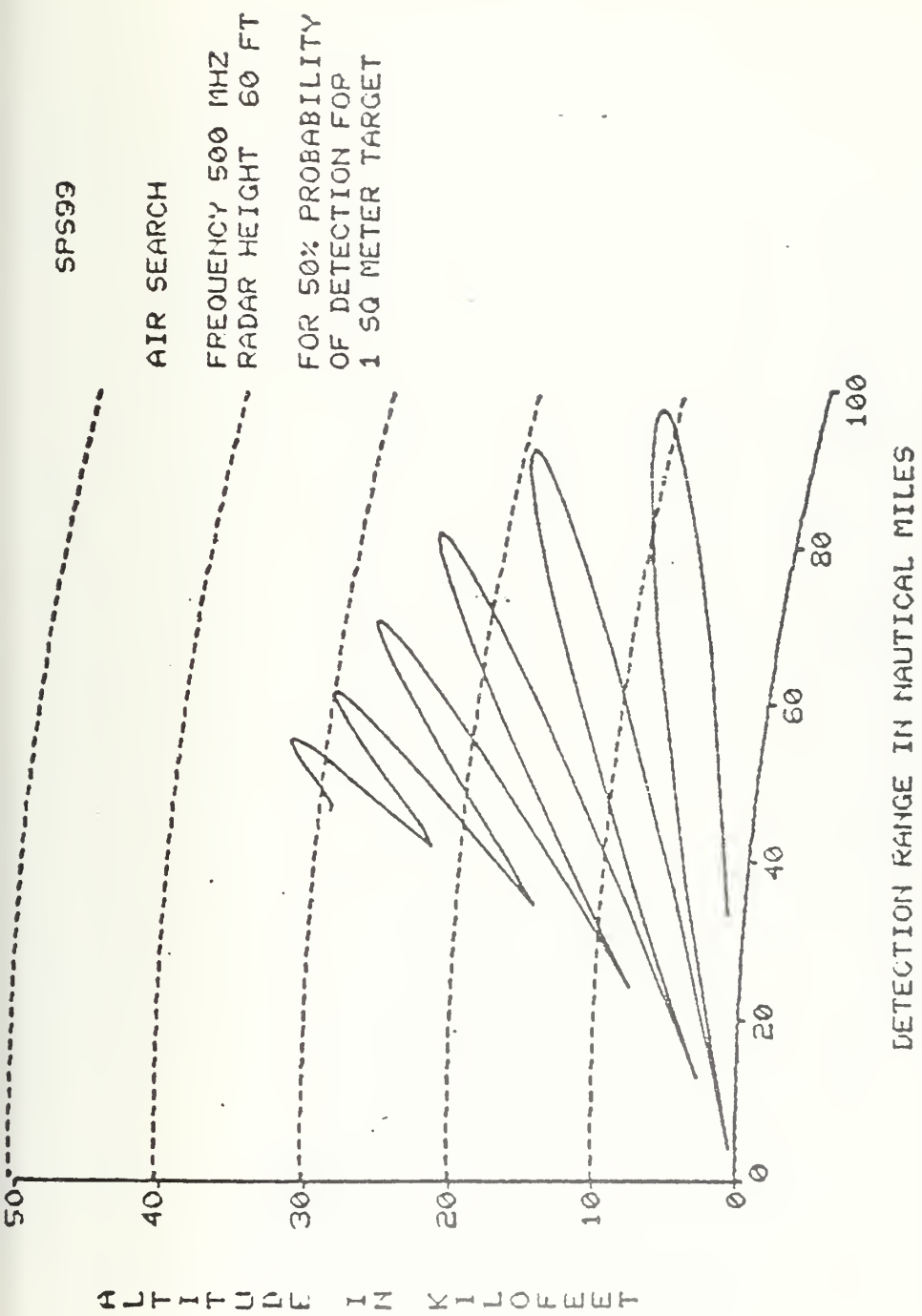


Figure 61
 Coverage Diagram (IREPS)

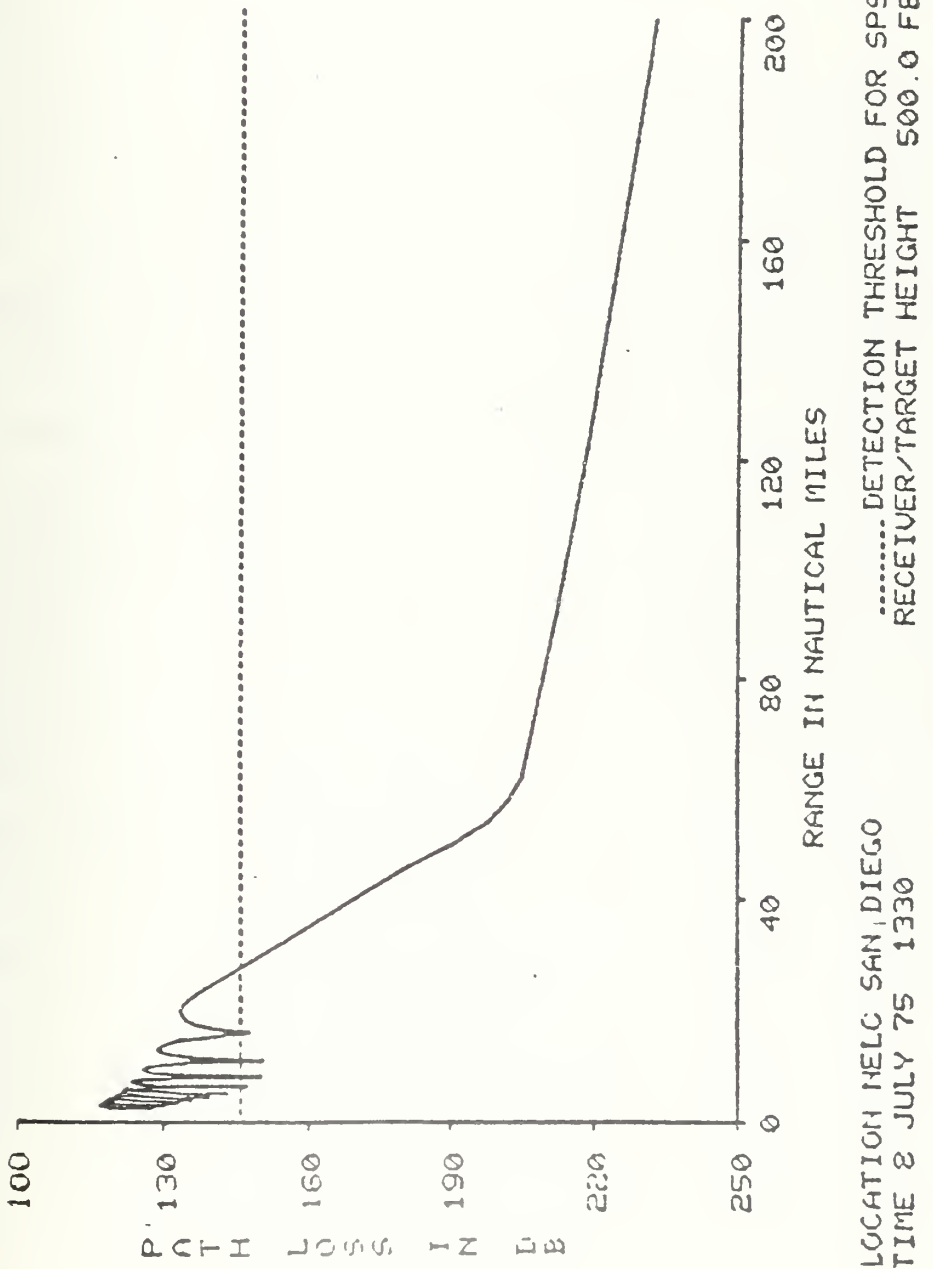


Figure 62
Path Loss Display (IREPS)

This system is not yet operational and is still undergoing testing. The value of the output formats in evaluating link anomalous propagation potential is clearly obvious. If data were available for each of the sites analyzed in the study a more exact picture of the statistics of propagation would be available.

Based on the available data for the Washington area several inferences can be made concerning anomalous propagation. For the frequencies in question the probability of extended ranges or ducting is between 8 and 10 percent while no statistics are presented for below normal refraction. For the locations from which the soundings are available it can be seen that surface ducting occurs most often in the daytime during Spring and that the ducts are predominantly less than 12 meters in thickness. The lowest occurrence of surface ducts at Quillayute is in the spring night which also has the highest incidence of elevated ducts. At Tatoosh which is a more classically marine climate, there are no ducts observed to occur during the autumn and winter either at night or during the day. The differences in the median refractivity at sea level are not significant and both values, 332 for Tatoosh and 324 for Quillayute, would produce an effective earth radius greater than $4/3$, and consequently better than average propagation conditions prevail. Until meteorological data is available for the actual sites the ray trace diagrams

can provide only an indication of the effect of a certain profile on the emitter in question rather than actual information concerning real conditions present in the link components.

APPENDIX A

Path Plotting Program

In order to plot a path profile on a curved earth surface either commercially available profile paper must be used or the profile can be manually or computer generated. Instructions for the construction of path profile paper for various values of earth radius can be found in Ref. 13. Computer generated profiles can be easily produced if a plotting package is available. For the purposes of this study a subroutine known as DRAWP was locally available. Other alternative plotting methods included the TEKTRONIX 4012 and HP 9830 plotting packages, both of which are available at the Naval Postgraduate School.

The program used made use of a transformation which allowed the terrain profile to be plotted on a linear graph by adjusting the height at a particular distance for the effective curvature of the earth. The profile is drawn by the CALCOMP plotter along with the earth surface at sea level. The program also fits a line to the terrain data by the method of least squares and forms the difference between the value of height found on the line and the actual value of the terrain height at the same distance. Aside from the actual terrain data points the only input parameters necessary to obtain this output are either the refractivity gradient or the surface refractivity, and the number of points input.

The output provided by the program includes a plot of the terrain on the effective earth surface, a table of height vs. input distance, a list of the terrain heights in kilometers, the effective earth radius, and the difference between each point on a least square curve and the actual terrain data points without the correction for earth curvature applied. In order to perform the curve to fit terrain referred to in Appendix B, a new set of points must be used taking only those the points visible to both transmitter and receiver instead of the entire terrain profile.

The format of the input data deck is presented below:

First Data Card:

Column 1: Code "1". surface refractivity will be used as input

Code "2". refractivity gradient will be used as input

Second Data Card:

Column 1-10: Number of data points
(right justified integer ≤ 200)

Column 10-20: Refractivity or gradient
(right justified integer)

Third Through Last Data Card:

The distance points in kilometers are listed in order using real numbers (i.e., F10.5 format) in columns 1-10, 11-20, ..., 61-70. The heights above sea level in feet follow directly after the distance listing in the same format. A new card is not started unless the last distance point was listed in Columns 61-70

An example of the latter cards is shown below

For the table of distance vs. height below

Distance (km)	Height (feet)
0.0	420.
1.0	500.
2.0	10.
3.0	125.5
4.0	780.
5.0	1000.

The final data cards would be as follows:

Column: 1-10 11-20 21-30 31-40 41-50 51-60 61-70

Card 3 0.0 1.0 2.0 3.0 4.0 5.0 420.

Card 4 500. 10. 125.5 780. 1000.

APPENDIX B

INPUT PARAMETER COMPUTATION

A. DETERMINATION OF DELTA-H

The program described in Appendix A was used to produce from the path geometry the parameters $d_{L1,2}$, $\theta_{e1,2}$ and Δh . The computation of Δh is only partially computer-aided by the fitting of a straight line to the uncorrected profile heights and subtracting the height of the line from the corresponding terrain height. This difference is output in the array D(I). The interdecile range is then extracted manually from this data by finding the value of the lower boundary of the 90th percentile and subtracting from it the value of the upper boundary of the 10th percentile. An example of the fit of this curve to actual terrain data is shown in the main body of this study.

B. DETERMINATION OF HE1,2

For line of sight paths the following determination was made for effective antenna heights:

1. A straight line is fitted to the corrected terrain profile heights.
2. The line is defined by

$$B(I) = A_0 + A_1(X(I))$$

in the program defined in Appendix A and should be modified for earth curvature by

$$B'(I) = B(I) - X^2/2A$$

3. The points chosen in the actual profile to which this line is fitted should be only those points which are visible to both transmitter and receiver.
4. The effective antenna height is then the difference between the fitted line and the height of the antenna above sea level.

The procedure described above defines a reflecting plane between the transmitter and receiver.

If, on inspection of the actual terrain and the least square curve, a good fit does not appear to have been obtained due to the roughness of the terrain other methods of obtaining effective antenna heights are available. If the foreground of the antenna represents a good reflecting surface then the antenna height over ground can be used, or multiple least square curves can be used if the path consists of a number of reflecting planes. In the event that terrain characteristics defy this sort of analysis, curves and formulae are available in Annex III to Ref. 5 which provide alternate methods for computing effective height.

The curve to fit terrain is also used in the determination of effective heights for the case of knife edge diffraction which is assumed to occur when the path length is less than the smooth-earth radio horizon for each antenna. In this case two curves are fitted to each of the diffracted paths forming a reflecting plane for each antenna.

For trans-horizon paths the effective heights are obtained by considering the actual height of the antenna above sea level and subtracting from that height the average height of the

terrain between the transmitter and receiver. To illustrate this, consider a link with transmitter height above sea level h_{to} . The heights at N equi-distant points are selected and the mean of the central 80% of these values is computed to produce \bar{h}_t where

$$\bar{h}_t = \frac{1}{.8N} \sum_{i=.1N}^{.9N} h_{ti}$$

e.g., $N = 31$; $\bar{h}_t = \frac{1}{25} \sum_{i=3}^{27} h_{ti} \quad i = 0, 1, 2, \dots, 30$

The effective transmitter height is then

$$h_{e1} = h_{to} - \bar{h}_t \quad \text{for } \bar{h}_t \leq h_{to}$$

If the mean value is greater than the height above sea level then the structural height of the antenna above ground is used.

C. DETERMINATION OF DL1,2 and TE1,2

The angular distance θ is readily obtained from the geometry of the profile as shown in Fig. 2. θ_{e1} , and θ_{e2} are measured and θ_e is calculated in the program as the maximum of either $\theta_{e1} + \theta_{e2}$ or $-d_L/a$. The distance d_L is the sum of the distances to the obstacle horizons, d_{L1} and d_{L2}

D. MODIFICATION TO TROPOPLOT

With the above means of determining the parameters

$\theta_{e1,2}$, $d_{L1,2}$, TROPOPLOT was modified as follows:

1. Delete the following statements from the main program:

```
IF (H1G.LE.2.) GO TO 12
IF (H1G.GE.2.).OR.H1G.LE.5.) GO TO 10
Z1 = 5.0
GO TO 11
10 Z1 = 1.0+DSIN(3.1415927*H1G/10.0)
11 H1E = H1G+Z1*DEXP(-2.0*H1G/DH)
IF (H2G.LE.2.0) GO TO 15
IF (H2G.GE.2.0.OR.H2G.LE.5.0) GO TO 13
Z2 = 5.0
GO TO 14
13 Z2 = 1.0+DSIN(3.1415927*H2G/10.0)
14 H2E = H2G+Z2*DEXP(-2.0*H2G/DH)
15 CONTINUE
DL1 = DLS1*DEXP(-.07*DSQRT(DH/DMAX1(5.0,H1E)))
DL2 = DLS2*DEXP(-.07*DSQRT(DH/DMAX1(5.0,H2E)))
TE1 = (.00065/DLS1)*((DLS1/DL1-1.)*DH-3.077*H1E)
TE2 = (.00065/DLS2)*((DLS2/DL2-1.)*DH-3.077*H2E)
```

2. Insert the following statements

```
909 FORMAT (4F10.5)
      READ(5,909) DL1, DL2, TE1, TE2
after the statement
22 FORMAT (4F10.5).
```

Having accomplished these insertions and deletions the input card deck as shown in Ref. 7 is changed as shown below for user-supplied data only:

First Data Card:

Column 01-10 "Type of Terrain" - Integer
Code: 4 User Terrain Data Used
No data suppression
5 User Terrain Data Used
No "output parameters" printed

Column 11-20 "DB Loss" - Integer
Code: 0 No DB data desired
(omit 2nd data card)
1 DB data desired

Column 21-30 "Distance Between Antennas" - Real
(1-2000) KM

Second Data Card:

Column 01-10 "TX Power Out" (Watts)
Positive Real Number

Column 11-20 "TX Antenna Gain" (db)
Positive Real Number

Column 21-30 "RX Antenna Gain" (db)
Positive Real Number

Column 31-40 "Transmitter Line Loss" (db)
Positive Real Number

Column 41-50 "Required Receiver Line Loss" (db)
Positive Real Number

Column 51-60 "Receiver Sensitivity" (dbm)
Positive Real Number

Third Data Card:

Column 01-10 "Surface Refractivity"
Integer (250-400) N-units

Column 11-20 "Surface Conductivity"
Real (mhos/meter)

Column 21-30 "Relative Dielectric Constant"
Real

Column 31-40 "Interdecile Range"
Delta-H

Fourth Data Card:

Column 01-10 "Antenna Polarization"
Real

Code: 01.00 Vertical Polarization
Code: -1.00 Horizontal Polarization

Column 11-20 "Frequency" Real
(20-40,000)

Column 11-20 "Calculated Antenna Height of
Transmitting Antenna"
Real (0.5-3000.0) Meters

Column 31-40 "Calculated Antenna Height
of Receiving Antenna"
Real (0.5-3000.0) Meters

Fifth Data Card:

Column 01-10 "Transmitter Obstacle Horizon, DL1" (km)
Real

Column 11-20 "Receiver Obstacle Horizon, DL2" (km)
Real

Column 21-30 "Transmitter Elevation (Depression)
Angle" (radians)
Real Positive (Negative)

Column 31-40 "Receiver Elevation (Depression)
Angle TE2" (radians)
Real Positive (Negative)

THIS IS A PROGRAM TO PLOT A TERRAIN PROFILE AND COMPUTE
 THE COEFFICIENTS OF A LEAST SQUARE LINE FITTED TO THE PROFILE.
 THE DIFFERENCE BETWEEN THE POINTS ON THE PROFILE AND THE
 ACTUAL TERRAIN ARE COMPUTED IN THE ARRAY D(I).
 THE TERRAIN PROFILE IS PLOTTED BY THE LOCAL SUBROUTINE
 CCFP.

```

C DIMENSION X(200),Y(200),H(200),E(200),Z(200),B(200),D(200)
C THE FRACTION OF THE EARTH'S RADIUS IS COMPUTED USING
C THE GRADIENT (TYPE=1.0) OR THE REFRACTIVITY
C (TYPE=2.0)
C (TYPE=2.0)      5 144) TYPE
C (TYPE=1.0)      10X11) TYPE
111  FCNTRAT (6,111)
10   INTEGER (215)
      REAL*4 ITB(12)/12*0./
      REAL*4 RTB(28)/28*0.*0/
      REAL*4 RGE(1.0)
      REAL (5,10) M,NS
      REAL (5,200) NS
      FER=1/(1-(.04665*EXP(.00577*NS)))
      FER=1/7
      COUNTINUE
55   READ (5,88) M,GRAD
88   FCNTRAT (215)
      FER=1/1-(6.4E-03)*GRAD
32   FCNTRATE (10X1-1,GRAD)
      COUNTINUE (6,22) GRAD
77   FCNTRATE (10X1'REFRACTIVE INDEX IS :',15)
200  FCNTRATE (7F10*5)
20   FACTUAL TERRAIN VALUES ARE READ IN FIRST LISTING THE DISTANCE FROM
THE TRANSMITTER KM AND THEN THE CORRESPONDING TERRAIN HEIGHTS IN FT
COUNTFILE READ (5,20,COUNTFILE=995)(X(I),I=1,M),(I(I),I=1,N)
      COUNTFILE=X(I)
      COUNTFILE=X(I)
56   COUNTFILE=(10X,'THE DISTANCE FROM XMTR',4X,'HEIGHT ABOVE SEA LEVEL')
300  FCNTRATE (6,1300)
      FCNTRATE (6,1300,F10.5,20X,F10.5)
400  FCNTRATE (6,1370)
      FCNTRATE (6,1400)((X(I))H(I))I=1,M)
      FCNTRATE (6,1300,'PROPAGATION PATH FILE',///)
20   FCNTRATE (6,1300)
      FCNTRATE (6,1300,'FRACTION OF EARTH RADIUS IS : ',2X,F10.5,///)
40   FCNTRATE (6,40) FER
      WRITE (6,40)
  
```



```

      DO 50 I=1,N
      SUMX=X(I)+SUMMX
      SCOUNTINUE(10X,'SUMMX =',F14.5)
      FCWRITE(6,100) SUMMX
      SUMY=Z(I)+SUMY
      FCWRITE(6,201) SUMY
      SCOUNTINUE(10X,'SUMY =',F10.5)
      FCWRITE(6,210) SUMY
      SUMXY=(X(I)*Z(I))+SUMXY
      SCOUNTINUE(SUMXY,'SUMXY =',F10.5)
      FCWRITE(6,301) SUMXY
      SUMXSQ=(X(I)**2)+SUMXSQ
      SCOUNTINUE(9X**SMXSQ =',F14.5)
      FCWRITE(6,401) SMXSQ
      DENOM=(SUMX**SQ)-(SUMXY**2)
      FCWRITE(6,402) DENOM
      AC=(SUMX*SQ)-(SUMXY*DENOM)
      FCFORMAT(6,500) AC
      A1=(N*(SUMXY)-(SUMX*SUMY))/DENOM
      FORMAT(10X,A1) A1
      WRITE(6,600) THE COEFFICIENT OF X IS =',F10.5
      D(I)=AC+A1*X(I)
      D(I)=ABSE(Z(I)-B(I))
      SCOUNTINUE(10X,'DISTANCE =',4X,'DIFFERENCE =',/ )
      FCWRITE(6,601) D(I)
      FCFORMAT(6,602)(X(I),D(I)),I=1,M)
      COUNTINE
      END

```

LIST OF REFERENCES

1. Bullington, K., "Radio Propagation Fundamentals," Bell System Technical Journal, v. 36, pp. 593-626, May 1957.
2. Panter, P. F., Communications Systems Design, pp. 371-405, McGraw-Hill, 1972.
3. Picquenard, A., Radio Wave Propagation, Wiley, 1974.
4. Naval Electronics Systems Command, Naval Shore Electronics Criteria, May 1972.
5. National Bureau of Standards Technical Note No. 101, Transmission Loss Predictions for Tropospheric Communications Circuits, by Rice, P. L., Longley, A. G., Norton, K. A. and Barsis, A. P., v. 1, 2, 7 May 1965.
6. ESSA Technical Report ERL 79-7TS-67, Prediction of Tropospheric Radio Transmission Loss Over Irregular Terrain, A Computer Method, by Longley, A. G., and Rice, P. L., July 1968.
7. Callaghan, J. M., "TROPOPLOT" an Improved Fortran Computer Program for Prediction of Long-Term Median Tropospheric Radio Transmission Loss Over Irregular Terrain, M.S. Thesis, U.S. Naval Postgraduate School, 1973.
8. ESSA Technical Report ERL 148-1%S 97, Comparison of Propagation Measurements with Predicted Values in the 20 to 10,000 MHz Range, by Longley, A. G. and Reasoner, R. K., January 1970.
9. National Bureau of Standards Monograph No. 22, Climatic Charts and Data of the Radio Refractive Index for the United States and the World, by Bean, B., Horn, J. and Ozanich, A. M., 1960.
10. Hitney, H. V. and Richter, J. H., "Integrated Refractive Effects Prediction System (IREPS)" Naval Engineers Journal, v. 88, April 1976.
11. National Bureau of Standards Monograph 92, Radio Meteorology, by Bean, B. R. and Dutton, E. J., 1 March 1966.
12. Du Castel, F., Tropospheric Radiowave Beyond the Horizon, Pergamon Press, 1966.
13. ITT, Reference Data for Radio Engineers, 12th ed., Ch. 26, 1975.

14. Sherar, R. C. and Rosenthal, J., "Don't Fall Into the Radar Hole," Proceedings of the Naval Institute, pp. 55-66, December 1973.
15. Freeman, R. L., Telecommunication Transmission Handbook, pp. 177-197, Wiley 1975.
16. Jordan, E. C. and Balmain, K. G., Electro-Magnetic Waves and Radiating Systems, Prentice-Hall, 1968.

DISTRIBUTION LIST

	No. Copies
1. Defense Documentation Center Cameron Station Alexandria, VA 22314	2
2. Library, Code 0212 Naval Postgraduate School Monterey, CA 93940	2
3. Assoc. Professor J. B. Knorr, Code 52Ko Department of Electrical Engineering Naval Postgraduate School Monterey, CA 93940	1
4. Department Chairman, Code 52 Department of Electrical Engineering Naval Postgraduate School Monterey, CA 93940	1
5. Assoc. Professor R. W. Adler, Code 52Ad Department of Electrical Engineering Naval Postgraduate School Monterey, CA 93940	1
6. Commanding Officer Naval Torpedo Station Attn: Dr. W.A. Middleton, Code 702 Keyport, WA 98345	1
7. Mr. H. V. Hitney, Code 2220 Naval Electronics Laboratory Center 271 Catalina Blvd. San Diego, CA 92152	1
8. Commanding Officer Naval Shipyard Attn: LCDR J. M. Callaghan, Code 106 Philadelphia, PA 19112	1
9. LT R. M. Cassidy 3716 Forest Grove Dr. Annandale, VA 22003	2
10. Commanding Officer Naval Torpedo Station Attn: Mr. Andy Hooper, Code 813A Keyport, WA 98345	1

thesC285
Computer prediction of tropospheric radi



3 2768 002 09092 0
DUDLEY KNOX LIBRARY